1 Photon interactions with atoms

1.1 Introduction

When a photon collides with an atom in its free state a number of things can happen. The photon may be absorbed and the atom left in an excited state or one or more atomic electrons may be removed and the atom becomes a singly or multiply charged ion. Alternatively, the photon may be scattered elastically without loss of energy or inelastically with subsequent excitation or single or multiple ionization of the atom. These processes are of fundamental importance for a wide variety of applications since the interactions of photons with atomic systems forms the basis of our understanding of the interaction of radiation with matter in general. It is the aim of this chapter to present a large subset of the basic experimental data on these processes.

Since photons can have energies (or wavelengths) over a broad range and the number of experiments which have been performed by alternative techniques to study these processes is large, there must be limits placed on the data presented. The criteria used to define the data presented are given below.

A. The data presented will be experimental data for ionization or scattering from free atoms only. This is an important limitation since at X-ray energies matter often behaves as if it were a collection of free atoms. However, one never can be sure that molecular or solid state effects may be neglected.

B. Photon absorption without ionization will not be considered. Basically, this is the subject of atomic spectroscopy and detailed tabulations of the wavelengths of spectral lines and of the probabilities of transitions between various atomic levels are available elsewhere [58Mo1, 69We1].

C. For photoionization, the data presented will be limited to the range of incident photon energies from the threshold for ionization (between 5 and 30 eV for neutral atoms) to 10 keV.

D. Although there have been a number of sophisticated theoretical calculations of photoionization and of elastic and inelastic photon scattering, with some exceptions, no data based on computed cross sections will be given.

E. Processes in which two or more photons interact simultaneously with a single atom will not be considered.

With the above criteria in mind, the data presented is arranged in three sections. Section 1.2 is concerned with total ionization cross sections for free atoms in their ground states in the energy range from threshold to 10 keV. The material is arranged in the following way. First, a brief discussion of the experimental techniques used in obtaining the data presented. Next, data are given for atomic hydrogen, for which few experiments have been done but theory is expected to be accurate. This is followed by data on the rare gases which, since they exist in free form comprise the bulk of the experimental data on free atoms. This is followed by data on the atmospheric gases oxygen and nitrogen, by data on the easily vaporized alkalis and finally by data on other atoms for which measurements have been made.

For all of the above elements there exists a large body of relative cross section measurements. These are not presented unless they can with reasonable certainty be normalized via other absolute measurements.

The data presented in Section 1.2 omits those energy ranges where autoionization or Auger processes occur which result in rapidly varying resonant cross sections. Such processes as well as simultaneous ionization and excitation and direct double ionization have been studied by a variety of experimental techniques and the data obtained is presented in Section 1.3. As in Section 1.2, there is a brief discussion of the experimental techniques used. The section also contains some data on the branching ratios; i.e., the ratios of alternative final states of the rest of the atom when a single electron is emitted and on the angular distribution of emitted electrons.

Finally, Section 1.4 is devoted to the experimental data on elastic and inelastic scattering. Here the energy range has been expanded and some data are given at high energies which was obtained from atoms not in their free state.

A number of alternative sources of the data presented here are available either in printed form or via on-line computer access. In general, these sources are intended for a particular application, are based either entirely or in part on theoretical calculations and often include data obtained via measurements on molecular gases or solids. Alternative sources of data including a brief description of each are listed in an appendix.

1.2 Total photoionization cross sections

1.2.1 Measurement techniques

If we assume that the photon source is weak enough so that only single photon-atom processes are possible and further that the energy of the photon beam is low enough that scattering may be neglected, but monochromatic with an energy above the first atomic ionization potential, then the cross section for total ionization may be obtained simply by measuring the attenuation of the photon beam as it passes through a gas of atoms. The cross section for total ionization in this case is given simply by Beer's law:

$$\sigma = \ln(I_o/I)/nl$$

Here I_o and I are the initial and final fluxes of the photon beam, l the length of path the beam passes through and n the gas density. If l is measured in cm and n is in atoms/cm^3 the cross section will be in units of cm^2. The units commonly used for photoionization cross sections are 10^{-18} cm^2 (megabarns), 10^{-21} cm^2 (kilobarns) and 10^{-24} cm^2 (barns). All of these units will be used here. Experimental data are sometimes expressed in units of reciprocal path length $k = n\sigma$ (cm^{-1}). When this is the case the results will be converted to cross sections using known density (n) values.

Alternatively, assuming again a monochromatic photon beam of known intensity, the photoionization cross section may be obtained by measuring the number and charge of the ions produced by absorption in a given path length or by measuring the number and energy of electrons. These methods have the added advantage that they allow one to separate single from double or multiple ionization and also make it possible to obtain cross sections differential in the direction and/or energy of the ejected electrons.

By far the bulk of the data on photoionization cross sections in this section has been obtained via straightforward photon attenuation measurements as described above. When this is not the case; i.e., when the data were obtained via collection of ions or electrons this will be noted.

The measurements reported in this section refer only to those energy ranges where the photoionization cross sections are expected to be slowly varying as a function of energy and hence

the energy distribution of the photon source (linewidth for discrete sources or spectral resolution for continuous sources such as synchrotron radiation using a monochromator) is relatively unimportant. However, some information on the experimental arrangement used will be given in some cases.

In a large part of the earlier literature which used photon line sources wavelengths rather than photon energies are reported. Although these measurements have the disadvantage of only being available at sometimes widely spaced energies, they have proven to be remarkably consistent since there is good agreement between experiments by different investigators. Most of the data obtained in the last several decades were obtained using synchrotron light sources which although they have the advantage of being continuous sources over a broad energy range require careful measurements to account for the detection of light not at the wavelength of the measurement.

Often, data are reported as a function of wavelength rather than of energy. When this is the case wavelengths have been converted to electron volts using the formula:

$$E\ (\text{eV}) = 1.2398 \cdot 10^{-4}/\lambda\ (\text{cm})$$

1.2.2 Cross sections for atomic hydrogen

In the energy range between the ionization threshold (13.598 eV) and 10 keV the cross section for atomic hydrogen can be calculated to high accuracy for the following reasons. Hydrogen is an atom with a single electron moving in a known central field. Thus the ground electronic state of the atom is known analytically as are the final continuum states corresponding to photoionization. This makes it possible to calculate the cross section accurately either by evaluating analytical formulas or by direct numerical solution of a one electron Schrodinger equation.

In Table 1 the calculated cross section for atomic hydrogen is shown over the range from threshold to 10 keV. The data in the range below 100 eV has been obtained by evaluating a simple formula for the cross section within dipole approximation [57Be1], and that at higher energies taken from the tabulations of Veigele [73Ve1] and Scofield [73Sc1].The calculated values are expected to be accurate to better than 1 %.

Although the photoionization cross section of atomic hydrogen can be calculated with high accuracy, measurements are difficult and serve only to provide a check on the theoretical results. The measurements are difficult since molecular hydrogen must be dissociated and some assumptions made concerning the relative absorption of molecular hydrogen since dissociation is incomplete. Absolute measurements of the cross section have been made at three energies near threshold [65Be1, 66Be2] and the results are compared with the theoretical results in Table 2. The agreement is good only at the lowest energy. The most definitive measurement for hydrogen was made by Palenius et al. [76Pa1] using a shock tube which resulted in almost 100 % dissociation of H_2. Their results extended from threshold to 20.36 eV and are also compared with theory in Table 2.

Although it is extremely difficult to measure the atomic hydrogen photoionization cross section measurements of molecular hydrogen are relatively simple to perform and a number of them have been performed. Tabulations of data of cross sections often use measurements on molecular gases or solids to infer cross sections for individual atoms assuming that molecular binding or solid state effects do not affect the cross sections. While this may be a good approximation at moderately high photon energies for some substances it is not for molecular hydrogen [74Co1].

Table 1. Cross sections for photoionization of atomic hydrogen as obtained from the formula described in the text and from the numerical calculations of Veigele and Scofield.

Energy [eV]	Cross section [10^{-21} cm^2]		
	Formula	73Ve1	73Sc1
1.360E+01 (I.P.)	6.303E+03		
2.000E+01	2.212E+03		
4.000E+01	3.059E+02		
6.000E+01	9.178E+01		
8.000E+01	3.838E+01		
1.000E+02	1.933E+01	1.93E+01	
2.000E+02	2.195E+00	2.20E+00	
4.000E+02	2.348E–01	2.32E–01	
6.000E+02	6.208E–02	6.15E–02	
8.000E+02	2.394E–02	2.36E–02	
1.000E+03	1.139E–02	1.12E–02	1.141E–02
2.000E+03		1.10E–03	1.111E–03
4.000E+03		1.05E–04	1.053E–04
6.000E+03		2.63E–05	2.627E–05
8.000E+03		9.79E–06	9.816E–06
1.000E+04		4.55E–06	4.558E–06

Table 2. Photoionization cross sections for atomic hydrogen as measured in [1]) [65Be1], [2]) [66Be2] and [76Pa1] and as computed by the analytic formula discussed in the text.

Energy [eV]	Cross section [10^{-18} cm^2]		Energy [eV]	Cross section [10^{-18} cm^2]	
	Measured	Formula		Measured	Formula
13.62	6.25	6.28	15.34	4.40	4.57
13.73	6.16	6.15	15.96	4.09	4.11
14.01	5.62	5.83	16.49	3.89	3.75
14.22	5.98	5.60	17.41	3.93	3.23
14.38	4.85	5.43	17.94	3.22	2.98
14.57	5.15 ± 0.18 [1])	5.25	18.70	2.99	2.63
14.59	4.83	5.24	19.10	2.82	2.51
14.70	2.90 ± 0.50 [2])	5.12	19.49	2.81	2.37
14.79	4.60	5.04	19.90	2.57	2.24
15.00	3.80 ± 0.80 [2])	4.85	20.36	2.23	2.11
15.08	4.19	4.78			

1.2.3 Cross sections for helium

Unlike hydrogen, exact calculations for helium cannot be made although much theoretical effort has been expended on such calculations and there is relatively good agreement with measurements. In contrast to hydrogen, measurements (at least at low energies) are fairly straightforward and the accuracy of the measurements is believed to be of the order of 1…2 %.

Since helium, unlike hydrogen is a two electron system, double as well as single ionization is possible at photon energies above the second ionization potential (79 eV) and measurements indicate that double ionization is of the order of 1…2 % of the total. All of the data reported here is for total ionization although there have been a number of measurements for the ratio of double to single ionization which will be discussed in Section 1.3.

The cross sections for photoionization are expected to be relatively smooth functions of photon energy except in the energy range below the double ionization threshold (79 eV) and extending to a region about 1 eV below the lowest energy resonance at 60.12 eV. For this reason data here is given only for the energy range below 59 eV and above 79 eV. Data in the resonance region will be reported in Section 1.3.

At energies above (1 keV for helium, measurements of the removal of photons from a beam cannot be used to infer photoionization cross sections since photon scattering becomes important. In the energy range considered here (the ionization threshold to 10 keV) helium is the only atom for which data is available in which scattering becomes important. In order to indicate the importance of scattering for helium, the percentage of the total attenuation cross section estimated [73Ve1] to be due to photoionization is shown in Table 3.

There have been a number of critical reviews of photoionization cross sections (or alternatively attenuation cross sections) for both helium and the other rare gases and they will be briefly described here. Samson [66Sa1] provided a set of data for all of the rare gases based on new measurements and existing theoretical and experimental data. Somewhat later Henke, as part of broader study of attenuation coefficients in materials included the rare gases helium, neon and argon [82He1].

West and Marr [76We1] gave a set of cross sections for helium, neon, argon and krypton based on new measurements by them between 36 and 310 eV and a review of earlier work and tables of their results were published [76Ma1]. Samson et al. [94Sa1] have recently made new measurements of helium from threshold to 120 eV and have provided a recommended set of data up to energies of 10 keV. Samson et al. [91Sa1] have also provided a new set of recommended values for the other rare gases based on highly accurate measurements made at low energies [89Sa1]. Finally Cooper [96Co1] has reviewed both the theoretical and experimental evidence on both photoionization and scattering cross sections for helium.

In the energy range below the autoionization region there is good agreement between the recent work of Samson et al. [94Sa1] and the earlier tabulation of Marr and West [76Ma1] as shown in Table 4 (the numbers shown for Marr and West were obtained from the published results via linear interpolation). The work of Samson et al. is based on new measurements whereas the work of Marr and West is based on a critical review of all of the measurements available to them at the time. Note that all of the results shown in Table 4 agree to within 3 %.

In the energy range between 80 and 300 eV there appears to be good agreement between the measurements of a number of investigators. Fig. 1 shows a comparison of the measurements of Henke [67He1], Denne [70De1], Watson [72Wa1] and an earlier measurement at 278 eV [31De1] with the recommended values of Samson et al. [94Sa1] Earlier measurements as well as those reported by Marr and West [76Ma1] appear to be somewhat higher than those shown.

In Table 5 the recommended values of Samson are given at 10 eV intervals in the energy range from 80 to 280 eV. Since the cross section is smoothly varying in this energy range this spacing should be adequate for interpolation. The expected accuracy of the data is better than 3 % for these data at energies below 150 eV and of the order of 5 % at higher energies.

Between 280 eV and 2.95 keV there are no measurements with the exception of a single measurement by Denne [70De1] at 523 eV. The quoted value $1.8 \cdot 10^{-21}$ cm^2 is so much lower than

any reasonable extrapolation to higher energies that it must be discounted. Table 6 gives a theoretical estimate of the photoionization cross section in this range based on the calculations of Railman and Manson [79Re1] and Scofield [73Sc1].

In the 1…10 keV range there are two measurements of photon attenuation, an old but careful measurement by Bearden [66Be1] and a recent measurement by Azuma et al. [95Az1]. Bearden's measurements were done with line sources at definite energies. His data which is only given to 2 place accuracy is shown in Table 7 and compared with the linearly interpolated values obtained from the work of Azuma et al. The results appear to agree to better than 10 %. Finally, a complete set of results of photon attenuation obtained by Azuma et al. is shown in Table 8. These authors have attempted to estimate the photoionization cross sections by subtracting theoretical scattering cross sections from their data but here only the total attenuation cross section is given. An estimate of the photoionization cross section may be obtained using the ratios given in Table 3.

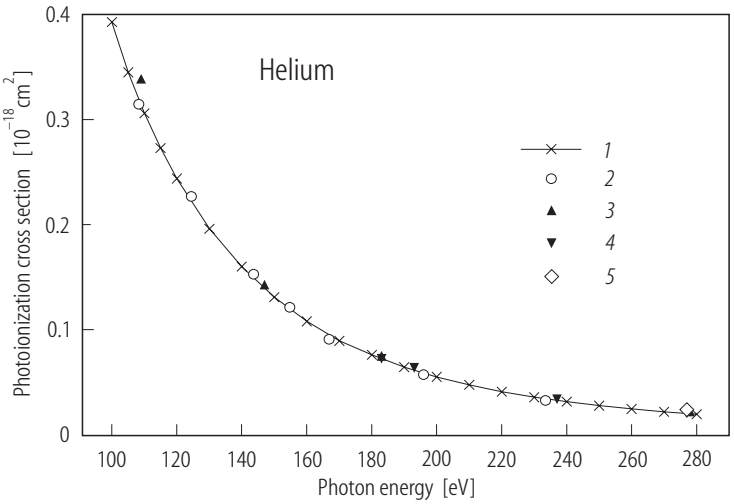

Fig. 1. Helium cross sections from 100 to 280 eV from various sources: *1* [94Sa1], *2* [72Wa1], *3* [67He1], *4* [70De1], *5* [31De1].

Table 3. Percentage of total attenuation due to photoionization for helium and neon for incident energies between 1 and 15 keV [73Ve1].

Energy [keV]	Helium [%]	Neon [%]
1.0	100	100
1.5	98	100
2.0	95	100
3.0	83	100
4.0	68	100
5.0	52	99
6.0	38	98
8.0	21	97
10.0	11	95
15.0	3	89

Table 4. A comparison of the cross sections for helium between threshold (24.59 eV) and 55 eV from [76Ma1] and [94Sa1].

Energy [eV]	Cross section [10^{-18} cm^2]	
	94Sa1	76Ma1
24.58	7.40	7.52
25.0	7.21	7.36
30.0	5.38	5.29
35.0	4.09	3.98
40.0	3.16	3.08
45.0	2.48	2.45
50.0	2.02	1.99
55.0	1.67	1.64

Table 5. Photoionization cross sections of helium at energies between 80 and 280 eV from [94Sa1].

Energy [eV]	Cross section [10^{-21} cm^2]
80.0	693.0
90.0	516.0
100.0	393.0
110.0	306.0
120.0	244.0
130.0	196.0
140.0	160.0
150.0	131.0
160.0	108.0
170.0	89.4
180.0	76.0
190.0	64.3
200.0	55.0
210.0	47.4
220.0	40.9
230.0	35.6
240.0	31.5
250.0	27.7
260.0	24.5
270.0	21.8
280.0	19.4

Table 6. Theoretical photoionization Cross sections of helium at energies between 300 eV and 3000 eV. From [73Sc1] and [79Re1].

Energy [eV]	Cross section [10^{-21} cm^2]
300.0	17.6000
450.0	5.1900
600.0	2.1000
750.0	1.0300
1000.0	0.4020
1500.0	0.1090
2000.0	0.0432
2500.0	0.0207
3000.0	0.0112

Table 7. A comparison of the measured photon attenuation cross sections of helium by Beardon [66Be1] and Azuma et al. [95Az1]. *) from [70Mc1].

Energy [keV]	Cross section [10^{-24} cm^2]		Ratio
	66Be1	95Az1	
2.98	13.3		
3.44	8.8	8.96	0.99
4.51	4.6	4.78	0.95
5.41	3.3	3.09	1.06
5.89 *)	2.8	2.66	1.04
6.40	2.3	2.44	0.94
8.15	1.9	1.82	1.04

Table 8. Measured photo attenuation cross sections of helium at energies between 3.35 and 14.0 keV from [95Az1].

Energy [keV]	Cross section [10^{-24} cm^2]
3.35	9.75
3.55	8.07
3.75	6.93
3.95	6.05
4.15	5.26
4.35	4.66
4.55	4.16
4.75	3.79
4.95	3.55
5.15	3.30
5.35	3.11
5.50	3.07
5.55	2.93
6.00	2.57
6.50	2.41
7.00	2.14
8.00	1.84
9.00	1.70
10.00	1.61
11.00	1.56
12.00	1.48
13.00	1.47
14.00	1.41

1.2.4 Cross sections for neon (Z = 10)

The experimental situation for measurements of total ionization cross sections for neon is similar to that of helium and the other rare gases. Recommended values have been given by Henke et al. [70He1], Samson [66Sa1] and Marr and West [76Ma1] based on critical reviews of the available experimental and theoretical evidence. In addition, Samson has provided an updated version of neon data based upon more recent unpublished data [91Sa1].

As in all elements there are energy ranges where resonances are expected to occur and the photoionization cross section shows rapid variations. In neon these ranges are (a) the narrow range between the two lowest states of the neon ion core (21.56…21.66 eV), (b), the range immediately below the ionization threshold for 2s electrons (L_1 edge) from 45 to 50 eV and (c), the range about the 1s ionization threshold (K edge) at 870 eV. Data in these ranges will be given in Section 1.3.

In the region below the second resonant range (threshold to 45 eV) there is good agreement between the new values of Samson and the recommended values of Marr and West as shown in Table 9. The major difference is in the range extending to about 5 eV above threshold where the new data of Samson is ≈ 3 % higher than the values of Marr and West.

In the energy range between 40 and 280 eV the neon cross section has been measured by essentially the same experimentalists as was the case for helium. Fig. 2 shows the results obtained by Marr and West [76Ma1], Henke [67He1], Denne [70De1], Watson [72Wa1], Cole et al. [78Co1] and the new results of Samson [91Sa1]. There is good agreement between all of these measurements with the exception that the results of Marr and West appear to be somewhat larger than the other measurements in the energy range from about 80 to 180 eV. Selected data from these authors is given in Table 10.

There have been few measurements in the energy range between 280 eV and 860 eV (10 eV below the K ionization threshold). The available measurements in this range from Henke [67He1], Bearden [66Be1] and Wuilleumier [69Wu1] are shown in Table 11.

In the energy range above the K ionization threshold to 10 keV there have been a number of measurements using X-ray line sources. A summary of these measurements is given in Table 12. In addition to the measurements using line sources, Wuilleumier's measurements using a continuum source are shown in Table 13. A comparison of his data with the line source data of Table 12 is shown in Fig. 3.

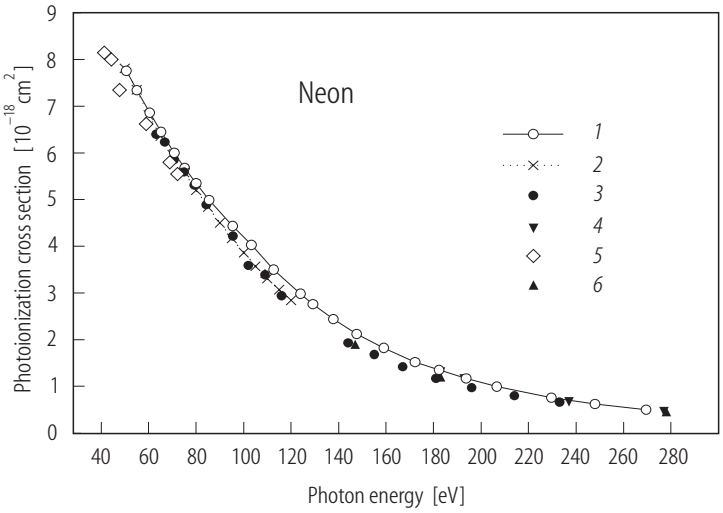

Fig. 2. Neon cross sections from 40 to 280 eV from various sources: *1* [76Ma1], *2* [91Sa1], *3* [72Wa1], *4* [70De1], *5* [78Co1], *6* [67He1].

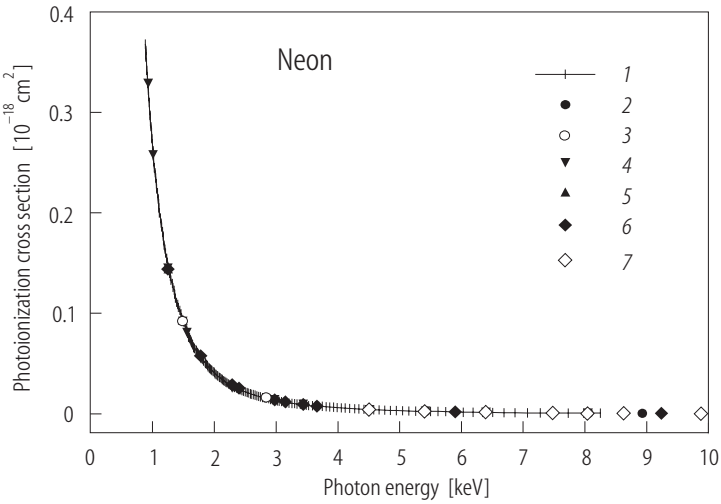

Fig. 3. Cross section for neon between 0.86 and 10 keV from various sources: *1* [69Wu1], *2* [30Co1], *3* [30Wo1], *4* [66Be1], *5* [67He1], *6* [70Mc2], *7* [74Mi1].

Overall, with the exception of the energy range from 50 to 280 eV mentioned above and the omitted resonance regions the good agreement between different experiments means that the total photoionization cross section for neon is known to an accuracy of about 3% over the entire energy range from threshold to 12 keV. Although most of the measurements were of photon attenuation rather than of the total photoionization cross section corrections for scattering are much smaller than for helium as shown in Table 3.

Table 9. Photo attenuation cross sections for neon at incident energies between 22 and 44 eV. Data from [91Sa1] and [76Ma1] (interpolated).

Energy [eV]	Cross section [10^{-18} cm^2]		Ratio
	91Sa1	76Ma1	
22.0	6.68	6.50	0.972
24.0	7.73	7.53	0.974
26.0	8.40	8.20	0.976
28.0	8.82	8.59	0.974
30.0	9.00	8.84	0.982
32.0	9.10	8.95	0.983
34.0	9.11	8.96	0.984
36.0	8.90	8.90	1.000
38.0	8.72	8.80	1.009
40.0	8.55	8.68	1.015
42.0	8.41	8.53	1.014
44.0	8.27	8.37	1.012

Table 10. Photo attenuation cross sections for neon at incident energies between 50 and 280 eV. [1]) from [72Wa1], [2]) [67He1], [3]) [70De1], [4]) [31De1].

Energy [eV]	Cross section [10^{-18} cm^2]			
	91Sa1	76Ma1	70De1	Other
50.00	7.81			
50.60		7.76		
55.00	7.35			
55.10		7.34		
60.00	6.81			
60.48		6.86		
63.10			6.40	
65.00	6.36			
65.25		6.45		
66.80			6.23	
70.00	5.96			
70.70			5.86	
70.85		6.00		
74.90			5.59	
75.00	5.58			
75.14		5.68		
79.30			5.31	
79.99		5.35		
80.00	5.20			
84.30			4.89	
85.00	4.84			
85.50		4.99		
90.00	4.50			
95.00	4.17			
95.37		4.43		
95.50			4.22	
100.00	3.86			
102.00			3.59	
103.30		4.03		
105.00	3.57			
109.00			3.39	
109.00				3.42 [1])
110.00	3.31			
112.70		3.50		
115.00	3.07			
116.00			2.94	
120.00	2.84			
124.00		2.98		
129.20		2.76		
137.80		2.44		
144.00			1.93	
147.00				1.90 [1])
147.60		2.12		
155.00			1.68	

Energy [eV]	Cross section [10^{-18} cm^2]			
	91Sa1	76Ma1	70De1	Other
159.00		1.82		
167.00			1.42	
172.20		1.52		
181.00			1.17	
182.30		1.35		
183.00				1.31 [2])
183.00				1.20 [1])
193.00				1.16 [1])
193.70		1.17		
196.00			0.968	
206.60		0.992		
214.00			0.796	
229.60		0.756		
233.00			0.662	
237.00				0.667 [2])
248.00		0.620		
269.50		0.500		
278.00				0459 [3])
278.00				0.457 [2])
278.00				0.439 [4])

Table 11. Photo attenuation cross sections for neon at incident energies between 280 and 860 eV.

Energy [eV]	Cross section [10^{-21} cm^2]	Ref.
391.0	185.0	67He1
526.0	87.1	67He1
676.0	43.9	67He1
774.0	30.1	67He1
825.0	25.9	69Wu1
830.0	25.6	69Wu1
836.0	25.3	69Wu1
842.0	24.9	69Wu1
847.0	24.7	69Wu1
852.0	25.0	66Be1
853.0	24.4	69Wu1
859.0	24.2	69Wu1

Table 12. Photo attenuation cross sections for neon at energies between 0.9 and 10 keV from various sources.

Energy [eV]	Cross section [10^{-21} cm^2]					
	30Wo1	66Be1	30Co1	67He1	70Mc2	74Mi1
930.0		329.000				
1012.0		258.000				
1254.0	144.000	145.000		144.000		
1487.0	92.160	92.300		93.000		
1557.0		81.000				
1778.0	57.880					
2293.0	25.990	25.800				
2395.0	25.570					
2838.0	16.020					
2984.0	13.940	14.100				
3151.0	11.930					
3444.0	9.350	9.450				
3662.0	7.740					
4508.0		4.360			4.190	4.243
5414.0	2.510	2.550				2.474
5420.0			2.520			
5895.0					1.910	
6404.0		1.500				1.507
7472.0						0.938
8041.0						0.750
8048.0		0.737				
8631.0						0.621
8930.0			0.533			
9243.0					0.503	
9876.0						0.410

Table 13. Photo attenuation cross sections for neon at energies between 0.87 and 10 keV [69Wu1].

Energy [eV]	Cross section [10^{-24} cm^2]	Energy [eV]	Cross section [10^{-24} cm^2]	Energy [eV]	Cross section [10^{-24} cm^2]
0.871E+03	0.387E+06	0.966E+03	0.291E+06	0.109E+04	0.214E+06
0.877E+03	0.373E+06	0.974E+03	0.286E+06	0.110E+04	0.209E+06
0.884E+03	0.368E+06	0.982E+03	0.280E+06	0.110E+04	0.205E+06
0.890E+03	0.362E+06	0.990E+03	0.274E+06	0.111E+04	0.200E+06
0.896E+03	0.355E+06	0.998E+03	0.268E+06	0.113E+04	0.195E+06
0.903E+03	0.349E+06	0.101E+04	0.262E+06	0.114E+04	0.190E+06
0.910E+03	0.342E+06	0.101E+04	0.257E+06	0.115E+04	0.186E+06
0.916E+03	0.335E+06	0.102E+04	0.251E+06	0.116E+04	0.181E+06
0.923E+03	0.329E+06	0.103E+04	0.245E+06	0.117E+04	0.177E+06
0.930E+03	0.322E+06	0.104E+04	0.240E+06	0.118E+04	0.173E+06
0.937E+03	0.316E+06	0.105E+04	0.235E+06	0.119E+04	0.168E+06
0.944E+03	0.310E+06	0.106E+04	0.229E+06	0.120E+04	0.164E+06
0.952E+03	0.303E+06	0.107E+04	0.224E+06	0.121E+04	0.160E+06
0.959E+03	0.297E+06	0.108E+04	0.220E+06	0.123E+04	0.155E+06

Energy [eV]	Cross section [10^{-24} cm^2]	Energy [eV]	Cross section [10^{-24} cm^2]	Energy [eV]	Cross section [10^{-24} cm^2]
0.124E+04	0.151E+06	0.192E+04	0.456E+05	0.317E+04	0.113E+05
0.125E+04	0.147E+06	0.193E+04	0.448E+05	0.321E+04	0.107E+05
0.126E+04	0.144E+06	0.195E+04	0.440E+05	0.326E+04	0.104E+05
0.128E+04	0.140E+06	0.196E+04	0.431E+05	0.330E+04	0.101E+05
0.129E+04	0.137E+06	0.198E+04	0.422E+05	0.334E+04	0.985E+04
0.130E+04	0.133E+06	0.200E+04	0.414E+05	0.339E+04	0.948E+04
0.132E+04	0.130E+06	0.201E+04	0.399E+05	0.344E+04	0.905E+04
0.133E+04	0.126E+06	0.203E+04	0.391E+05	0.349E+04	0.865E+04
0.135E+04	0.123E+06	0.205E+04	0.381E+05	0.353E+04	0.838E+04
0.136E+04	0.119E+06	0.206E+04	0.375E+05	0.359E+04	0.814E+04
0.137E+04	0.115E+06	0.208E+04	0.365E+05	0.364E+04	0.791E+04
0.139E+04	0.111E+06	0.210E+04	0.359E+05	0.369E+04	0.771E+04
0.141E+04	0.109E+06	0.212E+04	0.349E+05	0.375E+04	0.747E+04
0.142E+04	0.106E+06	0.213E+04	0.340E+05	0.381E+04	0.710E+04
0.144E+04	0.103E+06	0.215E+04	0.331E+05	0.387E+04	0.684E+04
0.146E+04	0.995E+05	0.217E+04	0.324E+05	0.393E+04	0.654E+04
0.147E+04	0.952E+05	0.219E+04	0.315E+05	0.399E+04	0.623E+04
0.149E+04	0.937E+05	0.221E+04	0.308E+05	0.406E+04	0.603E+04
0.151E+04	0.910E+05	0.223E+04	0.297E+05	0.412E+04	0.570E+04
0.153E+04	0.878E+05	0.225E+04	0.291E+05	0.419E+04	0.540E+04
0.155E+04	0.848E+05	0.227E+04	0.285E+05	0.427E+04	0.509E+04
0.156E+04	0.823E+05	0.229E+04	0.278E+05	0.434E+04	0.486E+04
0.157E+04	0.802E+05	0.231E+04	0.271E+05	0.442E+04	0.456E+04
0.158E+04	0.765E+05	0.233E+04	0.264E+05	0.450E+04	0.426E+04
0.159E+04	0.761E+05	0.236E+04	0.257E+05	0.458E+04	0.402E+04
0.160E+04	0.755E+05	0.238E+04	0.253E+05	0.467E+04	0.382E+04
0.161E+04	0.740E+05	0.240E+04	0.245E+05	0.476E+04	0.362E+04
0.162E+04	0.727E+05	0.243E+04	0.239E+05	0.485E+04	0.342E+04
0.163E+04	0.713E+05	0.245E+04	0.231E+05	0.495E+04	0.323E+04
0.164E+04	0.700E+05	0.247E+04	0.226E+05	0.505E+04	0.307E+04
0.165E+04	0.687E+05	0.250E+04	0.220E+05	0.515E+04	0.286E+04
0.166E+04	0.667E+05	0.253E+04	0.214E+05	0.526E+04	0.272E+04
0.167E+04	0.659E+05	0.255E+04	0.206E+05	0.538E+04	0.267E+04
0.168E+04	0.650E+05	0.258E+04	0.201E+05	0.550E+04	0.250E+04
0.170E+04	0.639E+05	0.260E+04	0.195E+05	0.562E+04	0.234E+04
0.171E+04	0.627E+05	0.263E+04	0.192E+05	0.575E+04	0.212E+04
0.172E+04	0.618E+05	0.266E+04	0.185E+05	0.589E+04	0.194E+04
0.173E+04	0.609E+05	0.269E+04	0.180E+05	0.603E+04	0.165E+04
0.174E+04	0.597E+05	0.272E+04	0.174E+05	0.619E+04	0.152E+04
0.176E+04	0.582E+05	0.275E+04	0.170E+05	0.634E+04	0.143E+04
0.177E+04	0.574E+05	0.278E+04	0.163E+05	0.651E+04	0.132E+04
0.178E+04	0.560E+05	0.281E+04	0.159E+05	0.669E+04	0.121E+04
0.179E+04	0.551E+05	0.284E+04	0.154E+05	0.687E+04	0.112E+04
0.181E+04	0.542E+05	0.288E+04	0.150E+05	0.707E+04	0.104E+04
0.182E+04	0.533E+05	0.291E+04	0.144E+05	0.728E+04	0.948E+03
0.183E+04	0.524E+05	0.295E+04	0.140E+05	0.750E+04	0.868E+03
0.185E+04	0.512E+05	0.298E+04	0.134E+05	0.773E+04	0.791E+03
0.186E+04	0.502E+05	0.302E+04	0.129E+05	0.798E+04	0.717E+03
0.187E+04	0.493E+05	0.305E+04	0.125E+05	0.825E+04	0.654E+03
0.189E+04	0.481E+05	0.309E+04	0.123E+05		
0.190E+04	0.467E+05	0.313E+04	0.118E+05		

1.2.5 Cross sections for argon (Z = 18)

For argon there have been a number of measurements in the energy range immediately above the first ionization potential (15.76 eV). As is the case in all of the heavier rare gases there is a resonance region between the ionization threshold and the first excited level of the ionic core (15.93 eV). Measurements in this energy range will be discussed in Section 1.3 as will the resonance regions near the inner subshell ionization potentials (26…30 eV, 245…255 eV and 3190…3220 eV).

In the energy range between 16 and 26 eV there have been a number of measurements of ionization cross sections. The recommended values of Samson [91Sa1]and the tabulation given by Marr and West [76Ma1] are given in Table 14 and are also shown in Fig. 4 along with data from Lee and Weissler [55Le1],Rustgi [64Ru1] and Carlson et al. [73Ca1]. The data of Carlson et al. was only presented in graphical form which means that a comparison to any better than 3 % is unwarranted. The figure shows that although there is good deal of scatter in the earlier data, there is essential agreement between the recommended data of Samson and the compilation of Marr and West to with about 3 %. Samson et al. [89Sa1] have made careful measurements of the rare gases with an expected accuracy of 1% at selected wavelengths. The results for argon at energies of 16.67,16.85 and 21.22 which form the basis of their recommended values are also shown in Fig. 4.

At energies above the resonance region between 30 and 100 eV the cross section drops rapidly to a minimum at approximately 48 eV and then rises to a maximum at approximately 70 eV. Data from various sources in this energy range are shown in Fig. 5. Owing to the rapid variation with energy the cross section is not known accurately to better than 10 % in this energy range. Values of the cross section obtained by various authors are shown in Table 15.

In the energy range between 100 and 240 eV data are shown in Table 16 from Marr and West [76Ma1], Lukirskii et al. [63Lu1], Watson [72Wa1], Henke [67He1] and Denne [70De1]. In general there is good agreement between the various data sets.

The available data in the energy range from 255 to 1000 eV is shown in Table 17. All of these measurements are of total attenuation and with the exception of the recent measurement by Yang et al. [87Ya1] and that of Wuilleumiur [69Wu1] were done using line sources. With the exception of a few points the agreement is better than 10 % over the entire energy range. At energies between 1 keV and the K ionization threshold the agreement between various sources is even better as is shown in Table 18. All of these measurements used line sources and all of the measurements were of total attenuation with the exception of the work of Woernle [30Wo1] who used a double ion chamber. The measurements of Wuilleumier [69Wu1] done at closely spaced energies are shown in Table 19 and are in good agreement with the line source data. The same type of data for energies above the K ionization threshold is shown in Tables 20 and 21. In general, there is agreement to better than 10 % in this energy range also.

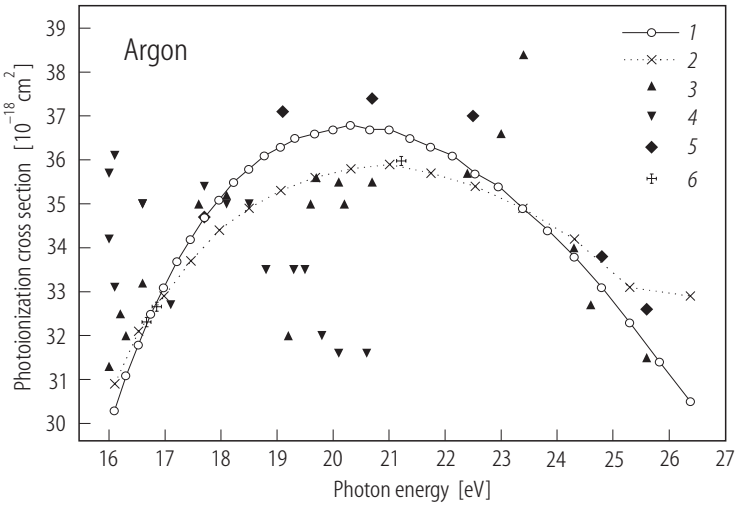

Fig. 4. Argon cross sections between 16 and 26 eV from various sources: *1* [76Ma1], *2* [91Sa1], *3* [64Ru1], *4* [55Le1], *5* [73Ca1], *6* [89Sa1].

Table 14. Photon attenuation cross sections for argon in the energy range between 16 and 26 eV.

Energy [eV]	Cross section [10^{-18} cm^2]			Energy [eV]	Cross section [10^{-18} cm^2]	
	76Ma1	91Sa1	89Sa1		76Ma1	91Sa1
16.10	30.3	30.9		19.68	36.6	35.6
16.67			32.3	20.00	36.7	35.7
16.31	31.1	31.7		20.32	36.8	35.8
16.53	31.8	32.1		20.66	36.7	35.9
16.75	32.5	32.5		21.01	36.7	35.9
16.85			32.7	21.38	36.5	35.8
16.98	33.1	32.9		21.75	36.3	35.7
17.22	33.7	33.3		22.14	36.1	35.6
17.46	34.2	33.7		22.54	35.7	35.4
17.71	34.7	34.1		22.96	35.4	35.2
17.97	35.1	34.4		23.39	34.9	34.9
18.23	35.5	34.6		23.84	34.4	34.4
18.50	35.8	34.9		24.31	33.8	34.2
18.78	36.1	35.1		24.80	33.1	33.7
19.07	36.3	35.3		25.30	32.3	33.1
19.37	36.5	35.5		25.83	31.4	32.6

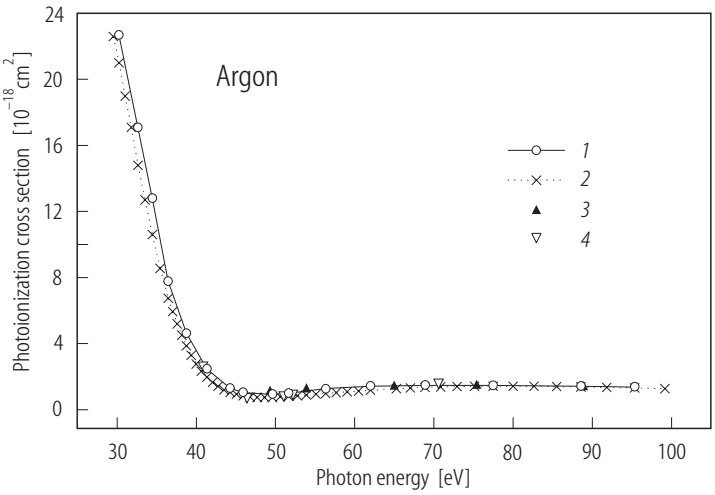

Fig. 5. Argon cross sections between 30 and 100 eV from various sources: *1* [76Ma1], *2* [63Lu1], *3* [91Sa1], *4* [64Al1].

Table 15. Photon attenuation cross sections for argon in the energy range between 30 and 100 eV.

Energy [eV]	Cross section [10^{-18} cm^2]				
	91Sa1	76Ma1	63Lu1	64Al1	72Wa1
30.24	21.0	22.7			
30.99	19.0	21.0			
31.79	17.1	19.1			
32.63	14.8	17.1			
34.44	10.6	12.8			
35.42	8.55	10.3			
36.46	6.75	7.77			
37.57	5.19	6.10			
38.15	4.51				
38.74	3.87	4.62			
39.99	2.77	3.41			
40.65	2.33				
40.80				2.6	
41.33	1.97	2.47			
42.03	1.66				
42.75	1.75	1.77			
43.50	1.20				
44.28	1.05	1.30			
45.08	0.94				
45.92	0.85	1.03			
46.40				0.7	
47.68	0.74	0.914			
48.62	0.74				
49.30			1.18		
49.59	0.75	0.916			
50.60	0.78				
51.00				0.8	
51.66	0.81	1.00			

Energy [eV]	Cross section [10^{-18} cm^2]				
	91Sa1	76Ma1	63Lu1	64Al1	72Wa1
52.20				0.9	
52.76	0.85				
53.90	0.89		1.32		
55.10	0.94				
56.35	0.99	1.28			
60.48	1.13				
61.99	1.18	1.42			
63.10					1.26
65.00			1.49		
65.25	1.27				
66.80					1.33
67.02	1.31				
68.88	1.35		1.48		
70.60				1.57	
70.70					1.38
70.85	1.38				
72.93	1.40				
74.90					1.40
75.14	1.41				
75.40			1.54		
77.49	1.42	1.47			
79.30					1.44
79.99	1.42				
82.65	1.41				
84.30					1.41
85.50	1.40				
85.56	1.38	1.41			
88.90			1.45		
91.84	1.35				
95.37	1.32	1.36			
95.50					1.33
99.18	1.28				

Table 16. Photon attenuation cross sections for argon in the energy range from 100 to 240 eV.

Energy [eV]	Cross section [10^{-18} cm^2]				
	72Wa1	63Lu1	67He1	70De1	76Ma1
101.7	1.262				
103.3					1.29
108.6	1.202				
108.9			1.293		
112.7					1.20
114.3		1.166			
116.3	1.105				

Energy [eV]	Cross section [10^{-18} cm^2]				
	72Wa1	63Lu1	67He1	70De1	76Ma1
124.0					1.10
124.5	1.049				
128.0	1.012				
130.5					1.05
133.5	0.938				
137.8					0.987
143.5	0.863				
145.9					0.923
147.2			0.842		
151.0				0.781	
151.2		0.736			
154.9	0.737				
155.0					0.856
165.3					0.785
166.9	0.666				
171.0		0.598			
171.7				0.660	
172.5	0.625				
177.1					0.709
180.8	0.584				
182.6			0.608		
183.4				0.592	
190.7					0.630
192.2		0.486			
192.6				0.543	
196.2	0.521				
217.2	0.443				
234.0		0.344			
236.9				0.360	

Table 17. Photon attenuation cross sections for argon in the energy range from 255 to 1000 eV. [1]) from [31De1], [2]) from [66Be1].

Energy [eV]	Cross section [10^{-18} cm^2]				
	87Ya1	63Lu1	67He1	69Wu1	Other
256.0		3.52			
267.0		3.10			
277.0					3.03 [1])
278.0			3.03		
282.0		2.70			
354.0		2.40			
391.4			2.00		
413.0		1.65			
442.0	1.53				
477.0	1.31				

Energy [eV]	Cross section [10^{-18} cm^2]				
	87Ya1	63Lu1	67He1	69Wu1	Other
496.0		1.08			
517.0	1.12				
526.0			1.06		
539.0	1.02				
564.0	0.933				
590.0	0.830				
620.0	0.737				
620.0		0.656			
651.0	0.668				
676.8			0.593		
687.0	0.580				
728.0	0.505				
773.0	0.432				
774.9			0.424		
824.0	0.365				
826.5		0.314			
852.0					0.305 [2])
865.0				0.324	
871.0				0.318	
877.0				0.312	
883.0	0.315				
884.0				0.305	
890.0				0.301	
896.0				0.295	
903.0				0.289	
910.0				0.284	
916.0				0.278	
923.0				0.272	
928.7			0.270		
930.0				0.267	0.268 [2])
937.0				0.262	
944.0				0.256	
950.0	0.262				
952.0				0.252	
959.0				0.246	
966.0	0.240				
974.0				0.236	
982.0				0.231	
990.0				0.226	
998.0				0.221	

Table 18. Photon attenuation cross sections for argon in the energy range between 1000 and 3190 eV. *) from [31Sp1].

Energy [eV]	Cross section [10^{-21} cm^2]				
	30Wo1	63Lu1	67He1	66Be1	75Lo1
1012.0				212.0	
1033.0		180.7			
1254.0	123.7		123.0	117.0	
1378.0		87.4			
1487.0	76.7		78.3	76.2	
1557.0				69.0	
1771.0		45.4			
1778.0	49.6				50.5 *)
2293.0	23.9			20.9	
2395.0	21.5				
2480.0		18.9			
2622.0					16.2
2838.0	13.4				
2839.0					12.9
2984.0	11.6			11.5	
2991.0					11.3 *)
3100.0		10.0			
3134.0	9.77				
3142.0					10.0 *)
3151.0	10.13				

Table 19. Photon attenuation cross sections for argon in the energy range from 1000 to 3190 eV from [69Wu1].

Energy [eV]	Cross section [10^{-21} cm^2]	Energy [eV]	Cross section [10^{-21} cm^2]	Energy [eV]	Cross section [10^{-21} cm^2]
1006.0	216.0	1167.0	146.0	1390.0	90.2
1014.0	211.0	1178.0	142.0	1406.0	87.0
1022.0	207.0	1190.0	138.0	1422.0	84.8
1031.0	202.0	1201.0	134.0	1438.0	82.1
1040.0	197.0	1213.0	131.0	1455.0	79.8
1048.0	192.0	1225.0	128.0	1473.0	77.1
1057.0	189.0	1237.0	124.0	1490.0	75.6
1066.0	185.0	1250.0	121.0	1509.0	73.3
1076.0	181.0	1262.0	118.0	1527.0	70.4
1085.0	177.0	1275.0	114.0	1546.0	68.3
1095.0	173.0	1289.0	111.0	1556.0	67.7
1104.0	168.0	1302.0	108.0	1566.0	67.1
1114.0	165.0	1316.0	105.0	1576.0	66.6
1125.0	161.0	1330.0	102.0	1586.0	64.4
1135.0	157.0	1345.0	99.7	1596.0	63.7
1145.0	153.0	1359.0	96.5	1607.0	63.3
1156.0	150.0	1374.0	93.1	1617.0	61.9

Energy [eV]	Cross section [10^{-21} cm^2]	Energy [eV]	Cross section [10^{-21} cm^2]	Energy [eV]	Cross section [10^{-21} cm^2]
1628.0	61.1	1933.0	36.9	2499.0	18.0
1638.0	60.3	1948.0	35.9	2525.0	17.5
1649.0	59.0	1964.0	34.8	2551.0	17.0
1660.0	57.0	1979.0	34.4	2577.0	16.6
1672.0	55.7	1995.0	33.4	2604.0	16.4
1683.0	55.1	2012.0	32.2	2632.0	16.3
1695.0	53.9	2028.0	31.3	2660.0	15.8
1706.0	52.7	2045.0	30.4	2689.0	15.4
1718.0	51.8	2062.0	29.5	2719.0	15.1
1730.0	50.8	2079.0	29.1	2749.0	14.5
1742.0	49.7	2097.0	28.8	2780.0	14.1
1755.0	49.0	2115.0	28.3	2812.0	13.7
1767.0	48.2	2133.0	27.0	2844.0	13.5
1780.0	47.2	2151.0	25.9	2877.0	13.1
1793.0	46.2	2170.0	24.8	2911.0	12.7
1806.0	44.4	2190.0	23.9	2945.0	12.1
1819.0	43.6	2209.0	23.4	2981.0	11.9
1833.0	41.9	2229.0	22.8	3017.0	11.4
1846.0	41.8	2249.0	22.5	3054.0	10.6
1860.0	40.3	2270.0	21.8	3093.0	10.3
1874.0	39.1	2291.0	21.2	3132.0	10.1
1889.0	38.1	2402.0	20.3	3172.0	10.0
1903.0	37.7	2450.0	19.6		
1918.0	37.4	2474.0	19.0		

Table 20. Photon attenuation cross sections for argon in the energy range from 3.25 to 10 keV from selected sources.

Energy [eV]	Cross section [10^{-21} cm^2]	Ref.	Energy [eV]	Cross section [10^{-21} cm^2]	Ref.
3336.0	87.560	31Sp1	6404.0	18.200	66Be1
3444.0	80.260	30Wo1	6925.0	11.690	75Lo1
3444.0	97.400	66Be1	7472.0	9.518	74Mi1
3662.0	67.990	30Wo1	8000.0	8.16	62Bu1
4089.0	48.050	75Lo1	8041.0	7.462	32Cr1
4508.0	37.000	70Mc2	8041.0	7.811	74Mi1
4508.0	37.210	74Mi1	8048.0	7.830	66Be1
5411.0	24.200	66Be1	8060.0	7.500	30Co1
5411.0	23.340	74Mi1	8067.0	7.429	31Sp1
5412.0	22.890	75Lo1	8631.0	6.353	74Mi1
5414.0	23.480	30Wo1	8631.0	6.324	75Lo1
5414.0	28.000	66Be1	8930.0	5.640	30Co1
5420.0	22.330	30Co1	9000.0	5.57	62Bu1
5428.0	22.820	31Sp1	9243.0	5.290	70Mc2
5895.0	18.200	70Mc2	9876.0	4.341	74Mi1
5946.0	18.700	30Co1	10000.0	4.18	62Bu1
6400.0	14.700	74Mi1			

Table 21. Photon attenuation cross sections for argon in the energy range from 3.25 to 8.5 keV from [69Wu1].

Energy [eV]	Cross section [10^{-21} cm^2]	Energy [eV]	Cross section [10^{-21} cm^2]
3255.0	91.0	4758.0	33.8
3299.0	88.9	4851.0	31.8
3343.0	85.9	4948.0	29.7
3389.0	83.7	5049.0	28.7
3436.0	79.1	5154.0	27.1
3485.0	77.3	5264.0	24.8
3534.0	74.2	5378.0	24.0
3586.0	72.2	5498.0	23.0
3638.0	69.6	5623.0	21.2
3693.0	66.9	5754.0	20.0
3749.0	64.5	5891.0	19.2
3806.0	62.2	6034.0	17.1
3866.0	58.2	6185.0	16.5
3927.0	55.1	6344.0	15.6
3990.0	53.9	6511.0	14.7
4056.0	52.4	6687.0	13.7
4124.0	48.8	6872.0	12.8
4193.0	45.6	7069.0	11.9
4266.0	43.9	7277.0	10.8
4340.0	42.4	7497.0	9.88
4418.0	40.9	7732.0	8.95
4498.0	39.3	7981.0	8.16
4582.0	37.1	8247.0	7.36
4668.0	36.2		

1.2.6 Cross sections for krypton (Z = 36)

There is a resonance range in krypton between the ionization potential (14.00 eV) and 14.7 eV and another one between 25 and 30 eV. The cross section in the range from 15 to 25 eV is shown in Fig. 6. The two curves show the recommended values of Marr and West [76Ma1] and Samson [91Sa1]. Earlier results of Pery-Thorne and Garton [60Pe1] and Rustgi et al. [64Ru2] show a good deal of scatter but the recommended values have the same general shape with the values of Samson being approximately 6 % higher than those of Marr and West. Their results are shown in tabular form in Table 22 along with the highly accurate values of Samson et al. [89Sa1] at three selected wavelengths.

The same is true in the energy range between 30 and 90 eV as shown in Fig. 7. The discrepancy is about 15 % at the minimum of the cross section. Both sets are much lower than the measured values of Lang and Watson [75La1]. All of these results are given in Table 23.

Between 100 and 200 eV there have been a number of measurements made in addition to the recommended values of Marr and West as shown in Fig. 8 and in Table 24. The earlier results of Lukirskii et al. [64Lu1] seem to scatter and those of Haensel et al. [69Ha2] seem too low at 150 eV. There is good agreement between the recommended values of Marr and West and the data of Henke [67He1] but the values of Lang et al. [75La1] are higher as they are at lower energies. In view of the

disagreement between these sources one must conclude that the cross section in this energy range is not known to better than 10 %.

In the energy range between 300 and 800 eV there are only a few measurements as shown in Table 25. The values of Henke in this energy range are probably the most reliable since they agree with the tabulation of Marr and West at lower energies and with the data of Wuilleumier [69Wu1] at higher energies as shown in Table 25.

The energy range between 1.6 and 2.0 keV contains the L edges and will be treated in Section 1.3. In the energy range from 2 to 10 keV the only measurements are those of Wuilleumier [69Wu1] and those of McCrary et al. [70Mc2]. Their data are shown in Table 26 and the agreement is excellent.

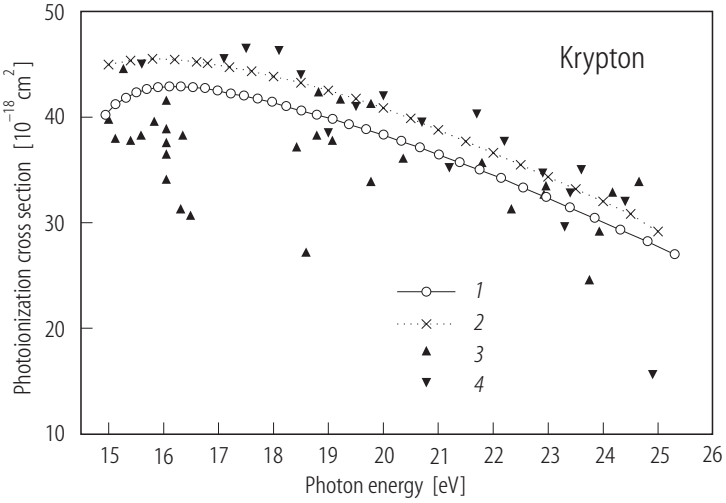

Fig. 6. Krypton cross sections from 15 to 26 eV from various sources: *1* [76Ma1], *2* [91Sa1], *3* [60Pe1], *4* [64Ru2].

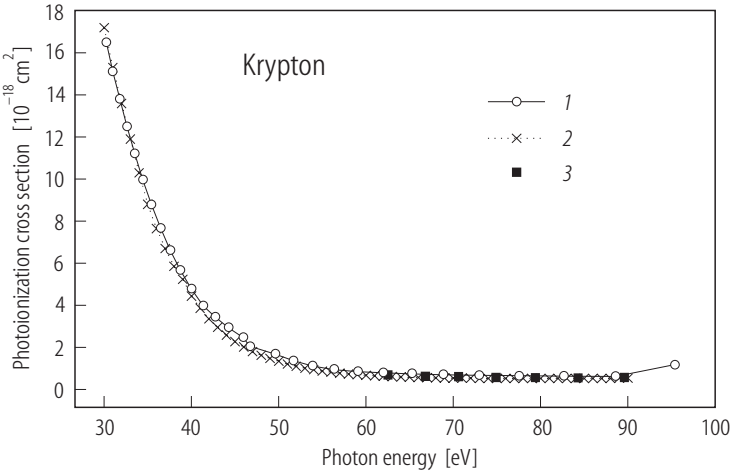

Fig. 7. Krypton cross sections from 30 and 90 eV from various sources: *1* [76Ma1], *2* [91Sa1], *3* [75La1].

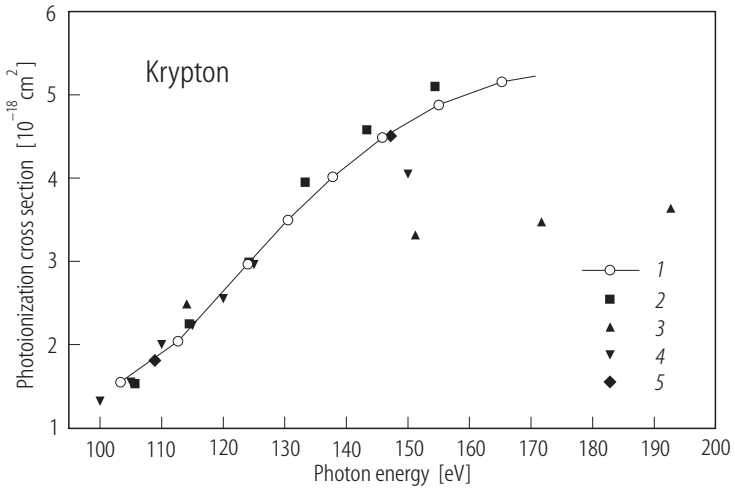

Fig. 8. Krypton cross sections from 100 to 200 eV from various sources: *1* [76Ma1], *2* [75La1], *3* [64Lu1], *4* [69Ha2], *5* [67He1].

Table 22. Photon attenuation cross sections for krypton in the energy range between 15 and 25 eV.

Energy [eV]	Cross section [10^{-18} cm^2]			Energy [eV]	Cross section [10^{-18} cm^2]		
	76Ma1	91Sa1	89Sa1		76Ma1	91Sa1	89Sa1
15.0		44.96		18.78	40.2		
15.12	41.2			19.0		42.53	
15.31	41.8			19.07	39.8		
15.4		45.34		19.37	39.3		
15.50	42.3			19.5		41.74	
15.69	42.6			19.68	38.8		
15.8		45.50		20.00	38.3	40.85	
15.89	42.8			20.32	37.7		
16.1	42.9			20.5		39.86	
16.2		45.44		20.66	37.1		
16.31	42.9			21.00	36.4	38.78	
16.40		45.36		21.22			38.31
16.53	42.8			21.38	35.7		
16.60		45.23		21.50		37.70	
16.67			44.90	21.75	35.0		
16.75	42.7			22.00		36.60	
16.80		45.08		22.14	34.2		
16.85			44.87	22.50		35.48	
16.98	42.5			22.54	33.3		
17.00		44.92		22.96	32.4		
17.20		44.73		23.00		34.34	
17.22	42.2			23.39	31.4		
17.40		44.54		23.50		33.19	
17.46	42.0			23.84	30.4		
17.60		44.34		24.00		32.02	
17.71	41.7			24.31	29.3		
17.80		44.12		24.50		30.82	
17.97	41.4			24.80	28.2		
18.00		43.84		25.00		29.15	
18.23	41.0			25.30	27.0		
18.50	40.6	43.25					

Table 23. Photon attenuation cross section of krypton in the energy range from 30 to 90 eV.

Energy [eV]	Cross section [10^{-18} cm^2]			Energy [eV]	Cross section [10^{-18} cm^2]		
	76Ma1	91Sa1	75La1		76Ma1	91Sa1	75La1
30.00		17.2		59.00		0.703	
30.24	16.5			59.04	0.838		
31.00	15.1	15.3		60.00		0.674	
31.79	13.8			61.00		0.650	
32.00		13.6		62.00	0.789	0.628	
32.63	12.5			62.50			0.692
33.00		11.9		63.00		0.610	
33.51	11.2			64.00		0.595	
34.00		10.3		65.00		0.582	
34.44	9.96			65.25	0.737		
35.00		8.80		66.00		0.570	
35.42	8.78			66.80			0.618
36.00		7.64		67.00		0.560	
36.46	7.67			68.00		0.552	
37.00		6.70		68.88	0.697		
37.57	6.62			69.00		0.544	
38.00		5.85		70.00		0.537	
38.74	5.66			70.60			0.610
39.00		5.24		71.00		0.534	
40.00	4.78	4.43		72.00		0.530	
41.00		3.86		72.93	0.671		
41.33	3.98			73.00		0.527	
42.00		3.36		74.00		0.525	
42.75	3.43			74.90			0.573
43.00		2.95		75.00		0.524	
44.00		2.58		76.00		0.523	
44.28	2.93			77.00		0.522	
45.00		2.28		77.49	0.652		
45.92	2.47			78.00		0.521	
46.00		2.02		79.00		0.520	
46.68	2.05			79.40			0.558
47.00		1.80		80.00		0.519	
48.00		1.62		81.00		0.518	
49.00		1.47		82.00		0.518	
49.59	1.68			82.65	0.633		
50.00		1.34		83.00		0.518	
51.00		1.21		84.00		0.519	
51.66	1.36			84.30			0.551
52.00		1.10		85.00		0.520	
53.00		1.01		86.00		0.522	
53.90	1.11			87.00		0.523	
54.00		0.934		88.00		0.525	
55.00		0.865		88.56	0.607		
56.00		0.817		89.00		0.528	
56.35	0.943			89.60			0.577
57.00		0.773		90.00		0.530	
58.00		0.735					

Table 24. Photon attenuation cross section for krypton in the energy range between 100 and 200 eV.

Energy [eV]	Cross section [10^{-18} cm^2]				
	76Ma1	75La1	69Ha2	67He1	64Lu1
100.0			1.32		
101.6		1.35			
103.3	1.55				
105.0			1.55		
105.7		1.53			
108.9				1.81	
110.0			2.00		
112.7	2.04				
114.1					2.49
114.5		2.25			
115.0			2.23		
120.0			2.55		
124.0	2.97				
124.2		2.99			
125.0			2.96		
130.5	3.50				
133.3		3.95			
137.8	4.01				
143.3		4.58			
145.9	4.49				
147.2				4.51	
150.0			4.05		
151.2					3.32
154.4		5.10			
155.0	4.88				
165.3	5.16				
171.7					3.47
177.1	5.31				
180.2		5.21			
182.6				4.98	
190.7	5.31				
192.7					3.64
195.6		5.32			

Table 25. Photon attenuation cross sections for krypton in the energy range between 300 and 1600 eV.

Energy [eV]	Cross section [10^{-18} cm^2]			
	67He1	69Ha2	64Lu1	76Ma1
300.0		3.90		
310.0				3.41
391.0	2.99			
394.0			2.00	
400.0	2.60			
525.0			1.32	
526.0	1.71			
677.0	1.01			
775.0	0.76			

Energy [eV]	Cross section [10^{-18} cm^2]		Energy [eV]	Cross section [10^{-18} cm^2]	
	69Wu1	67He1		69Wu1	67He1
825.0	0.666		1014.0	0.395	
830.0	0.650		1022.0	0.387	
836.0	0.640		1031.0	0.379	
842.0	0.631		1040.0	0.370	
847.0	0.623		1048.0	0.362	
853.0	0.610		1057.0	0.354	
859.0	0.600		1066.0	0.346	
865.0	0.589		1076.0	0.339	
871.0	0.579		1085.0	0.331	
877.0	0.568		1095.0	0.323	
884.0	0.557		1104.0	0.317	
890.0	0.550		1114.0	0.309	
896.0	0.538		1125.0	0.302	
903.0	0.527		1135.0	0.296	
910.0	0.518		1145.0	0.289	
916.0	0.508		1156.0	0.281	
923.0	0.498		1167.0	0.275	
928.0		0.494	1178.0	0.268	
930.0	0.491		1190.0	0.262	
937.0	0.484		1201.0	0.257	
944.0	0.474		1213.0	0.250	
952.0	0.463		1225.0	0.243	
959.0	0.454		1237.0	0.237	
966.0	0.444		1250.0	0.232	
974.0	0.436		1254.0		0.238
982.0	0.428		1262.0	0.226	
990.0	0.419		1275.0	0.220	
998.0	0.411		1289.0	0.215	
1006.0	0.402		1302.0	0.210	

Energy [eV]	Cross section [10^{-18} cm^2]		Energy [eV]	Cross section [10^{-18} cm^2]	
	69Wu1	67He01		69Wu1	67He01
1316.0	0.204		1487.0		0.152
1330.0	0.196		1490.0	0.148	
1345.0	0.193		1509.0	0.144	
1359.0	0.184		1527.0	0.140	
1374.0	0.182		1546.0	0.135	
1390.0	0.177		1556.0	0.133	
1406.0	0.172		1566.0	0.131	
1422.0	0.167		1576.0	0.129	
1438.0	0.162		1586.0	0.127	
1455.0	0.157		1596.0	0.125	
1473.0	0.152				

Table 26. Photon attenuation cross sections for krypton in the energy range between 1,600 and 10,000 eV from [69Wu1], *) values are from [70Mc2].

Energy [eV]	Cross section [10^{-21} cm^2]	Energy [eV]	Cross section [10^{-21} cm^2]	Energy [eV]	Cross section [10^{-21} cm^2]
1607.0	123.0	1925.0	582.0	2474.0	314.0
1617.0	121.0	1933.0	576.0	2499.0	306.0
1628.0	118.0	1948.0	565.0	2525.0	298.0
1638.0	116.0	1964.0	554.0	2551.0	289.0
1649.0	114.0	1979.0	543.0	2577.0	280.0
1660.0	113.0	1995.0	534.0	2604.0	274.0
1672.0	111.0	2012.0	522.0	2632.0	266.0
1680.0	462.0	2028.0	513.0	2660.0	259.0
1683.0	456.0	2045.0	504.0	2689.0	251.0
1695.0	483.0	2062.0	494.0	2719.0	243.0
1706.0	441.0	2079.0	484.0	2749.0	236.0
1718.0	433.0	2097.0	475.0	2780.0	229.0
1723.0	431.0	2115.0	465.0	2812.0	222.0
1732.0	623.0	2133.0	455.0	2844.0	215.0
1742.0	613.0	2151.0	447.0	2877.0	208.0
1755.0	603.0	2170.0	437.0	2911.0	202.0
1767.0	592.0	2190.0	429.0	2945.0	196.0
1780.0	582.0	2209.0	419.0	2981.0	189.0
1793.0	573.0	2229.0	410.0	3017.0	182.0
1806.0	564.0	2249.0	401.0	3054.0	177.0
1819.0	556.0	2270.0	391.0	3093.0	172.0
1833.0	548.0	2291.0	383.0	3132.0	166.0
1846.0	540.0	2312.0	373.0	3172.0	160.0
1860.0	533.0	2334.0	363.0	3213.0	155.0
1874.0	526.0	2356.0	356.0	3255.0	149.0
1889.0	520.0	2379.0	348.0	3299.0	144.0
1903.0	515.0	2402.0	339.0	3343.0	139.0
1917.0	507.0	2426.0	330.0	3389.0	134.0
1918.0	508.0	2450.0	323.0	3436.0	130.0

Energy [eV]	Cross section [10^{-21} cm^2]	Energy [eV]	Cross section [10^{-21} cm^2]	Energy [eV]	Cross section [10^{-21} cm^2]
3485.0	126.0	4418.0	69.7	5891.0	32.8
3534.0	121.0	4498.0	66.4	5895.0	31.6 *)
3586.0	117.0	4508.0	64.8 *)	6034.0	30.5
3638.0	113.0	4582.0	63.2	6185.0	28.1
3693.0	109.0	4668.0	60.5	6344.0	26.2
3749.0	106.0	4758.0	57.2	6511.0	24.6
3806.0	103.0	4851.0	54.5	6687.0	22.8
3866.0	99.1	4948.0	51.8	6872.0	21.3
3927.0	94.9	5049.0	49.3	7069.0	19.8
3990.0	90.9	5154.0	46.6	7277.0	17.8
4056.0	87.4	5264.0	44.0	7497.0	16.8
4124.0	83.5	5378.0	41.5	7732.0	15.3
4193.0	79.9	5498.0	39.2	7981.0	14.2
4266.0	76.2	5623.0	36.6	8247.0	13.5
4340.0	72.8	5754.0	34.6	9243.0	9.1 *)

1.2.7 Cross sections for xenon (Z = 54)

Xenon has resonance regions similar to those in krypton below 14 eV and in the energy range between 20 and 25 eV. Recommended values of the cross sections have been given by West and Morton [78We1] and by Samson [91Sa1] and are shown in Table 27 for the energy range between 14 and 20 eV and are shown along with earlier data by Rustgi et al. [64Ru2] in Fig. 9. As in krypton, the data of Rustgi et al. is scattered but there is good agreement between the two recommended data sets. As in krypton, the two highly accurate data points measured by Samson et al. [89Sa1] are also shown. The cross section is known in this energy range to better than 3 %.

Between 25 and 60 eV the cross section decreases rapidly as shown in Fig. 10. which gives data from the same sources as Fig. 9. As in Fig. 9, the data of Rustgi et al. is scattered, but there is good agreement between the two recommended data sets at the lower energies. At higher energies where the cross section is low Samson's results are 10…15 % lower than those of West and Morton as is shown in Table 28.

The cross section goes through a maximum at 100 eV and there have been a number of measurements of the cross section in the energy range between 70 and 140 eV as shown in Fig. 11. Data from a variety of sources is shown in Fig. 11 and tabulated in Table 29. There is good agreement between the recommended values of West and Morton and of Samson over the entire energy range.

There have also been a number of measurements in the energy range between 140 and 680 eV as shown in Fig. 12 and listed in Table 30. There is much better agreement between the various sets for energies up to about 300 eV. At higher energies there is moderately good agreement between the results of Henke [67He1] and Lukirskii [66Lu1].

The results of Wuilleumier [69Wu1] between 955 eV and 4770 eV are shown in Table 31. These data agree extremely well with the results made at various energies using line source sources. Data are also shown for Xenon in the energy range above the L thresholds from 5500 eV to 8247 eV [69Wu1] along with a single measurement made at 9243 eV [70Mc2] in Table 32.

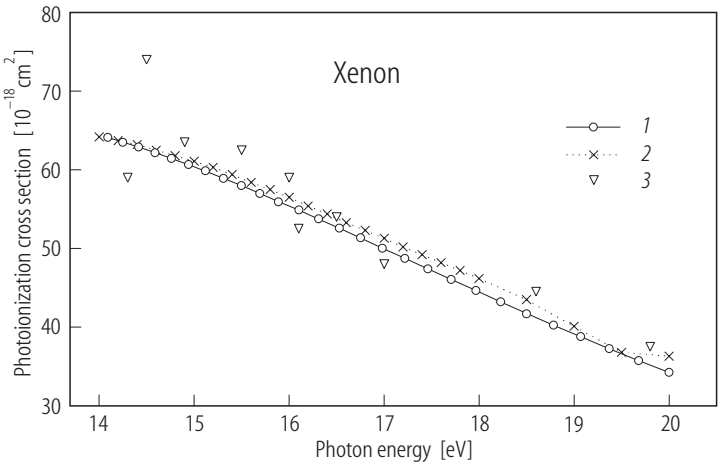

Fig. 9. Cross sections for xenon from 14 to 20 eV from various sources: *1* [78We1], *2* [91Sa1], *3* [64Ru2].

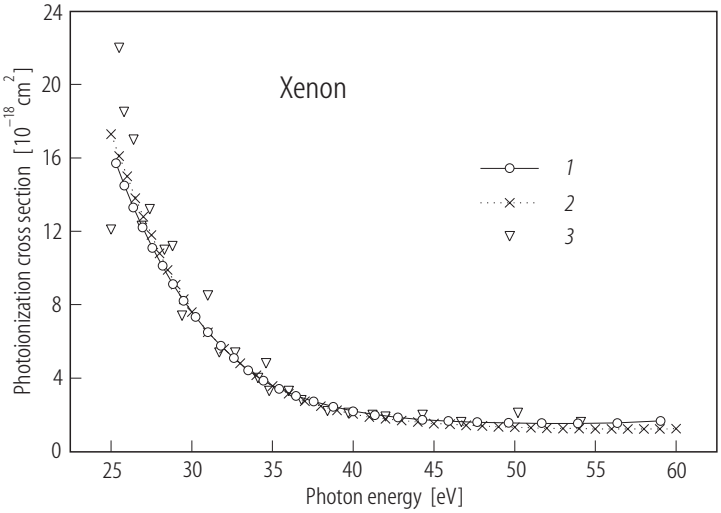

Fig. 10. Cross sections for xenon from 25 to 60 eV from various sources: *1* [78We1], *2* [91Sa1], *3* [64Ru2].

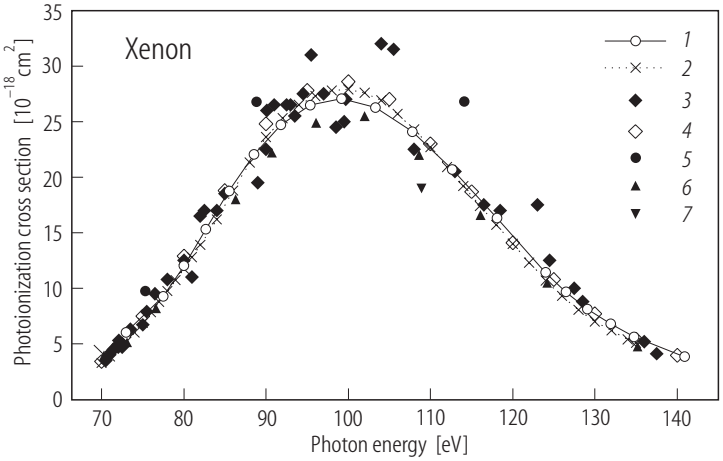

Fig. 11. Cross sections for xenon from 70 to 140 eV from various sources: *1* [78We1], *2* [91Sa1], *3* [64Ed1], *4* [69Ha2], *5* [64Lu1], *6* [75La1], *7* [67He1].

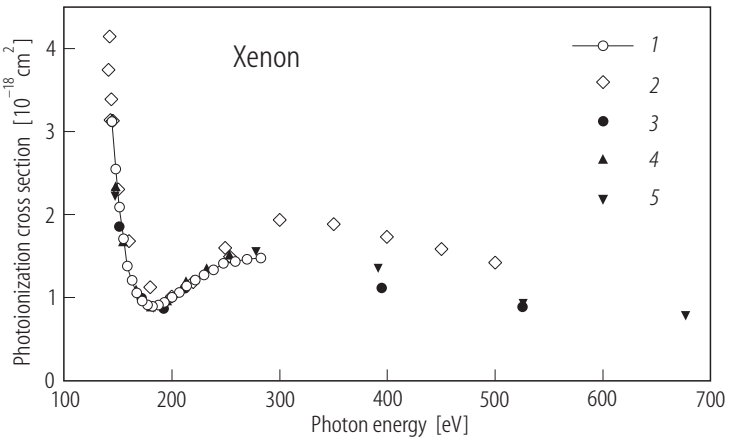

Fig. 12. Cross sections for xenon from 140 to 680 eV from various sources: *1* [78We1], *2* [69Ma2], *3* [66Lu1], *4* [64Lu1], *5* [67He1].

Table 27. Photon attenuation cross sections for xenon in the energy range from 14 to 20 eV.

Energy [eV]	Cross section [10^{-18} cm^2]			Energy [eV]	Cross section [10^{-18} cm^2]		
	78We1	91Sa1	89Sa1		78We1	91Sa1	89Sa1
14.00		64.2		16.53	52.55		
14.09	64.13			16.60		53.3	
14.20		63.7		16.67			52.65
14.25	63.53			16.75	51.32		
14.40		63.2		16.80		52.3	
14.42	62.88			16.85			51.88
14.59	62.19			16.98	50.05		
14.60		62.5		17.00		51.3	
14.76	61.45			17.20		50.2	
14.80		61.8		17.22	48.75		
14.94	60.67			17.40		49.2	
15.00		61.1		17.46	47.4		
15.12	59.83			17.60		48.2	
15.20		60.3		17.71	46.03		
15.31	58.94			17.80		47.2	
15.40		59.4		17.97	44.62		
15.50	58.00			18.00		46.2	
16.60		56.5		18.23	43.19		
15.69	57.01			18.50	41.73	43.5	
15.80		57.5		18.78	40.25		
15.89	55.96			19.00		40.1	
16.00		56.5		19.07	38.76		
16.10	54.87			19.37	37.26		
16.20		55.4		19.50		38.6	
16.31	53.74			19.68	35.75		
16.40		54.4		20.00	34.23	36.3	

Table 28. Photon attenuation cross section for xenon in the energy range from 25 to 60 eV.

Energy [eV]	Cross section [10^{-18} cm^2]		Energy [eV]	Cross section [10^{-18} cm^2]	
	78We1	91Sa1		78We1	91Sa1
25.00		17.3	38.00		2.47
25.30	15.72		38.74	2.44	
25.50		16.1	39.00		2.24
25.83	14.51		40.00	2.21	2.04
26.00		15.0	41.00		1.88
26.38	13.33		41.33	2.00	
26.50		13.8	42.00		1.77
26.95	12.21		42.75	1.86	
27.00		12.8	43.00		1.68
27.50		11.8	44.00		1.60
27.55	11.13		44.28	1.73	
28.00		10.8	45.00		1.52
28.18	10.10		45.92	1.66	
28.50		9.90	46.00		1.48
28.83	9.12		47.00		1.43
29.00		9.10	47.68	1.59	
29.50		8.30	48.00		1.39
29.52	8.20		49.00		1.35
30.00		7.60	49.59	1.56	
30.24	7.33		50.00		1.32
31.00	6.52	6.50	51.00		1.29
31.79	5.76		51.66	1.52	
32.00		5.60	52.00		1.26
32.63	5.06		53.00		1.25
33.00		4.80	53.90	1.52	
33.51	4.43		54.00		1.24
34.00		4.15	55.00		1.23
34.44	3.85		56.00		1.23
35.00		3.56	56.35	1.55	
35.42	3.41		57.00		1.23
36.00		3.11	58.00		1.23
36.46	3.04		59.00		1.23
37.00		2.74	59.04	1.67	
37.57	2.73		60.00		1.24

Table 29. Photon attenuation cross sections for xenon in the energy range from 70 to 140 eV. [1]) [64Lu1], [2]) [67He1].

Energy [eV]	Cross section [10^{-18} cm^2]					
	78We1	91Sa1	75La1	69Ha2	64Ed1	Other
68.88	3.89					
70.00		3.29			3.4	
70.30	3.95					
70.50					3.5	
71.00		3.86			4.0	
71.20					4.3	
71.40					4.5	
72.00		4.46			4.7	
72.00					4.9	
72.10					5.3	
72.50					4.7	
72.50					5.0	
72.93	6.01					
73.00		5.20				
73.10			5.14			
73.50					6.3	
74.00		6.00				
75.00		6.88		7.5	6.7	
75.32						9.74 [1])
75.50					7.9	
76.00		7.83				
76.50					9.5	
76.60			8.19			
77.00		8.78				
77.49	9.27					
78.00		9.74			10.8	
80.00	11.97	11.75		12.9	12.5	
81.00		12.78			11.0	
82.00		13.9			16.5	
82.50					17.0	
82.65	15.27					
83.00		15.0				
84.00		16.2			17.0	
85.00		17.5		18.8	18.5	
85.50	18.75					
86.00		18.8				
86.30			18.0			
87.00		20.1				
88.00		21.3				
88.56	22.04					
88.88						26.81 [1])
89.00		22.5			19.5	
90.00		23.6		24.8	22.5	
90.10					26.0	
90.70			22.2			

Energy [eV]	Cross section [10^{-18} cm^2]					
	78We1	91Sa1	75La1	69Ha2	64Ed1	Other
91.00		24.5			26.5	
91.84	24.7					
92.00		25.3				
92.50					26.5	
93.00		25.9			26.5	
93.50					25.5	
94.00		26.5				
94.50					27.5	
95.00		27.0		27.8		
95.37	26.5					
95.50					31.0	
96.00		27.3				
96.10			24.9			
97.00		27.6			27.5	
98.00		27.8				
98.50					24.5	
99.00		27.9				
99.18	27.1					
99.50					25.0	
99.70	27.0					
100.00		27.9		28.6		
101.00		27.8				
102.00		27.6	25.5			
103.30	26.3	27.3				
104.00		26.9			32.0	
105.00		26.4		27.0		
105.50					31.5	
106.00		25.7				
107.00		25.1				
107.80	24.1					
108.00		24.3			22.5	
108.60			22.0			
108.90						18.97 [2])
109.00		23.5				
110.00		22.7		23.0		
111.00		21.8				
112.00		20.9				
112.70	20.7					
113.00		20.0			20.5	
114.00		19.2				
114.10						26.81 [1])
115.00		18.3	18.7			
116.00		17.4				
116.10			16.6			
116.50					17.5	
117.00		16.5				
118.00		15.7				
118.10	16.3					
118.50					17.0	

Energy [eV]	Cross section [10^{-18} cm^2]					
	78We1	91Sa1	75La1	69Ha2	64Ed1	Other
119.00		14.8				
120.00		14.0		14.1		
121.00		13.2				
122.00		12.3				
123.00		11.5			17.5	
124.00	11.4	10.7				
124.20			10.5			
124.50					12.5	
125.00		10.0		10.8		
126.00		9.30				
126.50	9.64					
127.00		8.65				
127.50					10.0	
128.00		8.05				
128.50					8.8	
129.00		7.50				
129.10	8.11					
130.00		7.00		7.7		
131.00		6.60				
131.90	6.78					
132.00		6.20				
133.00		5.80				
134.00		5.40				
134.80	5.64					
135.00		5.10		5.4		
135.20			4.76			
136.00					5.2	
137.50					4.1	
140.00				3.96		

Table 30. Photon attenuation cross sections for xenon in the energy range from 140 to 680 eV. [1]) from [64Ed1], [2]) from [31De1], [3]) from [69De1].

Energy [eV]	Cross section [10^{-18} cm^2]				
	78We1	75La1	69Ha2	64Lu1, 66Lu1	67He1
140.9	3.82				
141.0			3.8		
141.8			4.2		
143.0			3.2		
143.7			3.4		
144.2	3.13				
145.0			3.2		
145.5					2.9 [1])
147.2					2.2

Energy [eV]	Cross section [10^{-18} cm^2]				
	78We1	75La1	69Ha2	64Lu1, 66Lu1	67He1
147.6	2.55	2.32			
149.0					2.6 [1])
150.0			2.3		
151.2	2.08			1.86	
154.0					2.3 [1])
154.4		1.66			
155.0	1.71				
158.9	1.42				
160.0			1.7		
163.1	1.21				
166.6		1.08			
167.5	1.06				
171.7				1.00	
172.2	0.96				
177.2	0.91				
180.0			1.1		
180.2		0.88			
182.3	0.89				
182.6					0.87
187.8	0.91				
192.7				0.87	
193.7	0.94				
195.6		0.95			
200.0	1.00		1.0		
206.6	1.06				
211.9				1.12	
213.0		1.18			
213.8	1.13				
220.0			1.2		
221.4	1.20				
229.6	1.27				
232.0		1.34			
238.4	1.33				
248.0	1.39				
250.0			1.6		
254.0		1.49			
258.3	1.43				
269.5	1.46				
278.0					1.56
278.0				1.38	1.47 [2])
281.8	1.48				
300.0			1.9		
350.0			1.9		
391.4					1.35
394.8				1.12	
395.0				1.32	
400.0			1.7		
450.0			1.6		

Energy [eV]	Cross section [10^{-18} cm^2]				
	78We1	75La1	69Ha2	64Lu1, 66Lu1	67He1
453.0				1.17	
500.0			1.4		
525.0				0.89	
526.0					0.93
557.0				0.65	
572.0				0.97	
637.0				0.65	
672.0	0.70 [3])				
675.0	0.80 [3])				
676.8					0.78
678.0	0.85 [3])				
680.0	1.00 [3])				

Table 31. Photon attenuation cross sections for xenon in the energy range from 950 to 4,750 eV. from [69Wu1], [1]) from [67He1], [2]) from [66Lu1], [3]) from [70Mc2].

Energy [eV]	Cross section [10^{-18} cm^2]	Energy [eV]	Cross section [10^{-18} cm^2]	Energy [eV]	Cross section [10^{-18} cm^2]
952.00	1.820	1190.00	1.330	1527.00	0.830
955.00	1.810	1201.00	1.310	1546.00	0.809
959.00	1.790	1213.00	1.290	1556.00	0.798
966.00	1.770	1225.00	1.270	1566.00	0.786
974.00	1.740	1237.00	1.250	1576.00	0.775
982.00	1.730	1250.00	1.220	1586.00	0.764
990.00	1.720	1254.00	1.35 [1])	1596.00	0.754
998.00	1.700	1254.00	1.17 [2])	1607.00	0.742
1006.00	1.680	1262.00	1.200	1617.00	0.732
1014.00	1.670	1275.00	1.180	1628.00	0.720
1022.00	1.650	1289.00	1.160	1638.00	0.710
1031.00	1.640	1302.00	1.130	1649.00	0.698
1040.00	1.620	1316.00	1.110	1660.00	0.691
1048.00	1.600	1330.00	1.090	1672.00	0.680
1057.00	1.590	1345.00	1.070	1683.00	0.670
1066.00	1.570	1359.00	1.050	1695.00	0.658
1076.00	1.560	1374.00	1.030	1706.00	0.646
1085.00	1.540	1390.00	1.040	1718.00	0.637
1095.00	1.520	1406.00	0.983	1730.00	0.628
1104.00	1.500	1422.00	0.962	1742.00	0.618
1114.00	1.480	1438.00	0.938	1755.00	0.607
1125.00	1.460	1455.00	0.917	1767.00	0.596
1135.00	1.440	1473.00	0.897	1776.00	0.600 [2])
1145.00	1.420	1487.00	0.98 [1])	1780.00	0.588
1156.00	1.400	1487.00	0.83 [2])	1793.00	0.577
1167.00	1.380	1490.00	0.873	1806.00	0.563
1178.00	1.360	1509.00	0.853	1819.00	0.554

Energy [eV]	Cross section [10^{-18} cm^2]	Energy [eV]	Cross section [10^{-18} cm^2]	Energy [eV]	Cross section [10^{-18} cm^2]
1833.00	0.546	2312.00	0.306	3132.00	0.147
1846.00	0.535	2334.00	0.300	3172.00	0.142
1860.00	0.523	2356.00	0.293	3213.00	0.138
1874.00	0.515	2379.00	0.286	3255.00	0.133
1889.00	0.506	2402.00	0.279	3299.00	0.128
1903.00	0.497	2426.00	0.274	3343.00	0.124
1918.00	0.488	2450.00	0.267	3389.00	0.119
1933.00	0.476	2474.00	0.258	3436.00	0.115
1948.00	0.468	2499.00	0.255	3485.00	0.111
1964.00	0.457	2525.00	0.249	3534.00	0.107
1979.00	0.448	2551.00	0.244	3586.00	0.103
1995.00	0.438	2577.00	0.239	3638.00	0.099
2012.00	0.429	2604.00	0.230	3693.00	0.095
2028.00	0.420	2632.00	0.226	3749.00	0.092
2045.00	0.411	2660.00	0.220	3806.00	0.088
2062.00	0.404	2689.00	0.216	3866.00	0.085
2079.00	0.394	2719.00	0.209	3927.00	0.081
2097.00	0.386	2749.00	0.203	3990.00	0.078
2115.00	0.379	2780.00	0.199	4056.00	0.075
2133.00	0.372	2812.00	0.193	4124.00	0.072
2151.00	0.365	2844.00	0.188	4193.00	0.068
2170.00	0.356	2877.00	0.184	4266.00	0.066
2190.00	0.349	2911.00	0.177	4340.00	0.064
2209.00	0.340	2945.00	0.172	4418.00	0.060
2229.00	0.333	2981.00	0.167	4498.00	0.058
2249.00	0.328	3017.00	0.163	4508.00	0.061 [3])
2270.00	0.321	3054.00	0.157	4582.00	0.056
2291.00	0.313	3093.00	0.151	4668.00	0.053

Table 32. Photon attenuation cross sections for xenon in the energy range between 4,850 and 10,000 eV. From [69Wu1]. *) from [70Mc2].

Energy [eV]	Cross section [10^{-18} cm^2]	Energy [eV]	Cross section [10^{-18} cm^2]	Energy [eV]	Cross section [10^{-18} cm^2]
4758.0	0.051	5378.0	0.158	6511.0	0.113
4791.0	0.144	5442.0	0.154	6687.0	0.105
4794.0	0.140	5461.0	0.182	6872.0	0.097
4851.0	0.138	5473.0	0.181	7069.0	0.090
4948.0	0.136	5498.0	0.178	7277.0	0.083
5049.0	0.134	5623.0	0.166	7497.0	0.077
5090.0	0.131	5754.0	0.156	7732.0	0.071
5114.0	0.179	5891.0	0.147	7981.0	0.065
5154.0	0.173	6034.0	0.138	8247.0	0.060
5208.0	0.169	6185.0	0.129	9243.0	0.046 *)
5264.0	0.160	6344.0	0.121		

1.2.8 Cross sections for atomic oxygen and nitrogen (Z = 8, 7)

Because they are important components of the earth's atmosphere the cross sections for absorption and ionization of both atomic and molecular oxygen and nitrogen have been the subject of numerous experimental and theoretical investigations and a recent compilation of data from both experimental and theoretical sources is available [92Fe1]. Here we list only the experimental data for the absolute photoionization cross sections of atomic oxygen and nitrogen in those energy ranges where there are no resonances. In these ranges the cross sections are expected to be smoothly varying functions of the energy. For atomic oxygen absolute measurements were made by Samson and Pareek [85Sa1] and van der Meer el al. [88Me1]. These measurements at 21.22 eV differed by about 40 % and it has been pointed out via a sum rule analysis [97Be1] that Samson and Pareek's value probably is more nearly correct. Earlier measurements were made by Comes [68Co1] and at lower energies by Kohl et al. [78Ko1]. Angel and Samson [88An1] extended the earlier measurements to higher energies and normalized the new data to that of Samson and Pareek at 21.22 eV. In Table 33 we show the cross sections from both of these sources from 28.8 eV; i.e., just above the energy where resonances occur, to 280 eV. The accuracy of these data is probably better than 10 %.

For atomic nitrogen absolute measurements have been made by Ehler et al. [55Eh1] by Comes [68Co2] at energies between threshold and 30 eV and by Samson and Angel [90Sa1] from threshold to 400 eV. Data from [90Sa1] from 44 eV, just above the range where resonant structure occurs, to 400 eV are given in Table 34.

There have been a number of measurements of relative cross sections and branching ratios for both nitrogen and oxygen at lower energies and these will be discussed in Section 1.3.

For Table 33 see p. 1-40.

Table 34. Photoionization cross sections for nitrogen in the energy range between 44 and 400 eV. From [90Sa1].

Energy [eV]	Cross section [10^{-18} cm^2]	Energy [eV]	Cross section [10^{-18} cm^2]	Energy [eV]	Cross section [10^{-18} cm^2]
44.1	5.65	80.0	1.57	160.0	0.313
46.0	5.30	85.0	1.34	170.0	0.272
48.0	4.94	90.0	1.17	180.0	0.238
50.0	4.60	95.0	1.04	190.0	0.211
52.0	4.30	100.0	0.92	200.0	0.187
54.0	4.00	105.0	0.82	220.0	0.150
56.0	3.80	110.0	0.740	240.0	0.123
58.0	3.55	115.0	0.668	260.0	0.102
60.0	3.33	120.0	0.606	280.0	0.086
65.0	2.80	130.0	0.504	300.0	0.074
70.0	2.34	140.0	0.425	350.0	0.052
75.0	1.96	150.0	0.363	400.0	0.038

Table 33. Total photoionization cross sections for oxygen in the energy range between 28 and 280 eV.

Energy [eV]	Cross section [10^{-18} cm^2]		Energy [eV]	Cross section [10^{-18} cm^2]	
	88An1	85Sa1		88An1	85Sa1
28.8	11.5		57.6		4.47
29.5	11.3		60.0	4.44	
29.8		11.2	61.1		3.97
30.2	11.0		62.1		3.94
30.3		11.0	64.3		3.58
30.6		11.1	67.3		3.41
31.0	11.8		68.8		2.88
31.3		10.0	70.0	3.43	
31.4		12.1	70.2		2.63
31.8	10.5		74.9		2.61
32.6	10.2		78.0		2.09
33.1		9.95	80.0	2.60	
33.5	9.90		80.3		1.93
34.4	9.57		81.6		2.30
35.3		9.37	89.6		1.81
35.4	9.25		90.0	2.06	
36.5	8.92		94.9		1.95
36.8		8.46	100.0	1.65	
37.6	8.60		103.2		1.34
37.7		8.70	110.0	1.39	
38.7	8.25		120.0	1.17	
40.0	7.90	7.97	130.0	1.00	
40.8	7.70	7.70	140.0	0.84	
41.3	7.55		150.0	0.73	
41.6		7.49	160.0	0.61	
42.1		7.20	170.0	0.52	
42.8	7.40		180.0	0.45	
44.3	6.85		190.0	0.38	
44.4		7.10	200.0	0.33	
45.9	6.50		210.0	0.28	
47.6		6.25	220.0	0.25	
47.7	6.15		230.0	0.22	
48.1		6.03	240.0	0.20	
48.7	6.00		250.0	0.18	
49.5		6.09	260.0	0.17	
50.0	5.77		270.0	0.17	
53.7		5.47	280.0	0.16	
56.1		4.91			

1.2.9 Cross sections for the alkalis (Z = 3, 11, 19, 37, 55)

Due to their low ionization potentials there have been a number of measurements of photoionization cross sections in the energy range below 25 eV. A summary of the earlier work has been given by Marr and Creek [68Ma1]. Measurements of absolute cross sections are difficult for two reasons. First, the cross sections in this energy range with the exception of lithium, are quite small (<< 1 Mb) and second, the measurements are always made on a species that contains some fraction of molecules and thus it is difficult to estimate the number of atoms that contribute to the absorption. As a result there are wide differences in both the absolute values of the cross sections reported as well as the variation of the cross section with energy.

At higher energies there have been measurements for lithium [82Me1], sodium [77Co1] and potassium [76Dr1] and a relative measurement for Cs [75Pe1].

For lithium, the results of Hudson and Carter [67Hu2] are shown in Fig. 13 between the ionization threshold, 5.39 eV and 22 eV. At higher energies the results of Mehlman et al. [82Me1] are shown along with an earlier measurement made on solid lithium [62Ba1] which illustrates that there is considerable difference in atomic and solid state cross sections at these energies. The results of Hudson and Carter are about 10 % lower than those of Marr and Creek [68Ma1] (not shown) but have the same dependence on energy. The results of Hudson and Carter and of Mehlman et al. are also shown in Table 35. There have been no measurements for lithium between 22 and 60 eV. However, there have been a number of measurements in the resonance region between 60 and 75 eV and between 140 and 175 eV which will be discussed in Section 1.3.

For sodium, Fig. 14 shows the low energy results of Hudson and Carter [67Hu2, 68Hu1] which are in agreement with an earlier measurement by Ditchburn et al. [53Di1] and a measurement at higher energies by Codling et al. [77Co1]. As with lithium, these data are also shown in Tables 36 and 37. Relative data in the resonance range between 30 and 70 eV [72Wo1] will be discussed in Section 1.3.

Table 38 gives the results of the measurements of Hudson and Carter [67Hu1] for potassium from the ionization threshold 4.34 eV to 18 eV and measurements at higher energies [76Dr1]. Also shown are results derived by Marr and Creek [68Ma1] from an analysis of their own results and previous measurements.

For rubidium and cesium measurements have only been made in the energy range from threshold (4.18 eV for rubidium, 3.89 eV for caesium) up to 11 eV. Results from various authors are shown in Table 39. For cesium the table shows that there is relatively good agreement between the results of Cook et al. [77Co2] and the relative measurements of Suemitsu and Samson [83Su1] concerning the energy dependence of the cross section. The results of Cook et al. are approximately a factor of 2 lower than the results of Marr and Creek [68Ma1]. In view of the small size of these cross sections and the difficulties of the measurements it is not surprising that there are large discrepancies.

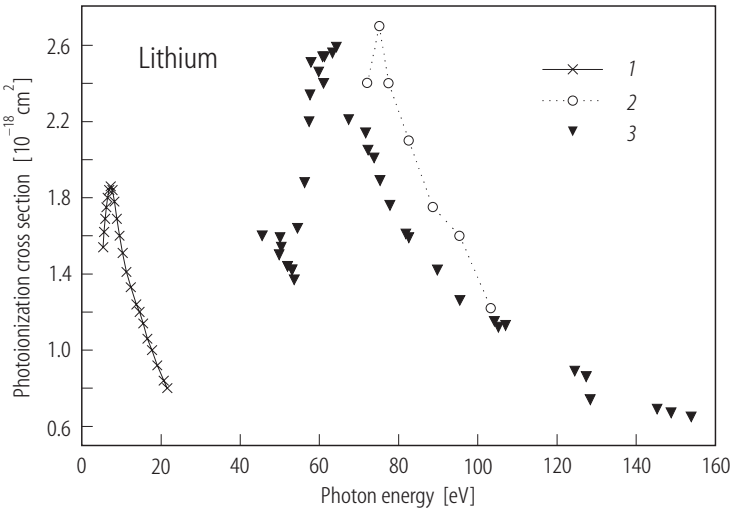

Fig. 13. Cross section for lithium between threshold and 160 eV from *1* [67Hu2] and *2* [82Me1]. The solid state measurements of *3* [62Ba1] are shown for comparison.

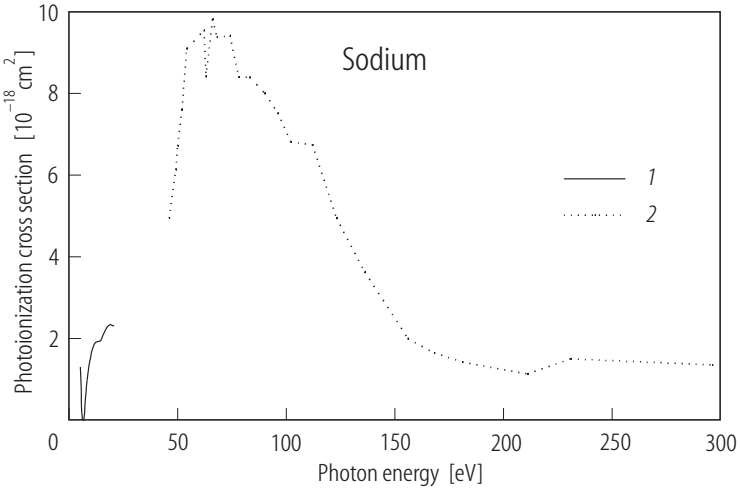

Fig. 14. Cross section for sodium from threshold to 300 eV from *1* [67Hu1, 68Hu1] and *2* [77Co1]. Note that the low energy data is shown multiplied by 10.

Table 35. Attenuation cross section for lithium in the energy ranges from 5.39 to 22.0 eV [67Hu2] and from 75 to 104 eV [82Me1].

Energy [eV]	Cross section [10^{-18} cm^2]	Energy [eV]	Cross section [10^{-18} cm^2]	Energy [eV]	Cross section [10^{-18} cm^2]
5.39	1.54	9.54	1.60	20.66	0.84
5.64	1.62	10.33	1.51	21.56	0.80
5.90	1.69	11.27	1.41	75.1	2.70
6.20	1.75	12.40	1.33	77.5	2.40
6.53	1.80	13.78	1.24	82.6	2.10
6.89	1.84	14.59	1.20	88.6	1.75
7.29	1.86	15.50	1.14	95.4	1.60
7.75	1.84	16.53	1.06	103.3	1.22
8.27	1.78	17.71	1.00		
8.85	1.69	19.07	0.92		

Table 36. Photon attenuation cross section for sodium in the energy range from 5 to 25 eV. From [67Hu2] and [68Hu1].

Energy [eV]	Cross section [10^{-18} cm^2]	Energy [eV]	Cross section [10^{-18} cm^2]	Energy [eV]	Cross section [10^{-18} cm^2]
5.14	0.130	7.29	0.038	13.05	0.192
5.17	0.126	7.51	0.057	13.78	0.193
5.28	0.110	7.75	0.072	14.59	0.195
5.39	0.092	8.00	0.085	15.50	0.207
5.51	0.070	8.27	0.097	16.53	0.219
5.64	0.045	8.55	0.110	17.71	0.230
5.77	0.022	8.86	0.122	19.07	0.240
5.91	0.008	9.18	0.134	20.66	0.230
6.05	0.001	9.54	0.145	20.66	0.250
6.20	0.000	9.92	0.155	21.56	0.240
6.36	0.000	10.33	0.166	22.54	0.230
6.53	0.000	10.78	0.175	23.62	0.220
6.70	0.001	11.27	0.182	24.80	0.190
6.89	0.006	11.81	0.189		
7.08	0.019	12.40	0.191		

Table 37. Photon attenuation cross section for sodium in the energy range between 46 and 290 eV. From [77Co1].

Energy [eV]	Cross section [10^{-18} cm^2]	Energy [eV]	Cross section [10^{-18} cm^2]	Energy [eV]	Cross section [10^{-18} cm^2]
46.00	4.95	68.00	9.38	123.00	4.95
49.00	6.14	74.00	9.42	136.00	3.63
50.00	6.72	78.00	8.40	156.00	2.00
52.00	7.61	83.00	8.40	168.00	1.65
54.00	9.10	90.00	8.01	181.00	1.42
62.00	9.55	96.00	7.52	211.00	1.13
63.00	8.42	102.00	6.81	231.00	1.50
66.00	9.82	112.00	6.75	246.00	1.35

Table 38. Photon attenuation cross section for potassium in the energy range between 5 and 18 eV. and between 25 and 35 eV.

Energy [eV]	Cross section [10^{-18} cm^2]		Energy [eV]	Cross section [10^{-18} cm^2]	
	67Hu1	68Ma1		67Hu1	68Ma1
4.96		0.065 ± 0.005	10.33	0.395	0.21 ± 0.02
5.39	0.060		11.27	0.413	
5.63	0.092		12.40	0.430	
5.90	0.125		13.78	0.460	
6.20	0.157		15.50	0.532	
6.53	0.188		17.71	0.700	
6.89	0.218				76Dr1
7.29	0.250	0.15 ± 0.01			
7.75	0.280		26.3		47.0 ± 9
8.27	0.313		32.5		31.0 ± 7
8.86	0.340		38.0		20.0 ± 4
9.54	0.370				

Table 39. Photoionization cross sections for rubidium and cesium in the energy range below 11 eV. *) value from [80Gr1].

Energy [eV]	Rb cross section [10^{-18} cm^2]		Cs cross section [10^{-18} cm^2]		
	68Ma1	83Su1	68Ma1	77Co2	83Su1
3.89			0.20 ± 0.01		0.10
3.90				0.086 ± 0.02	
3.92					0.095
3.96					0.077
4.00				0.068 ± 0.02	0.076
4.11					0.056
4.13				0.051 ± 0.02	0.054
4.18	0.1 ± 0.005				0.046
4.19		0.105			
4.28		0.062		0.037 ± 0.01	0.037
4.35		0.049			0.034
4.42		0.038			0.028
4.51		0.027			0.025
4.59		0.018			0.025
4.67		0.001	0.06 ± 0.01		0.028
4.76				0.023 ± 0.01	
5.00	0.008 ± 0.003	0.004			0.041
5.06		0.004			0.047
5.16				0.047 ± 0.02	
5.21		0.006			0.060
5.39		0.010			0.080
7.20				0.09 ± 0.027*	
7.28	0.10 ± 0.01		0.23 ± 0.015		
10.20	0.15 ± 0.02		0.33 ± 0.04		

1.2.10 Cross sections for other elements

While there have been a number of measurements of absolute cross sections for other elements made at low energies (below 25 eV) almost invariably these measurements are made in energy ranges where resonant structure dominates the cross section. The only exceptions are higher energy measurements of zinc, cadmium, mercury and chlorine. Data in the resonance ranges for these elements as well as selected data for other elements will be given in Section 1.3.

Harrison et al. [69Ha1] obtained relative data of single ionization of zinc in the energy range from threshold to 50 eV. In a later publication [69Ca1] these data were put on an absolute scale using the low energy measurements of Marr and Austin [69Ma2] and data on the formation of doubly charged ions was obtained. An estimate of the total attenuation cross section obtained from these data are shown in Table 40 in the structure-less range from 20 to 44 eV along with the rms deviance of the measurements.

A complicated structure exists in cadmium in the energy range below 20 eV [68Be1]. At higher energies cross sections for both single and double ionization have been measured [69Ca1] at energies up to 80 eV. Total attenuation has been measured from 20 to 250 eV by Codling et al. [78Co2]. The results of this measurement for energies between 40 and 250 eV are shown in Table 41.

Relative cross sections for the production of singly and doubly charged mercury were measured by Cairns et al. [70Ca1] and these data were normalized by Dehmer and Berkowitz [74De1] to previous data on oscillator strengths. The results in the energy range from 20 to 72 eV of these measurements are given in Table 42.

The cross section for atomic chlorine has been measured from threshold (13 eV) up to 80 eV by Samson et al. [86Sa1]. The results in the energy range from 30 to 80 eV, the range where no structure is expected are shown in Table 43.

Table 40. Photon attenuation cross section for zinc in the energy range between 18 and 51 eV. From [69Ha1] and [69Ca1].

Energy [eV]	Cross section [10^{-18} cm^2]
18.78	3.6 ± 1.2
19.68	4.6 ± 2.4
20.35	5.3 ± 1.3
20.69	4.6 ± 0.7
21.67	6.8 ± 0.8
22.38	6.1 ± 1.7
22.87	7.0 ± 0.4
24.40	7.0 ± 0.7
25.66	9.1 ± 0.9
26.37	8.2 ± 0.8
28.56	9.1 ± 0.9
29.80	12.1 ± 1.1
33.14	9.3 ± 2.0
43.80	12.4 ± 2.3

Table 43. Photoionization cross section for chlorine in the energy range from 30 to 80 eV. From [86Sa1].

Energy [eV]	Cross section [10^{-18} cm^2]
30.99	7.50
33.06	4.60
35.43	2.50
38.15	1.40
41.33	0.94
45.08	0.90
49.59	1.02
55.10	1.19
61.99	1.30
70.85	1.32
78.47	1.29

Table 41. Photon attenuation cross section for cadmium in the energy range between 41 and 250 eV. From [78Co2].

Energy [eV]	Cross section [10^{-18} cm^2]
41.92	12.64
44.23	14.52
50.13	15.76
56.54	16.27
62.56	14.69
66.15	14.44
69.49	14.42
73.08	14.42
78.21	13.88
83.33	12.69
89.36	11.44
95.00	9.81
103.80	7.35
113.80	4.58
124.70	3.78
135.60	1.98
155.10	0.58
167.95	0.51
179.50	0.66
189.70	0.71
193.80	0.99
210.40	1.22
228.70	1.53
247.70	1.83

Table 42. Photon attenuation cross section for mercury in the energy range from 20 to 72 eV. From [70Ca1].

Energy [eV]	Cross section [10^{-18} cm^2]
20.09	13.9
20.36	14.1
20.66	15.8
20.73	16.1
20.80	13.5
21.27	15.1
21.67	14.1
21.79	13.5
22.34	13.9
23.13	13.7
23.61	15.4
24.41	16.4
25.30	15.6
26.66	17.3
27.43	18.5
28.57	19.0
29.52	22.1
33.15	21.2
35.94	22.4
37.01	20.9
38.38	23.4
44.28	22.3
45.58	23.6
50.19	19.6
57.66	19.7
64.57	15.9
71.66	13.2

1.3 Cross sections due to resonances, branching ratios, multiple ionization and angular distributions

In the previous section data were presented for atomic photoionization or absorption in those energy ranges where the cross sections were expected to be slowly varying and consequently some energy ranges were omitted. Here data in those ranges will be given, but will for the most part not be presented in the form of tables, since in resonance regions the observed cross sections are strongly dependent on the instrumental bandpass used in making the measurements.

When single ionization occurs as a result of photoabsorption, the ions left behind may not be in their ground state. This is especially true at higher energies where most of the single ionization is from inner subshells of the atom. When this happens, the ions then decay via a complicated set of decay processes which emit both Auger electrons and fluorescence radiation and the end result is a

distribution of multiply charged ions. When ions and/or electrons are observed following photoabsorption it is possible to obtain information on both the intermediate and final states of the decay process and express the results in terms of branching ratios. Some data of this type will be presented.

Finally, when electrons are observed as a result of photoionizaton, in general their angular distributions will not be isotropic. At low energies the angular distribution of photoelectrons has a simple form and some data on angular distributions will be given.

1.3.1 Cross sections due to resonances

For the rare gases, which form the bulk of the data presented in the previous section, the spectral regions where resonances are expected to occur are well known. For helium, the range is from 60 eV, just below the position of the lowest doubly excited resonance, up to 79 eV., the threshold for direct double ionization. For the heavier rare gases, there will be resonances between the two lowest $^2P_{3/2}$-$^2P_{1/2}$ energy states of the singly charged ion in each case and resonance regions extending from about 10…12 eV below each inner shell ionization potential up to an energy corresponding to removal of both an inner shell and a valence shell electron. The ranges for He, Ne, Ar, Kr and Xe where resonances are expected are shown in Table 44.

For other atoms, the ranges corresponding to inner shell ionization are essentially the same as the rare gases; i.e., from about 10…12 eV below each inner shell ionization potential up to an energy corresponding to double ionization involving an inner shell electron. However, at lower energies resonances occur frequently and must be considered atom by atom.

Table 44. Energy ranges for photoionization in the rare gases where resonant structure is expected to occur.

Gas	Energy range [eV]					
	$^2P_{3/2}$-$^2P_{1/2}$	Inner subshells				
Helium		65-69				
Neon	21.56-21.66	44.0-43.4	860-910			
Argon	15.76-15.93	25.0-38.6	240-310	3200-3250		
Krypton	14.00-14.66	25.0-38.6	90-140	200-310	1650-1950	
Xenon	12.13-13.43	20.0-33.3	60-110	140-250	670-720	930-1200
Xenon						4780-5600

1.3.2 Resonances in helium

Resonances in helium were first discovered by Madden and Codling [63Ma1] in the energy range between 59 and 79 eV via an absorption measurement using synchrotron light and since that time there have been a number of measurements of helium resonances using alternative techniques. Since cross sections are rapidly varying near resonances the normal procedure has been to present graphs of cross sections or of transmitted intensity or observed ion or electron yields rather than try to give values of the cross section in tabular form. An example is shown in Fig. 15 in the resonance range between 59 and 66 eV [91Ch1]. The measurement here was an electron impact experiment at low

momentum transfer, but the results are expected to be equivalent to an absorption measurement. The results shown are in very good agreement with the recommended values of Samson et al. [94Sa1] as is shown in Table 45 which compares the results at energies between the resonances where the cross section is slowly varying.

It is important to note that the cross sections reported as in Fig. 15 are not "true" cross sections, but depend on the spectral resolution used in making the measurements. Due to the finite resolution the "true" cross section will always be larger than that reported at the peak of resonance and smaller at its minimum.

Higher resolution studies (see Fig. 16) have shown that unresolved structure exists at higher energies than is evident in Fig. 15. This means that if resonances are present the results only indicate the average cross section over the bandwidth of the measurement.

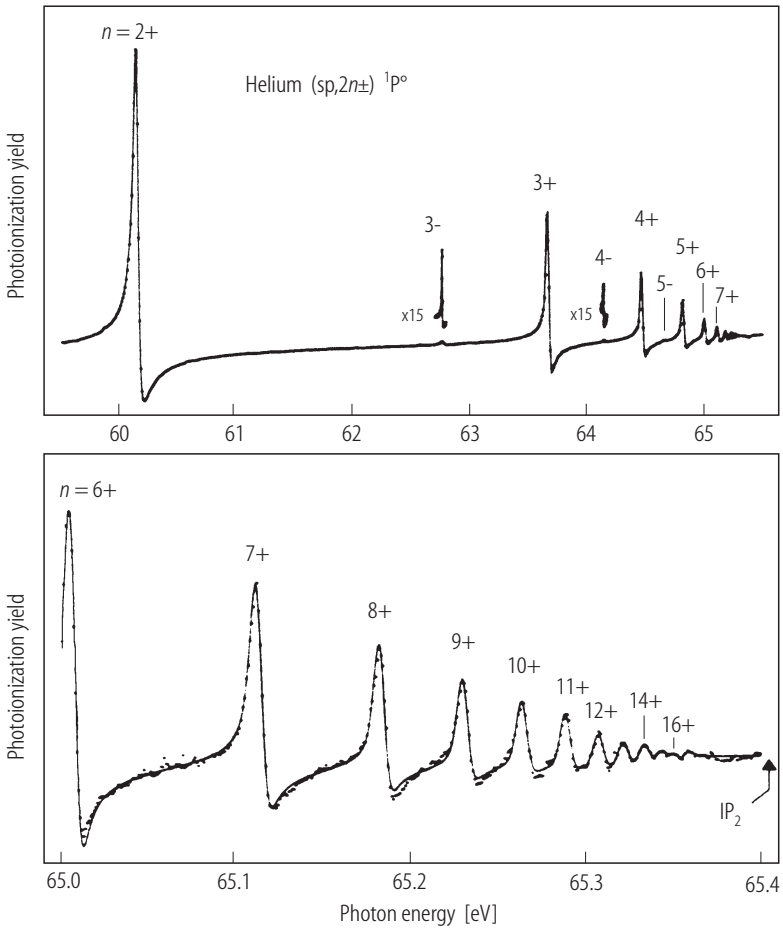

Fig. 16. Cross section for helium in the resonance region between 60 and 65.4 eV from [91Do1].

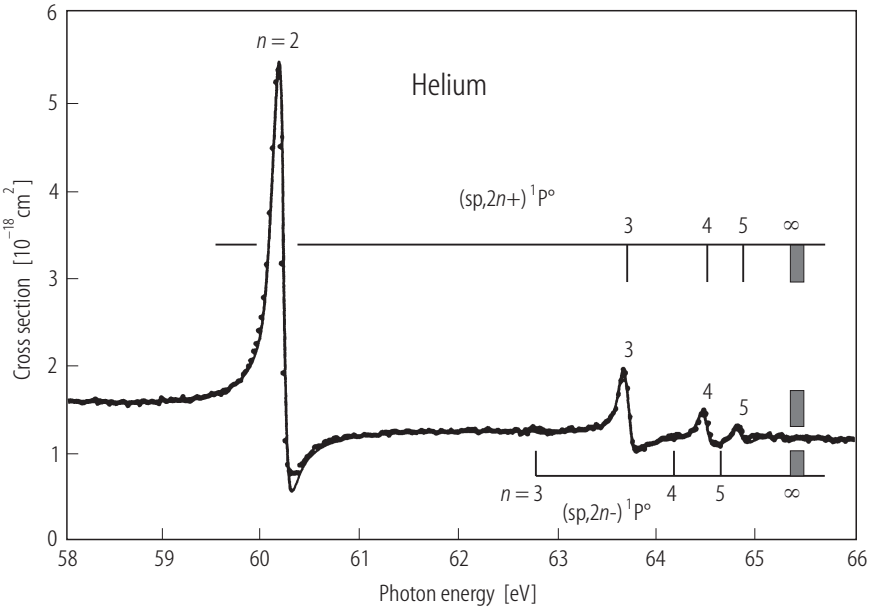

Fig. 15. Cross section for helium in the resonance region between 59 and 66 eV from [91Ch1].

Table 45. A comparison of measured cross sections of helium in the non-resonance range from 66 to 69 eV.

Energy [eV]	Cross section [10^{-18} cm^2]	
	94Sa1	91Ch1
66.0	1.15	1.15
67.0	1.11	1.10
68.0	1.06	1.06
69.0	1.02	1.02

1.3.3 Resonances between the two lowest ionization thresholds of the rare gases

For neon, argon, krypton and xenon removal of an outer subshell electron can leave the ion core in two possible states with a slight energy difference. Consequently, there will be two series of resonances in each case converging to the limit of higher energy as discovered by Beutler [35Be1].

For neon, the interval between the two limits is small (0.1 eV) and the structure has been observed by a number of techniques. Fig. 17 shows a measurement of the apparent cross section for neon taken with a band pass of 0.045 Å [79Ra1] and observing ions produced. Similar measurements were made at higher resolution observing both ions and electron for the lower energy part of the resonant region [90Ca1].

Since the early work of Beutler there have been a number of measurements of the resonances between the two lowest limits for argon, krypton and xenon. For these resonances, a careful measurement and an analysis of previous work have been carried out by Maeda et al. [93Ma1]. For the low energy resonances they obtained resonance parameters for each pair of resonances using the following formulas:

$$\sigma = \frac{\sigma_{as}(\varepsilon_s + q_s)^2}{1+\varepsilon_s^2} + \frac{\sigma_{ad}(\varepsilon_d + q_d)^2}{1+\varepsilon_d^2} + \sigma_b \quad (1)$$

$$\varepsilon_l = \frac{\tan[\pi(\nu_{1/2} + \mu_l)]}{W_l} \qquad \text{for } l = \text{s, d} \quad (2)$$

where the parameters σ_{as}, σ_{ad} and σ_b are partial cross sections, q_s and q_d are shape parameters, ε_l (l = s, d) are reduced energies and the parameters μ_l and W_l determine the energy position of the resonance relative to $\nu_{1/2}$, the energy (in cm^{-1}) of the upper series limit. The parameters for the lower resonances in each case along with estimates from other recent measurements are shown in Table 46.

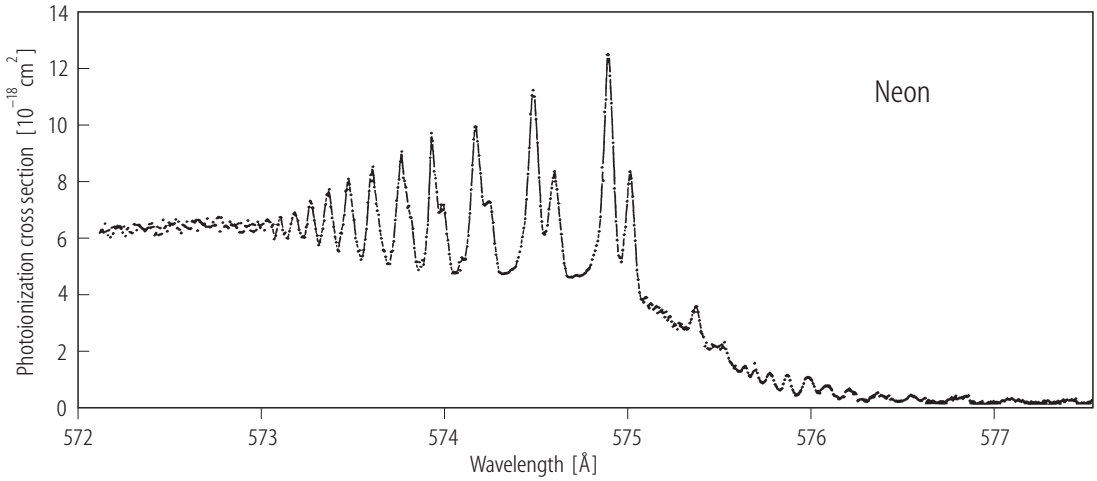

Fig. 17. Ionization yield for neon in the resonance region between 577 and 572 Å (21.5-21.7 eV) [79Ra1].

Table 46a. Energy width parameters W_s and W_d for argon, krypton and xenon resonances [93Ma1].

Atom	n	W_s	W_d	Atom	n	W_s	W_d
Argon	11	0.00544(65)	0.2122(70)		13	0.00911(85)	0.2070(55)
	12	0.00524(80)	0.2245(80)		14	0.00967(120)	0.2089(55)
	13	0.00438(100)	0.2296(90)	Xenon	8	0.00732(35)	0.2505(60)
	14	0.00461(130)	0.2258(90)		9	0.00657(40)	0.2465(65)
Krypton	8	0.00989(50)	0.1561(55)		10	0.00657(35)	0.2499(65)
	9	0.00952(55)	0.1741(55)		11	0.00642(50)	0.2499(65)
	10	0.00949(55)	0.1894(55)		12	0.00651(60)	0.2448(65)
	11	0.00938(60)	0.2040(50)		13	0.00645(80)	0.2505(65)
	12	0.00942(65)	0.1946(50)		14	0.00653(105)	0.2608(65)

Table 46b. Line shape parameters μ_1, q_1, σ_{al} and σ_1 for argon, krypton and xenon resonances [93Ma1].

Atom	n	μ_s	μ_d	q_s	q_d	σ_{as}	σ_{ad}	σ_b
Argon	11	0.138(1)	0.199(4)	14.8(5.1)	2.14(15)	1.28(80)	9.9(1.5)	9.5(1.5)
	12	0.137(1)	0.202(3)	16.5(6.8)	2.06(20)	0.96(75)	10.1(1.0)	10.7(2.0)
	13	0.139(1)	0.202(2)	14.8(6.5)	2.02(20)	1.21(85)	9.9(2.0)	11.1(2.0)
	14	0.136(1)	0.198(2)	15.9(6.5)	2.29(25)	0.91(75)	8.3(2.0)	11.9(3.0)
Krypton	8	0.099(1)	0.223(3)	36.9(6.5)	1.94(10)	0.20[10)	20.5(2.0)	11.7(1.5)
	8	0.097(1)	0.223(3)	23.2(5.0)	1.90(10)	0.45(20)	20.9(2.0)	12.8(2.0)
	10	0.096(1)	0.227(3)	26.0(5.0)	1.84(10)	0.34(15)	21.6(2.5)	11.2(1.5)
	11	0.095(1)	0.235(3)	19.2(3.5)	1.66(20)	0.61(20)	25.5(4.0)	9.1(3.5)
	12	0.094(1)	0.240(2)	25.5(5.5)	1.76(15)	0.31(15)	22.3(2.5)	11.1(2.0)
	13	0.094(1)	0.241(2)	21.4(4.0)	1.74(15)	0.46(15)	22.5(3.0)	11.0(2.0)
	14	0.094(1)	0.243(1)	25.5(5.5)	1.71(15)	0.27(15)	22.0(2.5)	11.2(2.0)
Xenon	8	0.025(1)	0.323(3)	22.7(6.0)	1.49(5)	0.66(35)	43.3(3.0)	6.8(3.0)
	9	0.021(1)	0.328(3)	15.8(2.5)	1.47(10)	1.33(45)	44.9(3.0)	6.3(3.0)
	10	0.019(1)	0.332(2)	13.9(2.5)	1.45(10)	1.65(55)	45.4(2.5)	5.3(2.0)
	11	0.017(1)	0.335(2)	13.2(2.5)	1.40(10)	1.97(65)	46.4(3.0)	5.9(2.0)
	12	0.016(1)	0.331(1)	15.3(3.0)	1.53(10)	1.32(55)	42.4(4.0)	8.7(1.5)
	13	0.014(1)	0.332(1)	14.7(2.5)	1.47(10)	1.35(55)	42.8(3.5)	7.1(2.0)
	14	0.014(1)	0.332(2)	17.6(3.0)	1.41(10)	0.90(35)	43.6(3.0)	7.7(2.0)

1.3.4 ns and doubly excited resonances in neon, argon, krypton and xenon

For the heavier rare gases a single series of autoionizing resonances converge to the inner *n*s subshell limits (n = 2, L_1 for neon, n = 3, M_1 for argon, etc.) which lie between 20 and 30 eV above the neutral ground state. In addition there are doubly excited resonances in each case which are intermingled with the series of s subshell resonances.

As example of a measurement of the photoionization cross section in the resonance region of neon between 40 and 55 eV is shown in Fig. 18 [92Ch1]. Here, as Fig. 15, the measurement was done by electron impact at low momentum transfer, but the results agree reasonably well with photoionization data obtained by direct measurement [65Sa1] as shown in the figure.

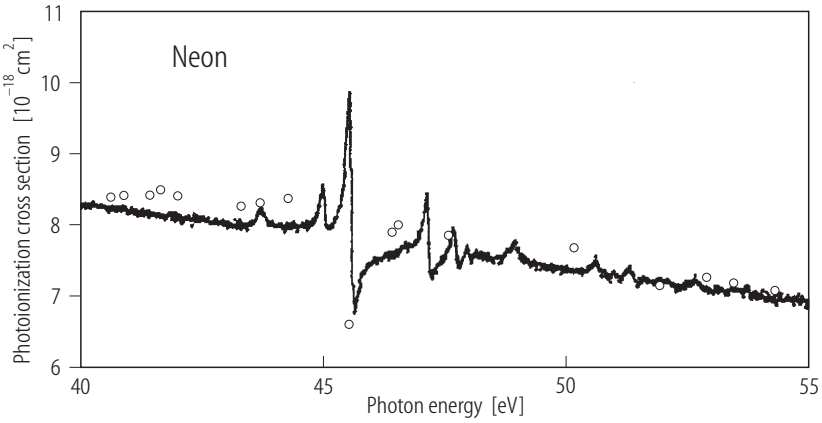

Fig. 18. Cross section for neon in the resonance region between 40 and 55 eV [92Ch1]. Circles are from [65Sa1].

As in the previous sections, the figure shows only an "apparent" cross section since the true cross section will be considerably larger (or smaller) in the vicinity of the resonances. Similar data for argon and krypton in the energy ranges from 25…31 and 22…31 eV is shown in Fig. 19 [63Sa1].

Although there have been few attempts to obtain absolute photoionization cross sections near resonances, the wavelengths (and therefore energies) of a number of the rare gas ns-np and doubly excited resonances are known (neon [67Co1]; argon [69Ma1]; krypton and xenon [72Co1]). Ederer [71Ed1] has obtained resonance parameters for some of the lower lying resonances in krypton and xenon and his analysis has been extended by Flemming et al. [91Fl1]. The analysis is similar to that of Maeda et al. and makes possible a representation of the true cross section in resonance regions.

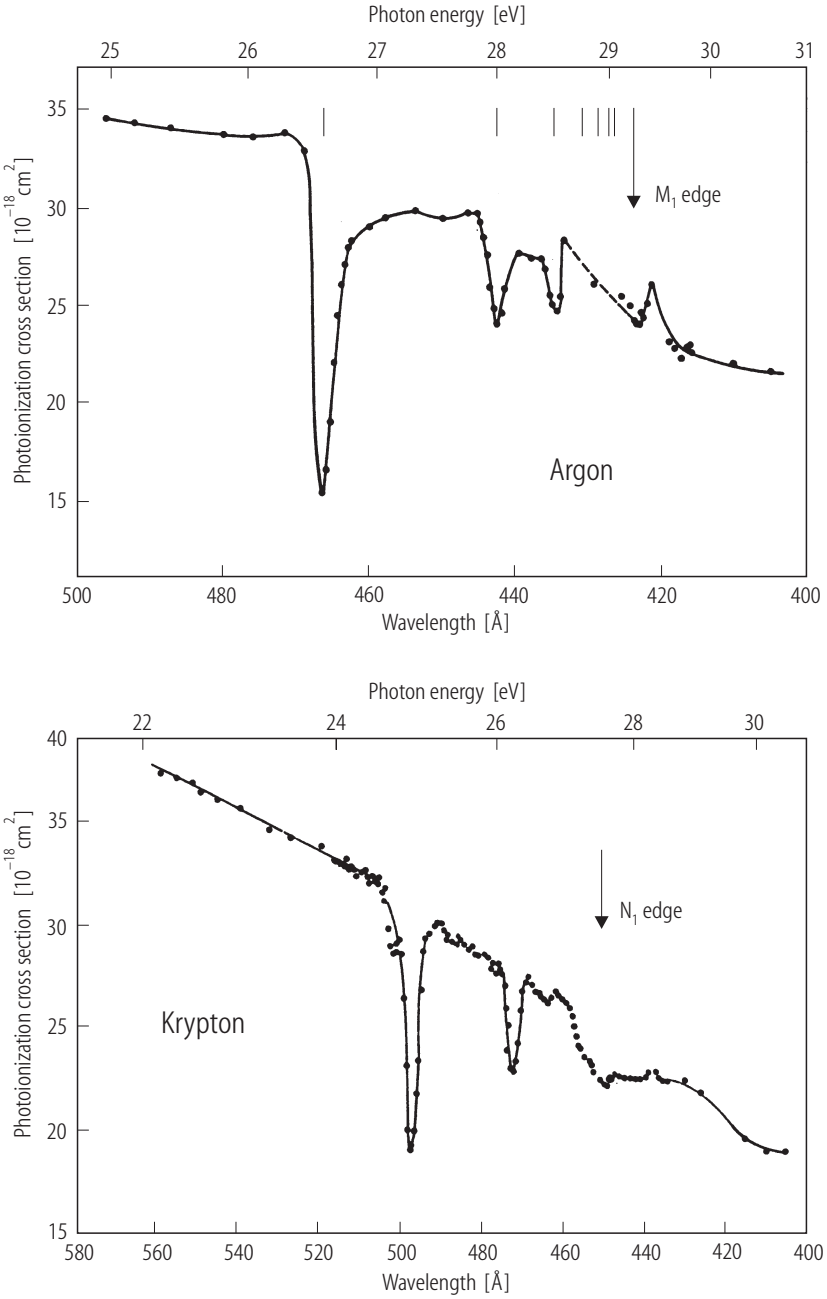

Fig. 19. Cross sections for argon and krypton in the resonance regions between 25-31 and 22-31 eV [63Sa1].

1.3.5 Deep inner shell resonance regions

In the vicinity of each inner shell ionization threshold in the rare gases, there will be a series of singly excited resonances below the limit and possibly doubly excited resonances in the energy range up to approximately 50 eV above the threshold. Typically these resonances are much weaker than those discussed in the previous sections and have larger widths due to the fact that the resonances can decay via a number of radiative and autoionization processes. As a result, measurements of total cross sections in the vicinity of inner shell thresholds are probably a more accurate estimate of the true cross section than those made at lower energies. A typical example is data near the K ionization threshold of neon, shown in Fig. 20 [69Wu1]. The resonances represent a series of single electron 1s-*n*p transitions (P3-P6) lying below the 1s ionization potential (870.1 eV). There is evidence for a double excitation resonance at higher energy (35 eV above the P3 peak in Fig. 20) but the resonance is less than 2 % of the observed apparent cross section. Values of the total absorption cross section in the vicinity of the ionization limit are given in Table 47.

The situation is similar for the energy ranges near the $L_{2,3}$ (240…260 eV) and K (3206 eV) thresholds of argon. Fig. 21 shows a high resolution measurement of the cross section just below the $L_{2,3}$ thresholds [81Gi1] and Table 48 gives data taken at lower resolution [69De1]. Evidence of the resonant structure near the K threshold of argon [83De1] is shown in Fig. 22 and cross section data in this energy range [Wu6901] are given in Table 49.

For the inner subshells of the heavier rare gases there is little evidence of structure near absorption thresholds since any discrete levels that exist are broadened by the many Auger and radiative decay processes that can occur. Thus the data shown in Tables 24 and 25 for krypton probably represents true cross sections at the energies listed. The same is true of the data for xenon shown in Tables 29 and 30. Arcon et al. [95Ar1) have made a detailed measurement of the attenuation cross section of xenon from 4700 to 6200 eV. They find that resonances never produce deviations larger than 3 % from a smooth energy dependence of the cross section.

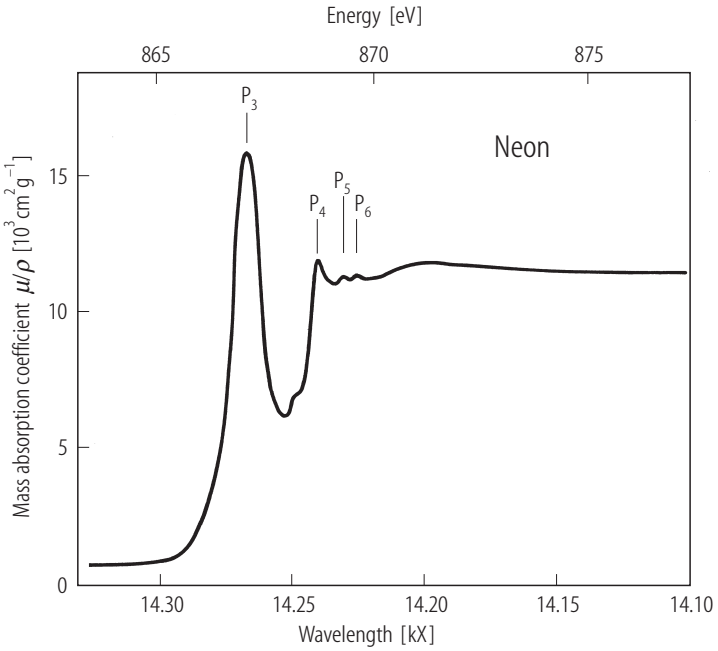

Fig. 20. Cross section for neon near the 1s ionization potential (870.1 eV) from [69Wu1].

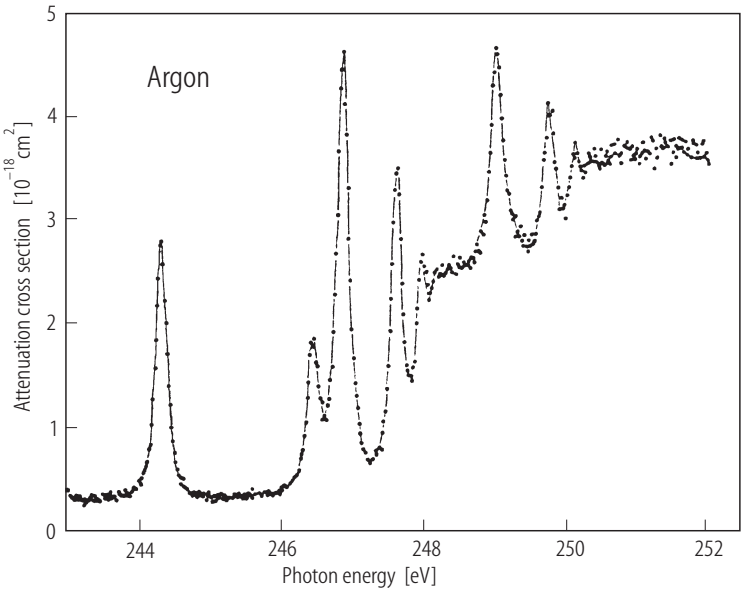

Fig. 21. Cross section for argon near the $L_{2,3}$ edges [81Gi1].

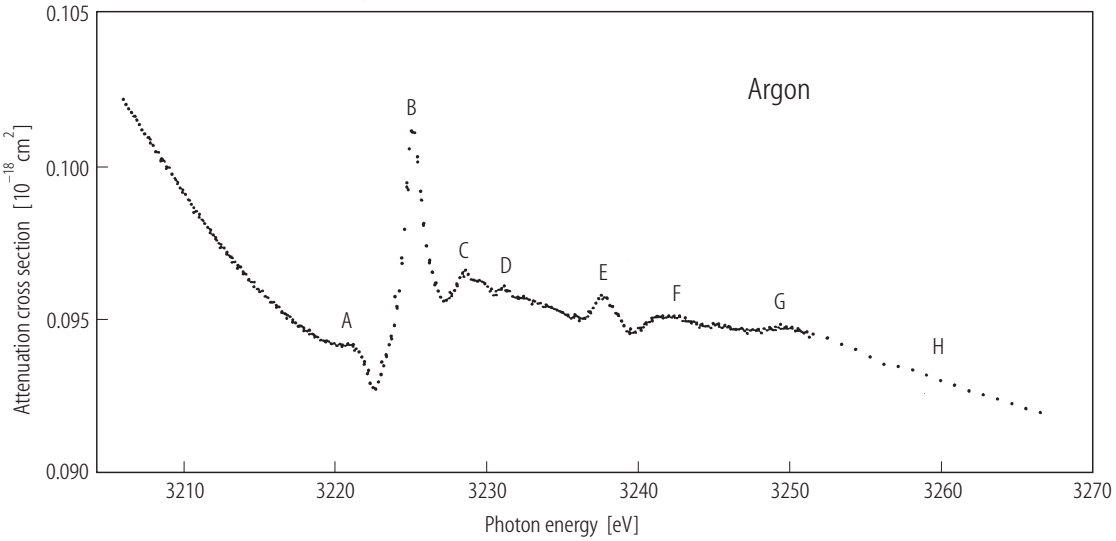

Fig. 22. Cross section for argon in the resonance range between 3205 and 3250 eV [83De1].

Table 47. Apparent photon attenuation cross sections for neon near the K absorption threshold [69Wu1].

Energy [eV]	Cross section [10^{-21} cm^2]	Energy [eV]	Cross section [10^{-21} cm^2]	Energy [eV]	Cross section [10^{-21} cm^2]
830.0	25.9	859.0	24.2	890.0	362.0
836.0	25.3	865.0	23.8	896.0	355.0
842.0	24.9	871.0	387.0	903.0	349.0
847.0	24.7	877.0	373.0	910.0	342.0
853.0	24.4	884.0	368.0		

Table 48. Apparent photon attenuation cross sections for argon near the $L_{2,3}$ absorption thresholds [69De1].

Energy [eV]	Cross section [10^{-18} cm^2]
240.0	0.31
241.0	0.35
242.0	0.35
243.0	0.39
244.0	0.44
245.0	1.11
246.0	0.72
247.0	1.18
248.0	1.86
249.0	1.73
250.0	3.81
251.0	4.27
252.0	4.59
253.0	4.68
254.0	4.62
255.0	4.58
256.0	4.48
257.0	4.37
258.0	4.29
259.0	4.20
260.0	4,14
261.0	4.07
262.0	4.03
263.0	4.03

Table 49. Apparent photon attenuation cross sections for argon near the K absorption threshold [69Wu1].

Energy [keV]	Cross section [10^{-21} cm^2]
3.017	11.4
3.054	10.6
3.093	10.3
3.132	10.1
3.172	10.0
3.196	9.7
3.205	98.8
3.213	93.7
3.255	91.0
3.299	88.9
3.343	85.9
3.389	83.7
3.436	79.1
3.485	77.3
3.534	74.2
3.586	72.2
3.638	69.6
3.693	66.9
3.749	64.5

1.3.6 Resonance regions in oxygen and nitrogen

Since these are open shell atoms, when ionization occurs the ion core can be left in a number of states and there will be resonant structure at energies lying just below the higher ionization thresholds. For oxygen the lowest ionization threshold is 13.61 eV but higher thresholds are at 16.93, 18.63 and 18.49 eV. The resonance structure below the 16.93 and 18.63 eV thresholds has been observed [67Hu3] and relative cross sections near these thresholds have been obtained [73De1]. For nitrogen the lowest ionization threshold is 14.54 eV and higher thresholds are at 16, 44, 18.59 and 20.4 eV. However, due to selection rules, no structure is expected below the 16.44 and 18.59 eV thresholds and none has been observed, but a single series of resonances has been observed between 17.7 and 20.4 eV and relative cross sections obtained the resonance region [74De2]. Cross sections for both oxygen [85Sa1, 88An1] and nitrogen [90Sa1] have been measured in the energy ranges where resonances are present and are shown in Table 50 and 51, respectively. The measurements shown are at energy values which do not correspond to known resonance positions and thus the values shown are expected to be true cross sections.

Table 50. Total photoionization cross sections for oxygen in the energy range between 13.7 and 25.4 eV. From [88An1].

Energy [eV]	Cross section [10^{-18} cm^2]
13.78	2.85
14.25	3.10
14.50	3.10
14.93	3.30
15.02	3.30
15.79	3.70
15.89	3.70
16.20	4.00
16.31	3.90
16.98	8.03
17.04	8.90
17.32	9.24
17.48	9.71
17.87	9.00
17.95	9.47
18.30	10.0
18.78	12.6
19.68	13.4
20.66	13.3
21.37	13.0
22.14	12.7
22.54	12.5
23.00	12.3
23.40	12.1
23.80	12.0
24.31	11.9
24.80	11.9
25.30	12.0

Table 51. Photoionization cross sections for nitrogen in the energy range between 14 and 44 eV. From [90Sa1].

Energy [eV]	Cross section [10^{-18} cm^2]
14.6	9.5
14.8	10.2
15.1	10.6
15.5	10.8
15.9	11.1
16.3	11.4
16.8	11.6
17.2	12.1
17.7	13.5
20.3	11.6
20.7	11.7
21.7	11.8
22.1	11.8
23.0	11.7
23.8	11.5
24.8	11.2
25.8	10.8
27.0	10.5
28.2	10.0
29.5	9.6
31.0	9.1
32.6	8.6
34.4	8.1
36.5	7.5
38.7	6.9
41.3	6.3

1.3.7 Resonances in the alkalis

Resonances have been observed near inner subshell ionization thresholds in lithium, sodium and potassium. In lithium there are autoionization resonances due to excitation of a single K shell electron which were first observed by Ederer et. al. [70Ed1]. Absolute measurements of the apparent cross sections in the resonant range between 58.91 eV (the position of the lowest resonance) and 81 eV. (the double ionization threshold were made by Mehlman et al. [78Me1, 82Me1]. The results in the energy range from 62 to 72 eV (200…172 Å) are shown in Fig. 23. More recently the resonance structure has been studied in detail in the energy range between 64.5 and 68 eV [96Ki1] and the results were found to agree closely with theoretical calculations [97Ch1].

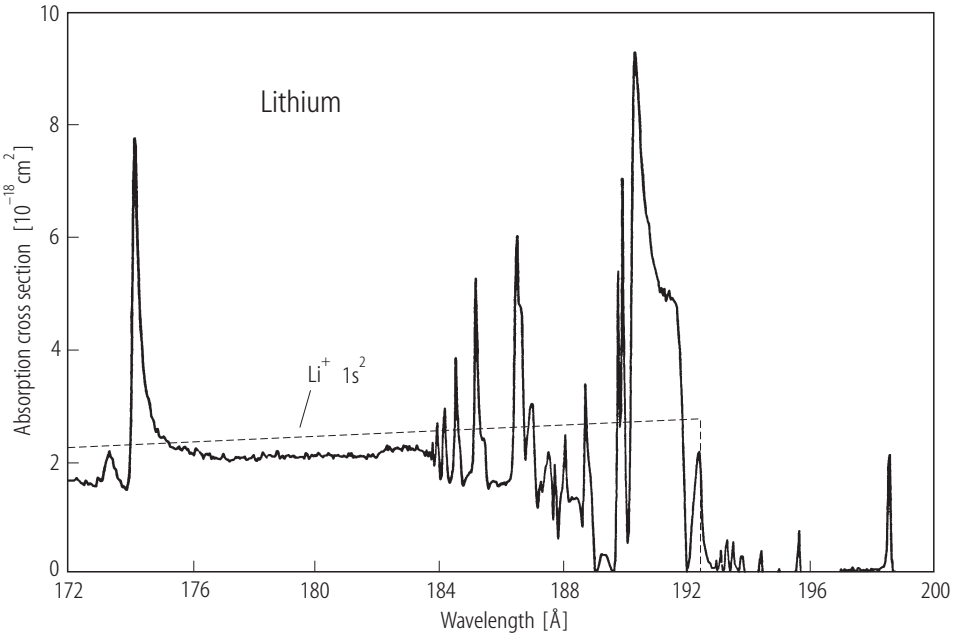

Fig. 23. Cross section for lithium in the resonance region between 200 and 172 Å (62-72 eV) from [78Me1]. The line labeled Li^+ $1s^2$ is from theory [79Re1].

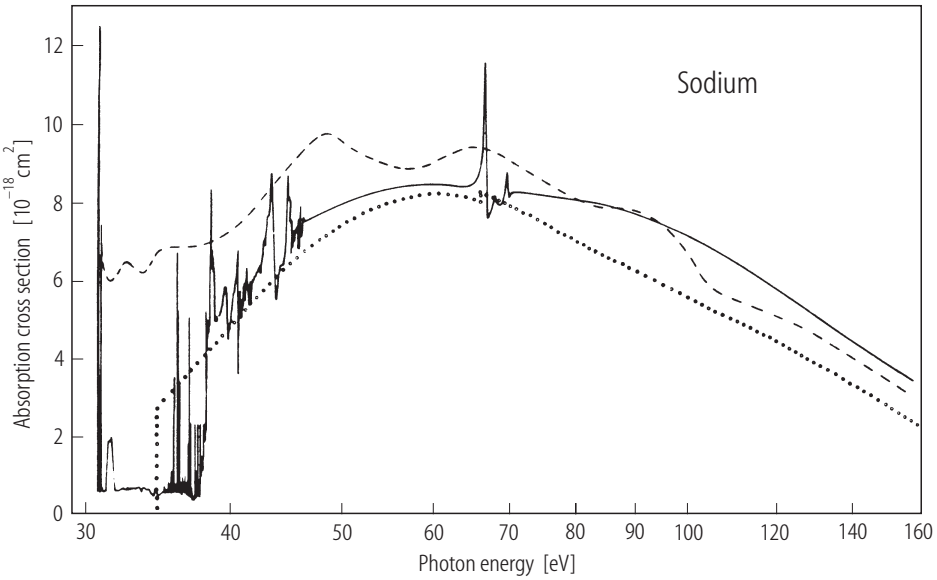

Fig. 24. Cross section for sodium in vapor (solid line) and solid (dashed line) phases compared with an atomic calculation (dotted line) from [72Wo1].

There is also a resonance region corresponding to excitation of two K shell electron which has been studied recently by a number of theoretical and experimental groups [96Wu1]. Resonances have been observed between 142.3 eV (the position of the lowest resonance [94Ki1] and 175.3 eV [97Az1]. Although it is possible that other resonances exist below the double ionization potential (203.4 eV), none have been observed.

Wolff et al. [72Wo1] have observed resonant structure for Na in the energy range between 35 and 75 eV in a relative measurement and a comparison of their results with solid state absorption and theory is shown in Fig. 24. Note that the normalized scale of the figure yield results approximately a factor of two higher than the results of Codling et. al. [77Co1] shown in Table 37.

Structure similar to this has been observed photographically in both potassium [34Be1] and rubidium [34Be2]. Hudson and Carter [67Hu1] have measured the apparent cross sections at the peaks of several of the resonances in potassium in the energy range between 18 and 21 eV.

For cesium Peterson et. al. [75Pe1] made a measurement of the relative cross section between 80 and 180 eV and found structure between 80 and 100 eV and between 160 and 180 eV.

1.3.8 Resonance regions in other elements

There have been a number of measurements of relative cross sections for elements other than those discussed above. Most of the earlier work was directed towards identifying resonances and was done with absorption measurements using photographic plates for detection with little or no attempt to derive relative cross sections. Later work involved ion and/or electron collection as well as attempts to obtain absolute cross sections from absorption measurements. A summary of this type of work for selected elements is given below.

Resonance structure was first observed in zinc by Beutler [33Be1]. A measurement of the absorption cross section in the energy range from threshold (9.39 eV) to 16.6 eV was made by Marr and Austin [69Ma2]. They find that the cross section at threshold is $(1.1 \pm 0.2)\cdot 10^{-18}$cm^2 and falls to a near zero minimum at 10.33 eV and there is a detailed resonance structure at higher energies. They report apparent cross sections over the entire energy range.

Ross and Marr [65Ro1] measured the absorption cross section for cadmium from threshold (9 eV) to 10.8 eV and found a threshold value of $(0.32 \pm 0.03)\cdot 10^{-18}$cm^2 and a decreasing cross section. The relative photoionization cross section from threshold to 19 eV was measured by collecting ions by Berkowitz and Lifshitz [68Be1] and the relative strengths of the resonances in the energy range from 10 to 18 eV previously identified by Beutler [33Be2] were reported. The work of Ross and Marr was extended by Marr and Austin [69Ma3] who measured the absorption cross section from threshold to 23.6 eV. They report apparent cross sections in the energy range between 13 and 23.63 eV.

Berkowitz and Lifshitz [68Be1]also obtained relative photoionization cross sections for mercury in the range between threshold (10.5 eV)and 18 eV and have identified a number of resonances in that range but no attempt was made to obtain absolute cross sections.

Chlorine is similar to atomic oxygen in that although the first ionization potential is at 13.01 eV., the ion can be left in excited states corresponding to higher thresholds of 14.45, 16.47 and 24.57 eV. Consequently there will be a complex resonant structure at energies immediately below these thresholds and structure has been observed via absorption measurements between 13 and 16.3 eV [83Ru1] and in photoelectron measurements in the energy ranges between 21.5 and 25 eV [92Me1]. Samson et al. [86Sa1] have measured the cross section at selected points in this energy range and at higher energies as shown in Table 43 and have assumed that the cross section is smoothly varying to obtain cross sections at specific energies. Their results are shown in Table 52.

The ionization threshold of barium is at 5.21 eV but there are a number of thresholds for ionization plus excitation extending up to 10.5 eV. Consequently, there is a complex resonant structure in this energy range which has been observed photographically [59Ga1, 73Br1]. Absolute cross sections were measured by Hudson et al. [70Hu1] between threshold and 7.3 eV and relative measurements were made by Saloman et al. [85Sa2] and the range was extended to 10.5 eV. Barium has a resonance at threshold and consequently the cross section is quite large in the threshold region. Carlsten and McIlrath [73Ca2] obtained a value at threshold of $5.6\cdot 10^{-17}$cm^2 which agrees with an estimate made by Armstrong and Wynn [79Ar1] based on their oscillator strength measurements but indicates that the absolute measurements of the cross sections by Hudson et al. are probably too low.

At higher energies relative photoabsorption and photoionizaton cross sections have been determined in the energy range from 85 to 140 eV. These data have recently been placed on an absolute basis by a careful measurement by van dem Borne et al. [95Bo1]. The results are shown in Fig. 25.

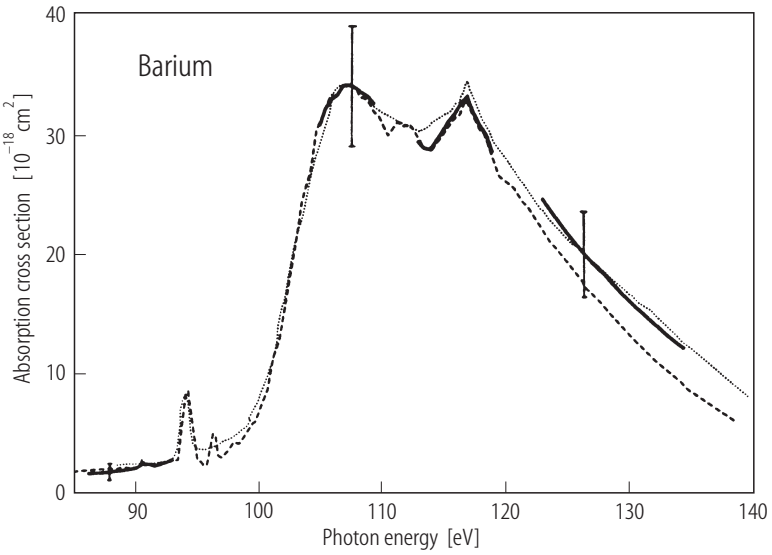

Fig. 25. Absolute cross section of barium from 90 to 130 eV from [95Bo1].

Table 52. Apparent photoionizaton cross section for chlorine in the energy range from 13.0 to 30 eV. From [86Sa1].

Energy [eV]	Cross section [10^{-18} cm^2]	Energy [eV]	Cross section [10^{-18} cm^2]
16.42	43.6	21.56	38.0
17.10	43.4	22.54	35.7
17.71	43.0	23.01	32.2
18.37	42.4	24.79	25.8
19.07	41.6	26.10	20.2
19.83	40.6	27.55	15.3
20.66	39.4	29.17	11.0

1.3.9 Branching ratios and angular distributions

The data presented in the preceding sections is, for the most part, cross sections for photo absorption in energy ranges where photoionization is the most important process. If measurements are made with monochromatic photon sources and either ions or electrons collected, it is possible to break down the total absorption cross section into a number of partial cross sections. With ion collection it is possible to measure cross sections for single,double and in general *n*-fold ionization and the total photoionization cross section will be the sum of these partial cross sections. When electrons are collected and their energy is specified, it is possible to obtain an alternative partitioning of the total photoionization cross section. Since energy is conserved, the difference between photon and electron

energy completely specifies the final state of the ion when a single electron is emitted. Thus by observing "main lines" in the photoelectron spectrum as photon energy is scanned, cross sections for single ionization of individual atomic subshells may be obtained. Alternatively, by observing "satellite lines" cross sections for ionization plus excitation or for double ionization may be measured. However, it is more difficult to obtain total photoionization cross sections via this technique for the following reasons. First, if multiple ionization occurs electrons must be collected over all energies allowed by conservation of energy. Second, typically electrons are collected at fixed angles with respect to the photon beam and its principal axis of polarization. Although at low energies the angular distribution of electrons ejected via photoionization relative to the photon beams polarization direction may be described by a single energy dependent parameter or, if the photon beam is unpolarized, to its direction, in general the photon polarization must be specified in order for cross sections measured at a "magic angle" to represent true partial cross sections. At higher energies corresponding to inner shell ionization measurements in general depend on both the direction and polarization of the photon beam and obtaining true partial cross sections is more difficult.

Although there has been a great deal of experimental work during the past several decades devoted to obtaining partial cross sections and electron angular distributions, most of the results have been presented in graphical form. Some of these results will be presented here and some references to alternative sources of data will be given in the appendix.

1.3.9.1 The ratio of double to single ionization for helium

Helium is the simplest atom which can be doubly ionized and the ratio of double to single ionization has been studied extensively by a number of groups and has been reviewed for both photon and charged particle impact recently [95MG1]. Helium is unusual in that at photon energies above 1 keV most of the cross section is due to scattering rather than absorption and there is considerable theoretical interest in the ratio at high energies.

A summary of experimental work on the ratio in the energy ranges between the double ionization threshold (79 eV) and 350 eV where photoionization is the dominant process and between 2 and 20 keV where ionization is due mainly to Compton scattering is given by Figs. 26 [98Sa1] and 27 [96Le1]. The ratio is less than 5 % at all energies and is between 1 and 2 % at high energies. More recent work [96Do1] and [96Sp1] indicates that the maximum of the ratio at low energies is less than 4 % and of the order of 1 % at higher energies.

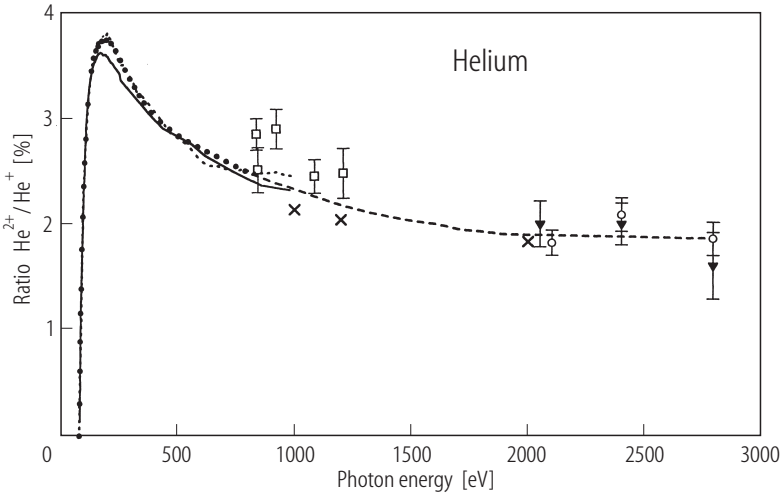

Fig. 26. Ratio of helium double to single ionization threshold (79 eV) to 3 keV from various sources [98Sa1].

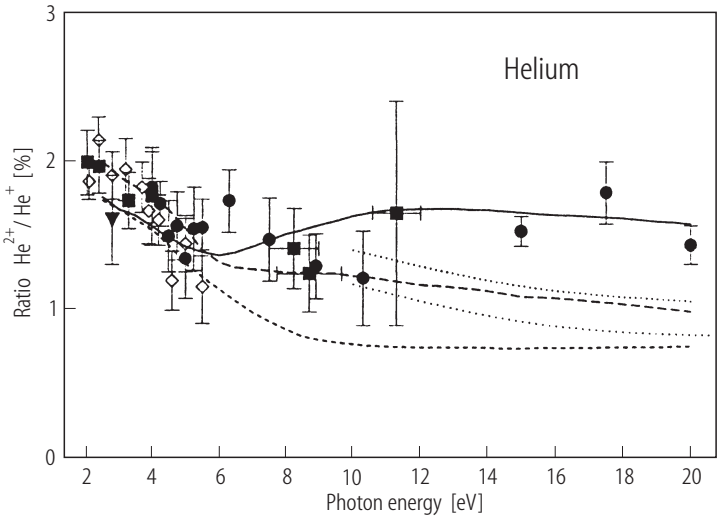

Fig. 27. Ratio of helium double to single ionization from 2 to 20 keV from various sources [96Le1].

1.3.9.2 Branching ratios for light elements

Although branching ratios between single, double and multiple ionization have been obtained by measuring the charge state of ions collected following photoionization for a number of elements, only for the light elements at low energies do the measurements reflect simple direct ionization processes. This is because at higher energies inner subshell ionization occurs followed by a cascade of radiative and Auger processes. Consequently the measured branching ratios must be interpreted in terms of cross sections for initial subshell ionization and relative probabilities for Auger and radiative decay processes. For neon, oxygen and nitrogen Auger processes cannot occur at energies below the 1s (K) shell ionizaton thresholds (865, 538 and 403 eV, respectively) and radiative processes are negligible. Consequently for these atoms measurements of the ratios of ions produced is a measure of direct multiple ionization.

There have been a number of measurements of the cross section for double ionization of neon between the threshold for double ionization (62.63 eV) and 280 eV and the results of various authors are shown in Fig. 28. Typically branching ratios of singly and doubly charged ions are measured and the results are put on an absolute scale by assuming that the total absorption cross section is the sum of single and double ionization cross sections. Samson and Angel [90Sa2] and Holland et al. [79Ho1] have made estimates of the double ionization cross section and their data is shown in Table 53 based on alternative values of the total cross section. Samson and Angel [88An1, 90Sa1,90Sa2] have measured the branching ratios for oxygen and nitrogen from their double ionization thresholds (48.76 and 44.15eV, respectively) to 280 eV. Using their total cross sections given in Tables 33 and 34 and their branching ratios, they have obtained cross sections for double ionization of oxygen and nitrogen and triple ionization of oxygen. Their results are given in Table 54.

Although the cross sections for double ionization of these elements are small near threshold they account for approximately 10 % of the total cross section at energies greater than 50 eV above the double ionization threshold.

Branching ratios for argon have been measured by a number of investigators and some of the earlier results for double ionization are shown in Fig. 29. For argon double ionization via Auger processes cannot take place at energies below 250 eV so the results shown in Fig. 29 represent direct double ionization. Cross sections for single, double and triple ionization in the energy range from 55 to 280 eV have been obtained by Holland et al. [79Ho1] by normalizing measured branching ratios to the total cross sections of Marr and West [76Ma1] and their results are given in Table 55. Although the double ionization cross sections are small they represent a large fraction of the total

cross sections at energies greater than 50 eV above the threshold. The double ionization cross section increases rapidly at 250 eV due to L sub shell ionization followed by Auger decay.

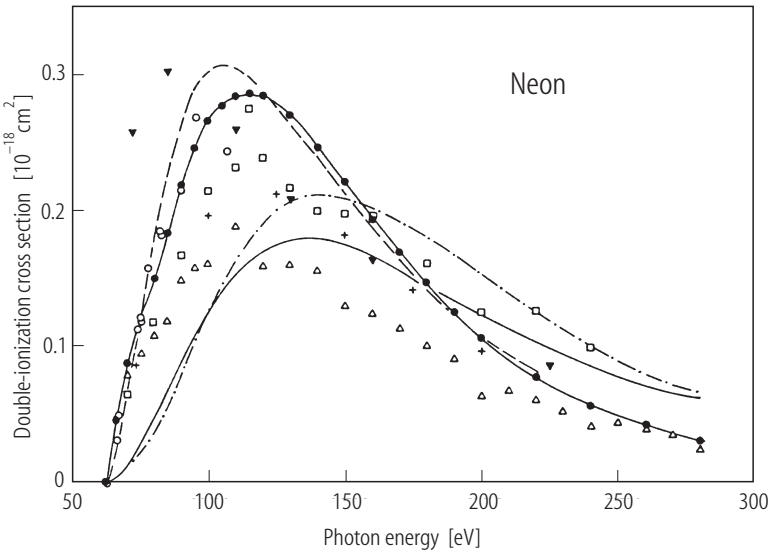

Fig. 28. Measurements of the cross section for neon double ionization from threshold (62.63 eV) to 280 eV from various sources [90Sa2].

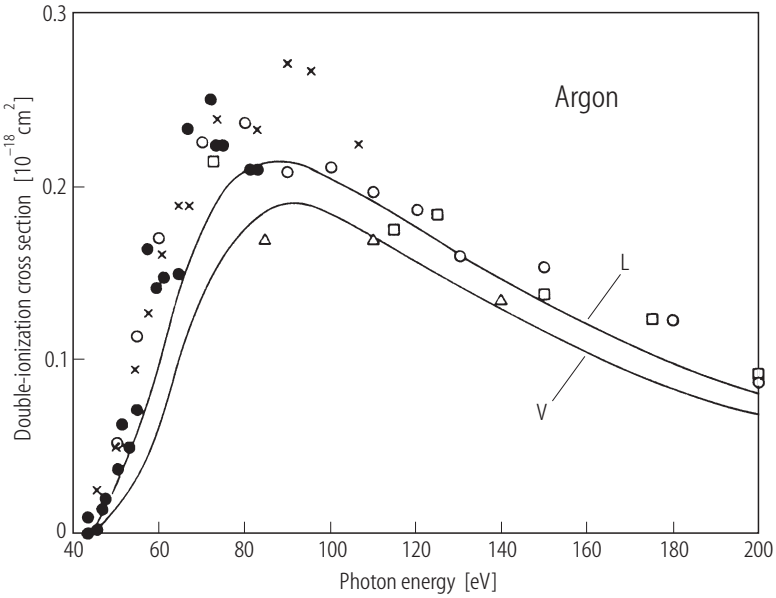

Fig. 29. Double ionization cross section for argon from various sources [A5]. Solid lines represent calculations: dipole-length (*L*) and velocity (*V*) approximation.

Table 53. Double ionization cross sections for neon at incident energies between 70 and 280 eV.

Energy [eV]	Cross section [10^{-18} cm^2]		Energy [eV]	Cross section [10^{-18} cm^2]	
	90Sa2	79Ho1		90Sa2	79Ho1
70.0	0.087	0.081	150.0	0.221	0.149
75.0	0.118	0.098	160.0	0.194	0.142
80.0	0.149	0.112	170.0	0.169	0.129
85.0	0.183	0.126	180.0	0.147	0.115
90.0	0.219	0.158	190.0	0.125	0.104
95.0	0.246	0.170	200.0	0.106	0.076
100.0	0.266	0.177	220.0	0.077	0.070
110.0	0.284	0.210	240.0	0.056	0.046
120.0	0.283	0.178	260.0	0.043	0.043
130.0	0.270	0.183	280.0	0.031	0.027
140.0	0.247	0.178			

Table 54. Double ionization cross sections for nitrogen and oxygen and triple ionization cross sections for oxygen at incident energies between 50 and 280 eV. From [90Sa1] and [88An1].

Energy [eV]	Cross section [10^{-18} cm^2]		
	σ_N^{++}	σ_O^{++}	σ_O^{+++}
50.0	0.117	0.002	
60.0	0.200	0.187	
70.0	0.186	0.225	
75.0	0.173		
80.0	0.159	0.230	
85.0	0.147		
90.0	0.135	0.221	
95.0	0.125		
100.0	0.115	0.205	
110.0	0.098	0.185	0.00028
120.0	0.084	0.164	0.00101
130.0	0.072	0.142	0.00165
140.0	0.062	0.121	0.00202
150.0	0.052	0.103	0.00220
160.0	0.043	0.084	0.00212
170.0	0.035	0.069	0.00195
180.0	0.028	0.058	0.00175
190.0	0.023	0.048	0.00151
200.0	0.019	0.039	0.00128
220.0	0.013	0.026	0.00087
240.0	0.010	0.018	0.00054
260.0	0.008	0.013	0.00037
280.0	0.008	0.011	0.00027

Table 55. Single, double and triple photoionization cross sections for argon in the energy range between 55 and 280 eV. From [79Ho1].

Energy [eV]	Cross section [10^{-18} cm^2]		
	σ^{+++}	σ^{++}	σ^{+}
55.0		0.136	1.06
60.0		0.194	1.20
65.0		0.201	1.25
70.0		0.220	1.26
80.0		0.224	1.24
90.0		0.227	1.17
100.0		0.198	1.12
110.0		0.200	1.02
120.0		0.184	0.96
130.0	0.010	0.161	0.88
140.0	0.017	0.155	0.80
150.0	0.008	0.134	0.75
160.0	0.007	0.119	0.69
170.0	0.010	0.119	0.63
180.0	0.014	0.103	0.59
190.0	0.006	0.098	0.53
200.0	0.018	0.086	0.48
210.0	0.013	0.087	0.43
220.0	0.010	0.098	0.37
230.0	0.015	0.104	0.32
240.0	0.015	0.147	0.25
250.0	0.378	3.77	0.41
260.0	0.398	3.45	0.30
270.0	0.506	3.04	0.28
280.0	0.529	2.69	0.28

1.3.9.3 Ionization plus excitation, partial subshell cross sections and angular distributions

For helium, results have already been presented for total ionization cross sections in both non resonant and resonant regions and for the ratios of double to single ionization. If electrons are collected following photoionization it is possible to obtain cross sections corresponding to ionization plus excitation, to obtain angular distributions of emitted electrons and to study the angular correlations between electrons emitted in double ionization by collecting two electrons in coincidence. Although these topics are currently being actively investigated most of the data is in the form of graphs. An example is given in Fig. 30 which shows the breakdown of the total cross section into partial cross sections corresponding to leaving the ion in various excited states obtained from various sources. Similar results for ionization plus excitation have been obtained for specific states for a number of atoms (see [A3, A8]).

For other atoms which have subshells it is possible to break down the total photoionization cross section into partial cross sections for single ionization or ionization plus excitation from various subshells. This was first done for neon by Wuilleumier and Krause [74Wu1]. Fig. 31 shows their breakdown of the total cross section from threshold to 2 keV into components which represent 1s, 2s or 2p single ionization and either ionization plus excitation or double ionization from these subshells.

Similar results are available for limited spectral ranges in all of the rare gases as well as in other elements (see [A3, A8]).

For low energy photoionization the angular distribution of any electron produced by photoabsorption will have the simple form

$$\frac{d\sigma}{d\Omega} = \frac{\sigma_n}{4\pi}[1+\frac{\beta}{2}(3\cos^2\theta - 1)] \quad (3)$$

where σ_n is the partial cross section for a particular process (single ionization or ionization plus excitation) and θ is the angle between photon polarization and electron ejection. At the "magic angle" 57.3° the differential cross section does not depend on the value of the angular distribution parameter β_n and measurements of partial cross sections are often made at this angle. However, using photoelectron spectroscopy it is possible to obtain both σ_n and β_n as functions of photon energy and such measurements have been made for a number of atoms. An example of this type of data [79Wu1] is given in Table 56 which gives the cross section for single 2p ionization and the β parameter for this process as a function of energy. Similar results are available for most of the subshells of the rare gases as well as for various excitation processes in other atoms (see [A3, A8]).

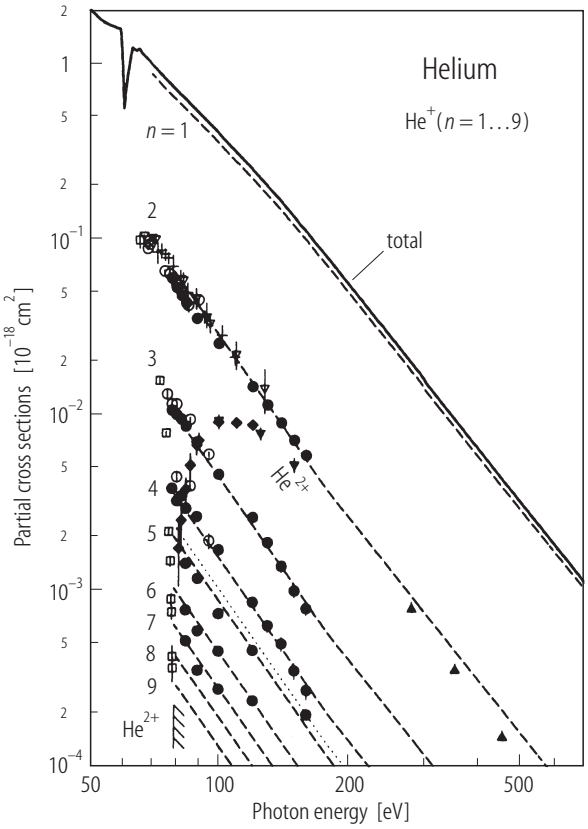

Fig. 30. Cross sections for ionization plus excitation of helium from various sources [A8].

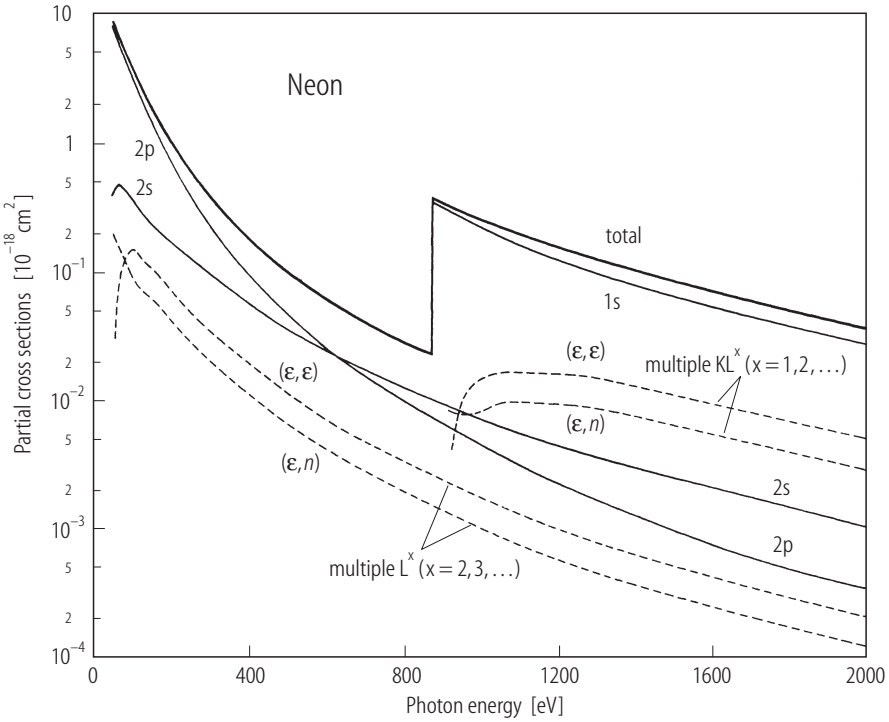

Fig. 31. Cross sections for ionization of neon inner shells and for ionization plus excitation [74Wu1].

Table 56. Photoionization cross sections and β parameters for neon 2p subshell ionization from 30 to 300 eV [79Wu1].

Energy [eV]	σ_{2p} [10^{-18} cm^2]	β	Energy [eV]	σ_{2p} [10^{-18} cm^2]
30.0	8.86	0.42	170.0	1.06
40.0	8.69	0.79	180.0	0.93
50.0	7.92	1.03	190.0	0.81
60.0	6.85	1.18	200.0	0.70
70.0	5.40	1.27	210.0	0.62
80.0	4.57	1.31	220.0	0.54
90.0	3.85	1.33	230.0	0.48
100.0	3.30		240.0	0.43
110.0	2.80		250.0	0.38
120.0	2.34		260.0	0.33
130.0	1.96		270.0	0.29
140.0	1.67		280.0	0.26
150.0	1.44		290.0	0.23
160.0	1.24		300.0	0.21

1.4 Elastic and inelastic scattering

1.4.1 Relationship of cross sections to the index of refraction and scattering factors

In contrast to the material presented in the previous two sections, there is comparatively little data on the scattering of photons from single atoms. There are two reasons for this. First, except at extremely high photon energies, the cross sections for photon scattering are much smaller than those for photon attenuation or ionization. As a result, experiments of single scattering from free atoms are more difficult and those that have been performed have been done mainly as a check on theoretical calculations rather than as a source of data to be used directly for applications. Second, while scattering from free atoms is an important process in applied fields, most of the experimental work has been performed within the basic context of scattering from aggregates of atoms. As a result, the experimental work attempts to provide information on optical constants at low energies or on scattering factors over an extended energy range which essentially provide a correction to the scattering from free electrons for each atom as a function of incident photon energy. A knowledge of the relationships between these quantities and scattering cross sections is essential to understand the experimental data and is given briefly below.

Basically, scattering from free atoms is of three types, namely:

a) Elastic scattering, where the photon transfers no energy to the atom.

b) Inelastic scattering, where there is a transfer of energy.

c) Resonant scattering, where the photon excites an atomic level which then re-emits a photon of the same energy, or the atom decays by emitting photons (or electrons) of different energies.

At low energies; i.e., below all ionization potentials inelastic scattering does not occur and the elastic scattering cross section for free atoms is simply related to the index of refraction. Resonant scattering occurs only for energies near atomic levels and results in an increase in cross sections and variations of the index of refraction known as anomalous dispersion. At higher energies inelastic scattering can occur but occurs mainly in the backward direction. Elastic and inelastic scattering are referred to as coherent or incoherent scattering or alternatively as Rayleigh (or Thomson) and Compton scattering. At higher energies resonant scattering can occur at energies near absorption edges and is termed resonant anomalous scattering. Although this is a subject of interest in molecules and solids, there have been few scattering measurements of this type for free atoms.

Since at low energies nuclear scattering and relativistic effects are negligible scattering from free atoms is assumed to be only from bound electrons. To the extent that the electrons in an atom are unbound, only elastic scattering can occur and the differential and total cross section for scattering will be given by the expressions:

$$\frac{\mathrm{d}\sigma}{\mathrm{d}\Omega} = \frac{1}{2} r_\mathrm{e}^2 (1 + \cos^2 \theta) \tag{4}$$

$$\sigma_\mathrm{tot} = \frac{8\pi}{3} r_\mathrm{e}^2 = 6.65 \cdot 10^{-25} \tag{5}$$

where $\mathrm{d}\sigma/\mathrm{d}\Omega$ is the differential cross section for scattering into angle θ, σ_tot is the total cross section and r_e is the electron radius. Coherent scattering from free atoms is modeled by defining correction factors that must be multiplied by the differential cross sections to account for the fact that the electrons are bound. Eq. 4 now becomes:

$$\frac{d\sigma}{d\Omega} = \frac{1}{2} r_e^2 (1+\cos^2\theta) f_1^2(q, Z) \tag{6}$$

where the momentum transfer q is defined in terms of the incident energy E_0 and scattering angle θ as

$$q = 2E_0 \sin\frac{\theta}{2} \tag{7}$$

and $f_1(q, Z)$ is a scattering factor which depends on the momentum transfer q (and hence the scattering angle θ)

When absorption can occur an imaginary component must be added to the scattering factor $f_2(0, Z)$ to indicate a loss of intensity in the forward direction. Both $f_1(0, Z)$ and $f_2(0, Z)$ depend on the incident photon energy and are related to one another and to the total absorption cross section. $f_2(0, Z)$ is proportional to the absorption cross section:

$$f_2(0, Z) = \frac{\pi}{2} CE\sigma(E, Z) \tag{8}$$

where $\sigma(E)$ is the absorption cross section. The constant C is 9.11 when the energy E is in eV and the cross section in barns (10^{-24}cm^2).

The forward scattering amplitude $f_1(0, Z)$ can be obtained from the absorption cross section via a dispersion relation:

$$f_1(0, Z) = Z + C\int_0^\infty \frac{\varepsilon^2 \sigma(\varepsilon, Z)}{E^2 - \varepsilon^2} d\varepsilon \tag{9}$$

The scattering factors described above depend on the atomic number Z and on photon energy E_0. One of the most important applications of the data described in the previous sections is the estimation of the scattering factor $f_1(0, Z)$ using Eq. 9. This requires a knowledge of the absorption cross section for each element over those energy ranges which make appreciable contributions to the integral in Eq. 9.

The forward scattering factor $f_1(0, Z)$ is also related to the index of refraction. The relationship is:

$$n = 1 - \delta\,;\ \delta = 2.72\cdot 10^{10}\ \lambda^2 f_1(0, Z) \tag{10}$$

where n is the index of refraction and λ the wavelength in Å.

Although inelastic scattering is important in molecules and solids at low energies; e.g., below 100 eV, the cross sections are negligible for all atoms compared to those for photoabsorption and elastic scattering. At higher energies the Compton effect has been studied mainly at large angles where it is possible to resolve photons elastically and inelastically scattered. In analogy to elastic scattering, inelastic scattering from free atoms is modeled by defining a correction factor which multiplies the free electron differential cross section for Compton scattering given by the Klein-Nishima formula:

$$\frac{d\sigma_{KN}}{d\Omega} = \frac{r_e^2}{2}[1+k(1-\cos\theta)]^{-2}\left[1+\cos^2\theta + \frac{k^2(1-\cos\theta)^2}{1+k(1-\cos\theta)}\right] \tag{11}$$

where θ is the scattering angle and k is the photon energy in mc^2 units (511 keV).

As for elastic scattering, atomic effects are modeled by multiplying by an incoherent scattering factor $S(q, Z)$ which depends on q, the momentum transferred in the collision and atomic number Z. The differential cross section is then:

$$\frac{d\sigma}{d\Omega} = \frac{d\sigma_{KN}}{d\Omega} S(q, Z) \tag{12}$$

and the total cross section can be obtained by integrating over all angles.

As stated previously, there has been little experimental work on scattering from free atoms although there have been theoretical calculations of form factors as described above and direct calculations of scattering cross sections for both elastic and inelastic scattering. The available experimental data falls into the following categories which will be described below:

A. Measurements of the index of refraction at energies below all excitation thresholds.

B. Measurements of elastic scattering cross sections at specific wavelengths both at low energies and in the X-ray range.

C. Measurements of inelastic scattering at high energies on solids where it is assumed that the atoms in the solid scatter as free atoms.

In order to show the relative importance of scattering and absorption, Table 57 gives theoretical estimates of the total cross sections for absorption,elastic and inelastic scattering from rare gases and hydrogen at various energies. Note that scattering is orders of magnitude smaller than absorption for all elements at energies below 100 eV, but becomes important for light elements in the energy range between 1 and 10 keV. For heavier elements scattering is negligible for energies below 10 keV but becomes important for all elements at energies above 100 keV.

Table 57. Cross sections for photoabsorption, coherent and incoherent scattering from [73Ve1].

Element	Energy [keV]	Cross section [10^{-24} cm^2]		
		Absorption	Coherent	Incoherent
Hydrogen	0.1	19300	0.664	0.001
Helium	0.1	359000	2.66	0.0008
Neon	0.1	4110000.0	66.5	0.0021
Argon	0.1	1310000.0	215.0	0.006
Hydrogen	1.0	10.9	0.579	0.085
Helium	1.0	413.0	2.52	0.072
Neon	1.0	266000.0	63.6	0.186
Argon	1.0	210000	202.0	0.471
Hydrogen	10	0.0046	0.0416	0.599
Helium	10	0.191	0.395	1.08
Neon	10	380	13.4	3.96
Argon	0	4120.0	49.2	6.18
Argon	100	3.7	1.4	8.5
Krypton	100	74.0	8.2	16.2
Xenon	100	383.0	23.0	23.7

1.4.2 Measurements of the index of refraction

The indices of refraction of the rare gases were measured by Cuthbertson and Cuthbertson in 1910 [10Cu1] at a number of wavelengths in the visible spectrum and much later the measurements for helium and neon were extended to shorter wavelengths [32Cu1].
This and other early work was found to be well represented by the simple formula:

$$n-1=\frac{C}{\nu_0^2-\nu^2} \tag{13}$$

Tables of the constants ν_0 and C for all of the rare gases and the ranges of wavelengths where the formula is valid are given in a review article by Korft and Breit [32Ko1]. A table of the values of $n - 1$ for wavelengths between 6200 and 2300 Å is given by Larsen [62La1]. Actually, all of the earlier measurements of the index of refraction made by various authors where there is no anomalous dispersion agree very well. This is demonstrated in Fig. 32 where the measurements of Cuthbertson and Cuthbertson are compared with the tabulated data of Larsen. The agreement is better than 1 %. Table 58 gives the index of refraction for neon as measured by Cuthbertson and Cuthbertson [32Cu1]. This table along with the tabulation given in [62La1] provided a compete set of experimental data in the normal dispersion range for all of the rare gases.

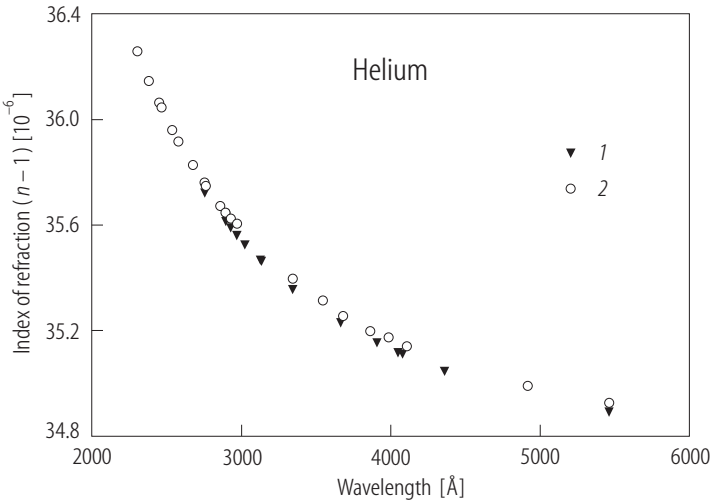

Fig. 32. Index of refraction of helium from *1* [10Cu1] and *2* [62La1].

Table 58. Refractive index of neon [32Cu1].

Wavelength [Å]	$(n-1)\cdot 10^6$	Wavelength [Å]	$(n-1)\cdot 10^6$
5462.23	67.250	3664.10	67.891
4917.40	67.372	3342.42	68.129
4359.54	67.540	3132.59	68.324
4078.97	67.662	3022.37	68.447
4047.68	67.675	2968.13	68.516
3907.56	67.744	2894.44	68.612

1.4.3 Measurements of elastic scattering

Although there were some earlier measurements of elastic scattering cross sections to compare with refractive indices [21Ca1, 25Da1, 51Va1], the major emphasis of this type of work was the study of polarization upon scattering in an attempt to obtain the polarizability of molecules. Definitive measurements on the rare gases were not done until the 1960's using ruby laser light (6943 Å) or Lyman α (1216 Å). The elastic differential cross section in these measurements is expressed as:

$$\frac{d\sigma}{d\Omega} = \sigma_R\left[(1-\rho)\cos^2\theta + \rho\right] \qquad (14)$$

where ρ is a depolarization ratio. For both atoms and molecules one expects a $\cos^2\theta$ distribution ($\rho = 0$) for horizontal polarization and an isotropic distribution ($\rho = 1$) for vertical polarization since the angular distribution depends only on the direction relative to the polarization of the incident beam. George et al. [63Ge1, 65Ge1] obtained a $\cos^2\theta$ distribution for horizontal polarization of 6943 Å light on argon and xenon but did not obtain a isotropic distribution for vertically polarized light. Subsequent experiments made on nitrogen molecules using 6943 Å [65Wa2, 68Ru1] gave an isotropic distribution for vertically polarized light in agreement with theory. The Rayleigh cross section σ_R is related to the index of refraction by:

$$\sigma_R = \frac{4\pi^2 (n-1)^2}{N^2 \lambda^4} \tag{15}$$

where N is Loschmidt's number $2.687 \cdot 10^{19}$ cm^{-3}; i.e., the number of atoms/cm^3 in an ideal gas at standard temperature and pressure and λ is the wavelength in cm. Table 59 gives the measured values obtained for σ_R for the rare gases and some molecular gases [65Ge1, 68Ru1] as well as the cross section obtained from the measured values of the index of refraction [62La1]. The results of 68Ru1 agree very well with the refractive index data. Both measurements were absolute.

Measurements of the refractive index or σ_R at 1216 Å for argon, krypton xenon and molecular hydrogen and nitrogen were made by Gill and Heddle [63Gi1] and of helium, neon, argon and molecular hydrogen and nitrogen by Shardanand and Mikawa [67Sh1]. Neither of these measurements were absolute, but they normalized using previous refractive index measurements [62He1] for nitrogen or theory [65Ch1] for helium. Table 60 gives the results of all of these measurements using the theoretical normalization.

In the X-ray range of energies (1…30 keV) there were a number of experiments performed before 1932 which measured the total scattering cross sections for various gases and both theoretical [31Wo1] and experimental work during that period has been summarized by Wollin [32Wo1]. Experiments were performed on helium,neon, argon and mercury and as well as hydrogen,oxygen and nitrogen in molecular form and the results compared with theoretical calculations. Practically all of the work was presented in graphical form and compared with theory. In these early experiments it was impossible to separate coherent and incoherent scattering, but the agreement with theory was remarkably good in most cases. Since it was assumed that the cross sections depended only on momentum transfer what was plotted was the scattering per electron as a function of momentum transfer, $\sin(\theta/2)/\lambda$ where θ is the scattering angle and λ the wavelength in Å (10^{-8} cm). An example of this type of experiment is shown in Fig. 33 for helium. The measurements were made at wavelengths of 0.39 [28Ba1] and 0.71 Å [31Wo2], (31.8 and 17.4 keV). The theoretical calculations are by Waller and Hartree [29Wa1].

A careful set of measurements were made by Chipman and Jennings [63Ch1] using 17.4 keV radiation for neon, argon, krypton and xenon. Their results are shown in Table 61. Their results for neon and argon are in good agreement with the earlier work of Wollin [31Wo2]. In order to estimate the elastic scattering form factor $f(q, Z)$ they estimated the cross sections due to inelastic scattering from theory and used measured values of the absorption cross section to correct their measured results. The results for all gases showed good agreement with theoretical calculations as shown in Table 62. The calculated form factors are from various sources (see [63Ch1]).

Ice et al. [78Ic1] measured cross sections for helium and molecular hydrogen at several energies and two angles using synchrotron light. Their results, when normalized to theory showed good agreement with theoretical calculations as shown in Table 63 for both gases. They also made absolute measurements at several energies and found that the measured cross sections were somewhat lower than theory, but within their estimated error.

Smend and Czerwinski [86Sm1] made measurements of the elastic scattering of 59.54 keV photons from krypton and xenon at angles between 20 and 120°. The measurements were compared with calculations of the scattering cross sections which included a small contribution for nuclear scattering. The results are shown in Table 64. The calculations in this case [80Ki1] are direct

calculations of the differential cross sections for elastic scattering which do not make the approximations inherent in using form factors.

There have been no measurements of inelastic scattering cross sections for free atoms or, alternatively measurements of the incoherent scattering factor $S(q, Z)$ for free atoms. However, there have been a number of measurements of this type for solids at energies where it is reasonable to expect the atoms in the solid to scatter as free atoms. An example of this type of data is given in Table 65 which compares the measured differential cross sections for a number of elements for scattering of 59.5 keV radiation at 120° [94Ku1] to those obtained via theory [75Hu1]. At this value of momentum transfer peaks due to inelastic and elastic scattering can be resolved so that only inelastic scattering is measured. The measurement in this case was normalized to the theoretical differential cross section for aluminum.

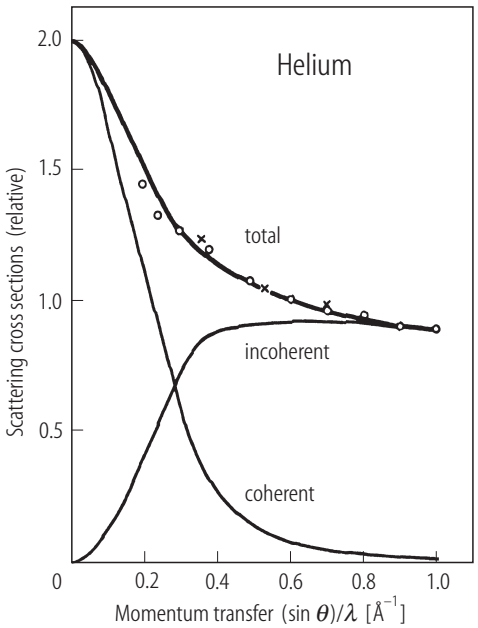

Fig. 33. Cross sections for scattering of 17.4 and 31.8 keV photons by helium from various sources [32Wo1].

Table 60. Rayleigh cross sections for scattering by 1216 Å light. From [63Gi1] and [67Sh1], theory [65Ch1].

Gas	Cross section [10^{-26} cm^2]	
	Experiment	Theory
He	0.41	0.41
Ne	1.8	1.7
Ar	76.0	76.0
Kr	714.0	
Xe	$2.3 \cdot 10^4$	
N_2	77.0	
H_2	26.0	

Table 59. Cross sections for elastic scattering by 6943 Å light.

Gas	Cross section [10^{-28} cm^2]		
	65Ge1	68Ru1	62La1
He	-	0.0296 ± 0.0014	0.0284
Ne	0.228	-	0.108
Ar	4.04	1.88 ± 0.09	1.85
Xe	27.4	11.55 ± 0.55	11.38
N_2	5.0	2.12 ± 0.09	2.10
H_2		0.438 ± 0.026	0.449
D_2		0.431 ± 0.021	0.449
N_2O		6.40 ± 0.31	6.40
CH_4		4.56 ± 0.22	4.49

Table 61. Measured values of $f_1^2(q, Z)$ (see eqs. 6 and 7) for the rare gases [63Ch1] before making corrections for absorption and inelastic scattering.

Neon		Argon		Krypton		Xenon	
θ	f_1^2	θ	f_1^2	θ	f_1^2	θ	f_1^2
3.76°	9.88	3.69°	17.72	3.73°	34.7	3.74°	52.8
4.59°	9.79	4.53°	17.54	4.57°	34.5	4.56°	52.4
7.33°	9.49	7.28°	16.77	7.31°	33.2	7.31°	50.5
10.22°	9.03	10.18°	15.71	10.20°	31.6	10.21°	48.2
14.13°	8.37	14.09°	14.14	14.13°	29.2	14.14°	44.7
22.05°	6.79	22.03°	11.40	22.08°	25.1	22.09°	38.7
27.02°	5.94	27.03°	10.20	27.07°	22.9	27.07°	35.8
32.01°	5.24	32.03°	9.36	32.06°	21.0	32.06°	33.0

Table 62. Estimated contributions of inelastic scattering f_{in} and absorption f_2 to the measurements shown in Table 60 and comparison of corrected f_1 (eqs. 6 and 7) with theory (f_{th}).

Gas	θ	f_{in}	f_2	f_1	f_{th}
Neon	3.76°	0.2	0.02	9.87	9.86
	4.59°	0.3	0.02	9.78	9.79
	7.33°	0.7	0.02	9.46	9.47
	10.22°	1.2	0.02	8.97	9.01
	14.13°	2.0	0.02	8.26	8.26
	22.05°	3.7	0.02	6.51	6.59
	27.02°	4.6	0.02	5.54	5.61
	32.01°	5.4	0.02	4.70	4.76
Argon	3.69°	0.6	0.20	17.71	17.62
	4.53°	0.8	0.20	17.52	17.43
	7.27°	1.7	0.20	16.72	16.61
	10.18°	2.7	0.20	15.63	15.50
	14.09°	4.3	0.20	13.99	13.85
	22.03°	6.7	0.20	11.10	10.92
	27.03°	7.8	0.20	9.81	9.61
	32.03°	8.8	0.20	8.88	8.68
Krypton	3.73°	1.0	2.8	34.61	35.41
	4.57°	1.0	2.8	34.34	35.12
	7.31°	2.0	2.8	33.05	33.88
	10.20°	4.0	2.8	31.43	32.24
	14.13°	6.0	2.8	29.00	29.83
	22.08°	9.0	2.8	24.80	25.50
	27.07°	11.0	2.8	22.43	23.40
	32.06°	12.0	2.8	20.54	21.63
Xenon	3.73°	1.0	2.2	52.70	53.06
	4.56°	1.0	2.2	52.30	52.62
	7.31°	4.0	2.2	50.38	50.71

Gas	θ	f_{in}	f_2	f_1	f_{th}
Xenon	10.21°	6.0	2.2	48.07	48.24
	14.14°	8.0	2.2	44.58	44.76
	22.09°	14.0	2.2	38.48	38.69
	27.07°	16.0	2.2	35.41	35.67
	32.06°	18.0	2.2	32.68	33.03

Table 63. Deviations of the measured relative differential cross sections of H_2 and helium from theoretical predictions ([75Be1] for H_2 and [73Br1] for helium).From [78Ic1]. [1]) Normalization point.

Gas	θ	Energy [keV]	$\frac{(d\sigma/d\Omega)_{exp}}{(d\sigma/d\Omega)_{theor}}$
He	60.9°	6.0	1.001
	135.6°	6.0	0.987
	60.9°	2.0	0.987
	135.6°	12.0	1.00 [1])
H_2	60.9°	5.0	0.996
	60.9°	6.0	1.007
	60.9°	7.0	0.986
	135.6°	5.0	1.001
	135.6°	6.0	1.005
	135.6°	7.0	1.00 [1])

Table 64. Experimental and theoretical differential cross sections for elastic scattering of 59.54 keV photons from krypton and xenon. Cross sections are in units of 10^{-24} cm^2 sr^{-1}. Theoretical values are from [80Ki1]. From [86Sm1].

θ	Krypton		Xenon	
	Experiment	Theory	Experiment	Theory
20°	11.86(20)	11.17	32.00(71)	30.24
30°	4.43(11)	4.190	16.62(32)	15.71
40°	2.38(5)	2.317	9.18(19)	8.067
50°	1.44(3)	1.467	4.74(11)	4.058
60°	0.888(22)	0.924	2.56(6)	2.292
70°	0.524(14)	0.579	1.67(4)	1.519
80°	0.350(6)	0.380	1.24(3)	1.149
90°	0.273(8)	0.272	1.07(3)	0.960
100°	0.221(7)	0.217	0.904(20)	0.867
110°	0.200(7)	0.191	0.873(23)	0.831
120°	0.179(6)	0.182	0.847(22)	0.830

Table 65. Experimental and theoretical differential cross sections for inelastic scattering of 59.54 keV photons at 120° from various elements. Cross sections are in units of 10^{-24} cm^2 sr^{-1}. Theoretical values are from [75Hu1]. Experimental values from [94Ku1].

Element (Z)	Cross section	
	Experiment	Theory
Ti (22)	0.8271	0.8306
Ni (28)	1.0336	1.0441
Zn (30)	1.1049	1.1159
Se (34)	1.2048	1.2558
Mo (42)	1.4326	1.5326
Ru (44)	1.4214	1.6019
Cd (48)	1.6615	1.7340
Sn (50)	1.6416	1.7898
Te (52)	1.6916	1.8662
Yt (70)	1.8813	2.4056
W (74)	1.9985	2.5467
Pb (82)	2.1043	2.7928

Appendix: Alternative sources of data

The aim of the present chapter has been to present critically evaluated experimental data on photon ionization and scattering from free atoms. This data base is necessarily incomplete since measurements covering the whole spectral range from the ionization threshold to 10 keV have only been made for rare gas atoms. However there are additional sources of data that may be used which are not covered in this report. Basically, these sources are of four different types, namely:

A. Other review articles which include data or references not presented here
B. Measurements made of molecules and/or solids
C. Theoretical calculations
D. Data bases which have been assembled for specific applications
E. On line data

Brief descriptions of these sources will be given here.

A. Other review articles

There have been a number of reviews which contain material similar to that reported here [A1-A8]. The entire subject of atomic photoionization was reviewed in 1982 by J. A. R. Samson [A5]. and the experimental techniques used discussed [A4] and these references are still useful, since they contain a comprehensive history of the subject, a discussion of experimental techniques and attempts to reference all of the experimental data available at that time. This work is complimented by the book by J. Berkowitz [A3] which, in addition to presenting much of the available data on both atoms and

molecules surveys the theory of the various processes. The chapters on partial cross sections and the angular distribution of photo electrons are especially useful.

More recently, Schmidt [A6] has provided a comprehensive review of the more recent work on rare gas photoionization using synchrotron radiation. He discusses recent theoretical and experimental developments and provides a detailed bibliography. Sonntag and Zimmermann [A7] have reviewed the recent work on relative measurements of metallic vapors using synchrotron sources. Finally, a recent book [A8] contains much useful information about recent photoionization measurements in atoms molecules and solids principally using synchrotron sources. The chapter on partial cross sections and angular distributions is particularly useful and provides much more detailed information than is contained in Section 1.3.

B. Measurements made on molecules and solids

Although photon processes on molecules and solids are not the subject of this report information of them particularly at higher energies where most of the photoionization comes from inner shells and is expected to be approximately the same as for free atoms. At lower energies information on the photoionization of molecules can be found in [A3, A8]. For oxygen and nitrogen a useful source is the compilation of Fennelly and Torr [92Fe1]. In the energy range above 100 eV most of the experimental data on photon attenuation has been tabulated by Saloman et. al. [A9, A10] for all elements and compared with theoretical calculations. The tabulation is extremely useful since the data is presented in both graphical and tabulated form. This data base in fact served as a starting point for the present tabulation.

C. Theoretical calculations

Since there is little or no data for most atoms, one must rely on theoretical calculations for those cases where no data exits. Such calculations have been carried out for photoionizaton, elastic and inelastic scattering over the entire energy range considered here and for all elements [A11-A16]. Early tabulations based on theory have been quoted previously, namely [73Ve1] which gives photoionization, elastic and inelastic scattering cross sections from 100 eV to 1 MeV for all elements based mostly on theoretical calculations, [73Sc1] which gives photoionization cross sections for all elements from 1 keV to 1.5 MeV, [79Re1] which gives photoionization cross sections for atoms and charged ions from 5 eV to 5 keV and for $Z < 31$, and [75Hu1] which gives elastic and inelastic scattering cross sections from 100 eV to 10 MeV for all elements. Other similar tabulations [A11-A14] have been made and may be useful for specific applications.

D. Data bases that have been assembled for specific purposes

While there are a number of data bases that contain data on photoionization and scattering cross sections we list here only those that are based largely on experimental information which has been supplemented by theoretical calculations. Photoionization cross sections for all elements are available in the energy range from 100 eV to 100 keV [A10] which are based on theoretical calculations [73Sc1]. The tabulation lists also experimental results for each element and compares both graphically and in tabular form the experimental results with theory. References to all of the experimental papers quoted are given. Similar data over a broader energy range is available in [A17, A18]. Data for photoionization, and elastic and inelastic form factors for all elements in the energy range from 50 eV to 30 keV which are based on a careful analysis of all of the available experimental and theoretical data available is given in [A19]. The data for photoionization given in this reference is compared with that of [A10] in some detail in [A9]. A tabulation similar to that of [A19] based solely on theoretical cross sections is also available [A16].

E. On line data

It is possible to obtain data on photoionization via the world-wide web from a number of sources. One of the easiest ways at present to obtain access to these sources is to contact directly one of two

addresses, namely ORNL (Oak Ridge National Laboratory; http://www-cfadc.phy.ornl.gov/) or the Weizmann Institute (http://plasma-gate.weizmann.ac.il/). Both of these sources maintain links to data bases which contain both numerical and bibliographic information on photoionization and scattering processes.

Currently the main links to data bases from ORNL which contain data on photon processes are the atomic data base for astrophysics at the University of Kentucky, which contains theoretical cross sections for photoionization; the Corex Data base at McMaster University, which provides data on inner shell excitation processes for atoms and molecules and Topbase, the data base for opacity at the University of Strasbourg which provides theoretical photoionization cross sections for atoms and ions for light elements. The most useful links that can be reached from the Weizmann address are the Interactive Elastic-Atom Scattering Database at Lawrence Livermore Laboratories, which provides theoretical cross sections for elastic photon scattering for all elements and DABAX, the data base for X-rays of the European Synchrotron Radiation Facility, which provides on lie X-ray scattering factors and photoabsorption cross sections from various tabulations, and the Henke Scattering Factors data base, maintained by Uppsala University which provides the scattering factors of [A19] online.

References for 1

10Cu1 Cuthbertson, C., Cuthbertson, M.: Proc R. Soc. London A **84** (1910) 13.

21Ca1 Cabannes, J.: Ann. Phys. **15** (1921) 5.

25Da1 Daure, P.: C. R. **180** (1925) 2032.

28Ba1 Barrett, C.S.: Phys. Rev. **32** (1928) 223.

29Wa1 Waller, I., Hartree, D.R.: Proc. R. Soc. A **124** (1929) 119.

30Co1 Colvert, W.W.: Phys. Rev. **36** (1930) 1619-1624. (5.42-25.0 keV: Ne, Ar)

30Wo1 Woernle, B.: Ann. Phys. (Leipzig) **5** (1930) 475-506. (1.254-5.946 keV: Ne, Ar)

31De1 Dershem, E., Schein, M.: Phys. Rev. **37** (1931) 1238-1245. (0.277 keV: He, Ne, Ar, Kr, Xe)

31Sp1 Spencer, R.G.: Phys. Rev. **39** (1932) 178 (see also: Phys. Rev. **38** (1931) 1932). (1.778-8.066 keV: Ar)

31Wo1 Woo, Y.H.: Proc Nat. Acad. Sci **17** (1931) 467.

31Wo2 Wollan, E.O.: Phys. Rev **37** (1931)862.

32Cu1 Cuthbertson, C., Cuthbertson, M.: Proc R. Soc. London A **135** (1932) 44.

32Cr1 Crowther, J.A., Orton, L.H.H.: Philos. Mag. **13** (1932) 505-523 (see also: Philos. Mag. **10** (1930) 329-342). (6.407-8.056 keV: Ar)

32Ko1 Korft, S.A., Breit, G.: Rev. Mod. Phys. **4** (1932) 471.

32Wo1 Wollan, E.O.: Rev. Mod Phys. **4** (1932) 205.

33Be1 Beutler, H., Guggenheimer, K.: Z. Phys. **87** (1933) 176.

33Be2 Beutler, H.: Z. Phys. **85** (1933) 710.

34Be1 Beutler, H., Guggenheimer, K.: Z. Phys. **88** (1934) 25.

34Be2 Beutler, H., Guggenheimer, K.: Z. Phys. **88** (1934) 141.

35Be1 Beutler, H.: Z. Phys. **93** (1935) 177.

51Va1 Vaucouleurs, G.: Ann. Phys. **6** (1951) 211.

53Di1 Ditchburn, R.W., Jutsum, P.J., Marr, G.V.: Proc. R. Soc. London A **219** (1953) 89.

55Eh1 Ehler, A.W., Weissler, G.L.: J. Opt. Soc. Am. B **6** (1955) 2326-2330. (18-30 eV: N)

55Le1 Lee, P., Weissler, G.L.: Phys. Rev. **99** (1955) 540-542. (0.0147-0.0517 keV: He, Ar)

57Be1 Bethe, H.A., Salpeter, E.E.: Quantum Mechanics of one- and two-electron atoms, New York: Academic Press (1957), p. 304.

58Mo1 Moore, C.E.: Atomic Energy levels NBS Circular **467** (1958).

59Ga1 Garton, W.R.S., Codling, K.: Proc. Phys. Soc. London A **75** (1959) 87.
60Pe1 Pery-Thorne, A., Garton, W.R.S.: Proc. Phys. Soc. London **76** (1960) 833-843. (0.01463-0.02465 keV: Kr)
62Ba1 Baker, D. J., Tombouulian, D.U.: Phys. Rev. **128** (1962) 677-680. (45.5-153.87 eV: Li)
62Bu1 Buckman, W.G.: Thesis, Vanderbilt Univ., Tenn. (1962). (6.-24. keV: Ar)
62He1 Heddle,D.W.O.: JQSRT **2** (1962) 349.
62La1 Larsen, R., in: Zahlenwerte and Funktionen aus Physik, Chemie, Astronomie, Geophysik und Technik, Vol. II, part 8, Berlin: Springer (1962), p. 6-82.
63Ch1 Chipman, D.R., Jennings, L.D.: Phys. Rev. **37** (1963) 862.
63Ge1 George, T.V., Slama, L., Yokoyama, M., Goldstein, L.: Phys. Rev. Lett. **11** (1963) 403.
63Gi1 Gill, P., Heddle, D.W.O.: J. Opt. Soc. Am. **53** (1963) 847.
63Ma1 Madden, R.P., Codling, K.: Phys. Rev. Lett. **10** (1963) 516.
63Lu1 Lukirskii, A.P., Zimkina, T.M.: Izv. Akad. Nauk SSSR **27** (1963) 808-811; Engl. Transl. in: Bull. Acad. Sci. USSR, Phys. Ser. **27** (1963) 817-820. (0.0493-3.10 keV: Ar)
63Sa1 Samson, J.A.R.: Phys. Rev. **132** (1963) 2122.
64Al1 Alexander, R.W., Ederer, D.L., Tomboulian, D.H.: Bull. Am. Phys. Soc. (Ser. 2) **9** (1964) 626. (40.8-117.7 eV: Ar)
64Ed1 Ederer, D.L.: Phys. Rev. Lett. **13** (1964) 760-762. (0.0455-0.154 keV: Xe)
64Lu1 Lukirskii, A.P., Brytov, I.A., Zimkina, T.M.: Opt. Spectrosc. **17** (1964) 234-237. (0.04949-0.5253 keV: He, Kr, Xe)
64Ru1 Rustgi, O.P.: J. Opt. Soc. Am. **54** (1964) 464-466. (0.0125-0.0742 keV: Ar)
64Ru2 Rustgi, O.P., Fisher, E.I., Fuller, C.H.: J. Opt. Soc. Am. **54** (1964) 745-746. (0.0135-0.0541 keV: Kr, Xe)
65Be1 Beynon, J.D.E., Cairns,R.B.: Proc. Phys. Soc. **86** (1965) 1343-1349. (0.014576 keV: H)
65Ch1 Chan, Y.M., Dalgarno, A.: Proc. Phys. Soc. London **85** (1965) 227.
65Ge1 George, T.V., Goldstein, L, Yokoyama, M.: Phys. Rev. **137** (1965) 369.
65Ro1 Ross, K.J., Marr, G.V.: Proc.Phys. Soc. London **85** (1965) 193. (9-10.8 eV: Cd)
65Sa1 Samson, J.A.R.: J. Opt. Soc. Am. **55** (1965) 935-937. (0.02156-0.04379 keV: Ne)
65Wa2 Watson, R.D., Clark, M.D.: Phys. Rev. Lett. **14** (1965) 1057.
66Be1 Bearden, A.J.: J. Appl. Phys. **37** (1966) 1681-1692. (0.852-40. keV: He, Ne, Ar)
66Be2 Beynon, J.D.E.: Proc. Phys. Soc. **89** (1966) 59-61. (0.01476-0.015 keV: H)
66Lu1 Lukirskii, A.P., Brytov, I.A., Gribovskii, S.A.: Opt. Spektrosk. **20** (1966) 368-369; Engl. Transl. in: Opt. Spectrosc. **20** (1966) 203-204. (0.279-1.776 keV: Xe)
66Sa1 Samson, J.A.R.: Adv. At. Mol. Phys. **2** (1966) 177-261. (0.0122-0.0592 keV: He, Ne, Ar, Kr, Xe)
67Co1 Codling, K., Madden, R.P., Ederer, D.L.: Phys. Rev. **155** (1967) 26.
67He1 Henke, B.L., Elgin, R.L., Lent, R.E., Ledingham,R.B.: Norelco Rep. **14** (1967) 112-131. (0.1089-1.487 keV: He, Ne, Ar, Kr, Xe)
67Hu1 Hudson, R.D., Carter, V.L.: J. Opt. Soc. Am. **57** (1967) 1471-1474. (0.00434-0.02021 keV: K)
67Hu2 Hudson, R.D., Carter, V.L.: J. Opt. Soc. Am. **57** (1967) 651-654. (0.00514-0.02156 keV: Li, Na)
67Hu3 Huffman, R.E., Larrabee, J.C., Tanaka,Y.: J. Chem. Phys. **46** (1967) 2213.
67Sh1 Shardanand, Mikawa, Y.: JQSRT **7** (1967) 605.
68Be1 Berkowitz, J., Lifshitz, C.: J. Phys. B **1** (1968) 438-44. (8.99-18 eV:Cd, Hg).
68Co1 Comes, F.J., Speier, F., Elzer, A.: Z. Naturforsch. A **3** (1968) 125-133. (13-28 eV: O)
68Co2 Comes, F.J., Elzer, A.: Z. Naturforsch. A **23** (1968) 133-136. (14-30 eV: N)
68Hu1 Hudson, R.D., Carter, V.L.: J. Opt. Soc. Am. **58** (1968) 430-431. (17.711-24.796 eV: Na)
68Ma1 Marr, G.V., Creek, D.M.: Proc. R. Soc. A **304** (1968) 233.

68Ru1 Rudder, R.R., Bach, P.R.: J. Opt. Soc. Am. **58** (1968) 1260.

69Ca1 Cairns, R.B., Harrison, H., Schoen, R.I.: J. Chem. Phys. **53** (1969) 5440-5443. (9- 83 eV: Cd, 27- 65 eV: Zn)

69De1 Deslattes, R.D.: Phys. Rev. **186** (1969) 1.

69Ha1 Harrison, H., Schoen, R.I., Cairns, R.B., Schubert, K.E.: J. Chem. Phys. **50** (1969) 3930-3936. (9.97 -50.19 eV: Zn)

69Ha2 Haensel, R., Keitel, G., Schreiber, P., Kunz, C.: Phys. Rev. **188** (1969) 1375-1380 (see also: Schreiber, P.: Internal Report DESY-F41-69/6 (1970)). (0.064-0.500 keV: Kr, Xe)

69Ma1 Madden, R.P., Ederer, D.L., Codling, K.: Phys. Rev. **177** (1969) 136.

69Ma2 Marr, G.V., Austin, J.M.: J. Phys. B **2** (1969) 107-114. (9.47-16.6 eV: Zn)

69Ma3 Marr, G.V., Austin, J.M.: Proc. R. Soc. A **310** (1969) 137. (9-23 eV: Cd)

69We1 Wiese, W.L., Smith, M.W., Glennon, B.M.: Atomic Transition Probabilities Vol. I.II NRSDS-NBS-4,22 (1966,1969).

69Wu1 Wuilleumier, F.: Thesis, Lab. Chim. Phys., Paris (1969) (see also: C. R. Acad. Sci. **257** (1963) 855-858; ibid **269** (1969) 968-971; J. Phys. (Paris) **26** (1965) 776-784; Phys. Rev. A **6** (1972) 2067-2077). 0.825-8.247 keV: Ne, Ar, Kr, Xe)

70Ca1 Cairns, R.B., Harrison, H., Schoen, R.I.: J. Chem. Phys. **53** (1970) 96-101. (10-72 eV: Hg)

70De1 Denne, D.R.: J. Phys. D **3** (1970) 1392-1398. (0.151-0.523 keV: He, Ne, Ar)

70Ed1 Ederer, D.L., Lucatorto, T., Madden, R.P.: Phys. Rev. Lett. **25** (1970) 1537.

70He1 Henke, B.L., Elgin, R.L.: X-Ray Absorption Tables for the 2- to 200 Å Region, Adv. X-Ray Anal. **13** (1970) 639-664.

70Mc1 McCrary, J.H., Looney, L.D., Atwater, H.F.: J. Appl. Phys. **41** (1970) 3570-3572. (5.895 keV: He)

70Mc2 McCrary, J.H., Looney, L.D., Constanten, C.P., Atwater, H.F.:Phys. Rev.A **2** (1970) 2489-2497 (see also: McCrary, J.H., Ziegler, L.H., Looney, L.D.: J. Appl. Phys. **40** (1969) 2690-2693. (4.508-145.43 keV: Ne, Ar, Kr, Xe)

70Hu1 Hudson, R.D., Carter, V.L., Young, P.A.: Phys. Rev. A **2** (1970) 643. (5.2-7.3 eV:Ba)

71Ed1 Ederer, D.L.: Phys. Rev. A **4** (1971) 2263.

72Co1 Codling, K., Madden, R.P.: J. Res. Natl. Bur. Stand. A **76** (1972) 1.

72Wa1 Watson, W.S.: J. Phys. B **5** (1972) 2292-2303. (0.0631-.2335 keV: He, Ne, Ar)

72Wo1 Wolff, H.W., Radler, K., Sonntag, B., Haensel, R.: Z. Phys. **257** (1972) 353-368. (30- 160 eV: Na)

73Br1 Brown, C.M., Tilford, S.G., Ginter, M.L.: J. Opt. Soc. **63** (1973) 1454.

73Ca1 Carlson, R.W., Judge, D.L., Ogawa, M., Lee, L. C.: Appl. Opt. **12** (1973) 409-412. (0.0177-0.0681 keV: Ar)

73Ca2 Carlsten, J.L., McIlrath, T.C.: J. Phys. B **6** (1973) L284.

73De1 Dehmer, P.M., Berkowitz, J., Chupka,W.A.: J. Chem. Phys. **59** (1973) 5777.

73Sc1 Scofield, J.H.: Theoretical Photoionization Cross Sections from 1 to 1500 keV, Lawrence Livermore National Laboratory Report UCRL-51326 (1973).

73Ve1 Veigele, Wm.J.: Photon Cross Sections from 0.1 keV to 1 MeV for Elements $Z = 1$ to $Z = 94$, At. Data **5** (1973) 51-111.

74Co1 Cooper, J.W.: Phys. Rev. A **9** (1974) 2236.

74De1 Dehmer, J.L., Berkowitz, J.: Phys. Rev. A **10** (1974) 484-490. (15-70 eV: Hg)

74De2 Dehmer, P.M., Berkowitz, J., Chupka, W.A.: J. Chem. Phys. **60** (1974) 2676.

74Mi1 Millar, R.H., Greening, J.R.: J. Phys. B **7** (1974) 2332-2344. (4.508-25.192 keV: Ne, Ar)

74Wu1 Wuilleumier, F., Krause, M. O.: Phys. Rev. A **10** (1974) 242.

75Be1 Bentley, J.J., Stewart, R.F.: J. Chem. Phys. **62** (1975) 875.

75Hu1 Hubbell, J.W., Veigele, W.J., Briggs, E.A., Brown, R.T., Cromer, D.T., Howerton, R.J.: J. Phys. Chem. Ref. Data **4** (1975) 471-538.

75La1 Lang, J., Watson, W.S.: J. Phys. B **8** (1975) L339-L343. (0.0611-0.254 keV: Kr, Xe)

75Lo1 Loomis, T.C., Keith, H.D.: Appl. Spectrosc. **29** (1975) 316-322. (2.622-11.209 keV: Ar)

75Pe1 Peterson, H., Radler, K., Sonntag, B., Haensel, R.: J. Phys. B **8** (1975) 31. (80-180 eV: Cs)

76Dr1 Driver, R.D. J. Phys. B **9** (1976) 817-827. (24- 40 eV: K)

76Ma1 Marr, G.V., West, J.B.: At. Data Nucl. Data Tables **18** (1976) 497.

76Pa1 Palenius, H.P., Kohl, J.L., Parkinson, W.H.: Phys. Rev. A **13** (1976) 1805-1816. (13.6-20.36 eV: H)

76We1 West, J.B., Marr, G.V.: Proc. R. Soc. London A **349** (1976) 397-421 (36.46-306.6 eV: He, Ne, Ar, Kr)

77Co1 Codling, K., Hamley, J.R., West, J.B.: J. Phys. B **10** (1977) 2797-2807 (0.046-0.296 keV: Na)

77Co2 Cook, T.B., Dunning, F.B., Foltz, G.W., Stebbings, R.F.: Phys. Rev A **15** (1977) 1526-1529. (3.8-5.2 eV:Cs)

78Co1 Cole, B.E., Dexter, R.N.: JQSRT **19** (1978) 467-471. (0.0365-0.248 keV: He, C, N, O, F, Ne, Cl)

78Co2 Codling, K., Hamley, J.R., West, J.B.: J. Phys. B **11** (1978) 1713-1716. (41.92-247.7 eV: Cd)

78Ic1 Ice, G.E., Chen, M.H., Crasemann, B.: Phys. Rev. A **17** (1978) 650.

78Ko1 Kohl, J.L., Lafyatis, G.P., Palenius, H.P., Parkinson, W.H.: Phys. Rev. A **18** (1978) 571-574. (13.1-10.5 eV: O)

78Me1 Mehlman, G., Ederer, D.L., Saloman, E.B., Cooper, J.W.: J.Phys.B **11** (1978) L689.

78We1 West, J.B., Morton, J.: At. Data Nucl. Data Tables **22** (1978) 103-107. (13.45- 14,530 eV: Xe compilation)

79Ar1 Armstrong, J.A., Wynne, J.J.: J. Opt. Soc. **69** (1979) 211.

79Ho1 Holland, D.M.P., Codling, K., West, J.B., Marr, G.V.: J. Phys. B **12** (1979) 2465.

79Ra1 Radler, K., Berkowitz, J.: J. Chem. Phys. **70** (1979) 216.

79Re1 Reilman, R.F., Manson, S.T.: Photoabsorption Cross Sections for Positive Atomic Ions with $Z \leq 30$, Astrophys. J. Suppl. **40** (1979) 815-880.

79Wu1 Wuilleumier, F., Krause, M.O.: J. Electron. Spectros. Relat. Phenom. **15** (1979) 15.

80Gr1 Grattan, K.T.V., Hutchinson, M.H.R., Theocharous, E.S.: J. Phys. B **13** (1980) 2931-2935. (7.2 eV: Cs)

80Ki1 Kissel, L., Pratt, R.H., Roy, S.C.: Phys. Rev. A **22** (1980) 1970.

81Gi1 Gilberg, E., Hanus, M.J., Folz, B.: Rev. Sci. Instr. **52** (1981) 662.

82He1 Henke, B.L., Lee, P., Tahaka, T.J., Shimabukuro, R.L., Fujikawa, B.K.: At. Data Nucl. Data Tables **27** (1982) 1.

82Me1 Mehlman, G., Cooper, J.W., Saloman, E.B.: Phys. Rev. A **25** (1982) 2113-2122. (71-107 eV: Li)

83De1 Deslattes, R.D., LaVilla, R.E., Cowan, P.L., Henins, A.: Phys. Rev. A **27** (1983) 923.

83Ru1 Rusic, B., Berkowitz, J.: Phys. Rev. Lett. **50** (1983) 675.

83Su1 Suemitsu, H., Samson J.A.R.: Phys. Rev. A **28** (1983) 2752. (3.66-4.42 eV: Rb, Cs)

85Sa1 Samson, J.A.R., Pareek, P.N.: Phys. Rev. A **31** (1985) 1470-1476. (14.86-103.2 eV: O)

85Sa2 Saloman, E.B., Cooper, J.W., Mehlman, G.: Phys. Rev. A **32** (1985) 1878. (5.2-10.5 eV: Ba)

86Sa1 Samson, J. A. R., Shefer,Y., Angel, G. C. Phys. Rev. Lett. **56** (1986) 2020-2022. (13.0-70 eV:Cl)

86Sm1 Smend, F., Czerwinski, H.: Z. Phys. D **1** (1986) 139.

87Ya1 Yang, B.X., Kirz, J.: Appl. Opt. **26** (1987) 3823-3826. (0.326-1.01 keV: Ar)

88An1 Angel, G.C., Samson, J.A.R.: Phys. Rev. A **38** (1988) 5578-5585. (13.6-280 eV: O)

88Me1 van der Meer, W.J., van der Meulen, P., Volmer, M., de Lange, C.A.: Chem. Phys. **126** (1988) 385-93. (21.22 eV: O)
89Sa1 Samson, J.A.R., Yin, L.: J. Opt. Soc. Am. B **6** (1989) 2326- 2333. (16.7-21.2 eV: Ar, Kr, Xe)
90Ca1 Caldwell, C.D., Krause, M.O.: J. Phys. B **23** (1990) 2233.
90Sa1 Samson, J.A.R., Angel, G.C.: Phys. Rev. A **42** (1990) 1307-1312. (44-400 eV: N)
90Sa2 Samson, J.A.R., Angel, G.C.: Phys. Rev. A **42** (1990) 5328.
91Ch1 Chan, W.F. Cooper, G, Brion, C.E.: Phys. Rev. A **44** (1991) 186.
91Do1 Domke, M., Xue, A., Puschmann, T., Mandel, E., Hudson, E., Shirley, D.A., Kaindl, G., Greene, C.H., Sadeghpour, H.R., Peterson, H.: Phys. Rev. Lett. **66** (1991) 1306.
91Fl1 Flemming, M.G., Wu, J-Z., Caldwell, C.D.: Phys. Rev. A **44** (1991) 1733.
91Sa1 Samson, J.A.R., Yin, L., Haddad, G.N., Angel, G.C.: J. Phys. (Paris) IV suppl. Vol **1** (1991) Cl99-107 and private communication. (Ne: 21-705 eV, Ar: 16-248 eV, Kr: 15-125 eV, Xe:13.6-135 eV) (recommended data)
92Ch1 Chan, W.F., Cooper, G., Guo, X., Brion, C.E.: Phys. Rev. A **45** (1992) 1420.
92Fe1 Fennelly, J.A., Torr, D.G.: At. Data Nucl. Data Tables, **51** (1992) 321.
92Me1 Meulen, P., Krause, M.O., Caldwell, C.D., Whitfield, S.B., Lange, C.A.: Phys. Rev. A **46** (1992) 2468. (21.5-25 eV: Cl)
93Ma1 Maeda, K., Ueda, K., Ito, K.: J. Phys. B **26** (1993) 1541.
94Ki1 Kiernan, L.M., Mosnier, J-P., Kennedy, E.T., Costello, J.T., Sonntag, B.F.: Phys. Rev. Lett. **72** (1994) 2359.
94Ku1 Kurucu, Y., Erzeneoglu, S., Sahin,Y., Durak, R.: Nuovo Cimento **16** (1994) 555.
94Sa1 Samson, J.A.R., He, Z.X., Yin, L., Haddad, G.N.: J. Phys. B **27** (1994) 887.
95Ar1 Arcon, I., Kodre, A., Stuhec, M., Glavic-Cindro, D.: Phys. Rev. A **51** (1995) 147.
95Bo1 Borne, A. Federmann, F., Lee, M.K., Sonntag, B.: J. Phys. B **28** (1995) 2591.
95Az1 Azuma, Y., Berry, H.G, Gemmell, D.S., Suleiman, J., Westerlind, M., Sellin, I.A., Woicik, J.C., Kirkland, J.P.: Phys. Rev. A **51** (1995) 447, 453.
95MG1 McGuire, J.H., Berrah, N., Bartlett, R.J., Samson, J.A.R., Tanis, J.A., Cocke, C.L., Schlachter, A.S.: J. Phys. B **28** (1995) 913.
96Co1 Cooper, J.W.: Radiat. Phys. Chem. **47** (1996) 927-934.
96Do1 Doerner, R. et al.: Phys. Rev. Lett. **76** (1996) 2654.
96Ki1 Kiernan, L.M.: J. Phys. B **29** (1996) L181.
96Le1 Levin, J.C., Armen, B., Sellin, I.A.: Phys. Rev. Lett. **76** (1996) 1220.
96Sp1 Spielberger, L. et al.: Phys. Rev. Lett. **76** (1996) 4685.
96Wu1 Wuilleumier, F.J., Diehl, S., Cubaynes, D., Bizau, J-M., in: X-Ray and Inner Shell Processes, AIP Press, New York: Woodbury (1996), p 625.
97Ch1 Chung, K.T.: Phys. Rev. Lett. **78** (1997) 1416.
97Az1 Azuma, Y. et al.: Phys. Rev. Lett. **79** (1997) 2419.
97Be1 Berkowitz, J.: J. Phys. B **30** (1997) 583.
98Sa1 Samson, J.A.R., Stolte, W.C., He, Z.X., Cutler, J.N., Lu, Y., Bartlett, R.J.: Phys. Rev. A **57** (1998) 1906.

A1 Hudson, R.D., Kieffer, L.J.: Compilation of Atomic Ultraviolet Photoabsorption Cross Sections for Wavelengths between 3000 and 10 Å, At. Data **2** (1971) 205-262.
A2 Kieffer, L.J.: Bibliograpy of Low Energy Electron and Photon Cross Section Data, NBS Special Pub. **426** (1976) and NBS Special Pub. **426**, Suppl. 1 (1979).
A3 Berkowitz, J.: Photoabsorption, Photoionization, and Photoelectron Spectroscopy, New York: Academic Press (1979).
A4 Samson, J.A.R.: Techniques of Vacuum Ultraviolet Spectroscopy, New York: Wiley (1967).

A5 Samson, J.A.R.: Atomic Photoionization (p. 123-213), Encyclopedia of Physics (W. Mehlhorn, ed.), Berlin: Springer (1982).
A6 Schmidt, V.: Photoionization of Atoms Using Synchrotron Radiation, Rep. Prog. Phys. **55** (1992) 1483.
A7 Sonntag, B., Zimmermann, P.: Rep. Prog. Phys. **55** (1992) 911.
A8 VUV and Soft X-Ray Photoionization (U. Becker, D.A. Shirley, eds.), New York: Plenum Press (1996).
A9 Saloman, E.B., Hubbell, J.H.: X-Ray Attenuation Coefficients (Total Cross Sections): Comparison of the Experimental Data Base with the Recommended Values of Henke and the Theoretical Values of Scofield for Energies Between 0.1-100 keV, Natl. Bur. Stand. Int. Rep. NBSIR 86-3431 (1986).
A10 Saloman, E.B., Hubbell, J.H., Scofield, J.H.: X-Ray Attenuation Cross Sections for Energies 100 eV to 100 keV and Elements Z = 1 to Z = 92, Atomic Data and Nuclear Data Tables **38** (1988) 1-197.
A11 Band, I.M., Yu, I.K., Trzhaskovskaya: Photoionization Cross Sections and Photoelectron Angular Distributions for X-Ray Lines Energies in the Range 0.132-4.509 keV. Targets:$1 \le Z \le 100$, At. Data Nucl. Data Tables **23** (1979) 443.
A12 Huang, K.N., Johnson, W.R., Cheng, K.T.: Theoretical Photoionization Parameters for the Noble Gases Argon, Krypton and Xenon, At. Data Nucl. Data Tables, **26** (1981) 33.
A13 Yeh, J.J., Lindau, I.: Atomic Subshell Photoionization Cross Sections and Asymmetry Parameters: $1 \le Z \le 103$, At. Data Nucl. Data Tables **32** (1985) 1.
A14 Verner, D.A., Yakovlevd, G., Band, I.M., Trzhakovskaya, M.B.: Subshell Photoioniza tion Cross Sections and Ionization Energies of Atoms and Ions from He to Zn, At. Data Nucl. Data Tables **55** (1993) 233.
A15 Wang, J., Sagar, R.P., Schmider, H., Smith, V.H.: X-Ray Elastic and Inelastic Scattering Factors for Neutral Atoms Z = 2-92, At. Data Nucl. Data Tables **53** (1993) 233.
A16 Chantler, C.T.: Theoretical Form Factor, Attenuation and Scattering Tabulation for Z = 1-92 from E = 1-10 eV to E = 0.4-1.0 MeV, J. Phys. Chem. Ref. Data **24** (1995) 71.
A17 Saloman, E.B., Hubbell, J.H., Berger, M.J.: Natl. Bur. Stand. Data Base of Photon Absorption Cross Sections from 10 eV to 100 GeV, Proc. SPIE **911** (1988) 100-106.
A18 Cullen, D.E., Chen, M.H., Hubbell, J.H., Perkins, S.T., Plechaty, E.F., Rathkopf, J.A., Scofield, J.H.: Tables and Graphs of Photon-Interaction Cross Sections from 10 eV to 100 GeV, Derived from the LLNL Evaluated Photon Data Library. Part A: Z = 1-50. Part B: Z = 51-100, Lawrence Livermore Lab. Rep. UCRL-50400, Vol. **6**, Rev. 4 (1989).
A19 Henke, B.L., Gullikson, E.M., Davis, J.C.: X-Ray Interactions: Photoabsorption, Scattering, Transmission, and Reflection at E = 50-30,000 eV, Z = 1-92, At. Data Nucl. Data Tables **54** (1993) 181-342.

Acknowledgements

The author is indebted to J.H. Hubbell who not only made his collection of photon attenuation cross section reprints available to him, but provided much useful information on data sources, to E.B. Saloman, who made available the information contained in the NIST X-ray attenuation data base and to J.A.R. Samson who read preliminary versions of this work and provided in useful form some of the data contained here.